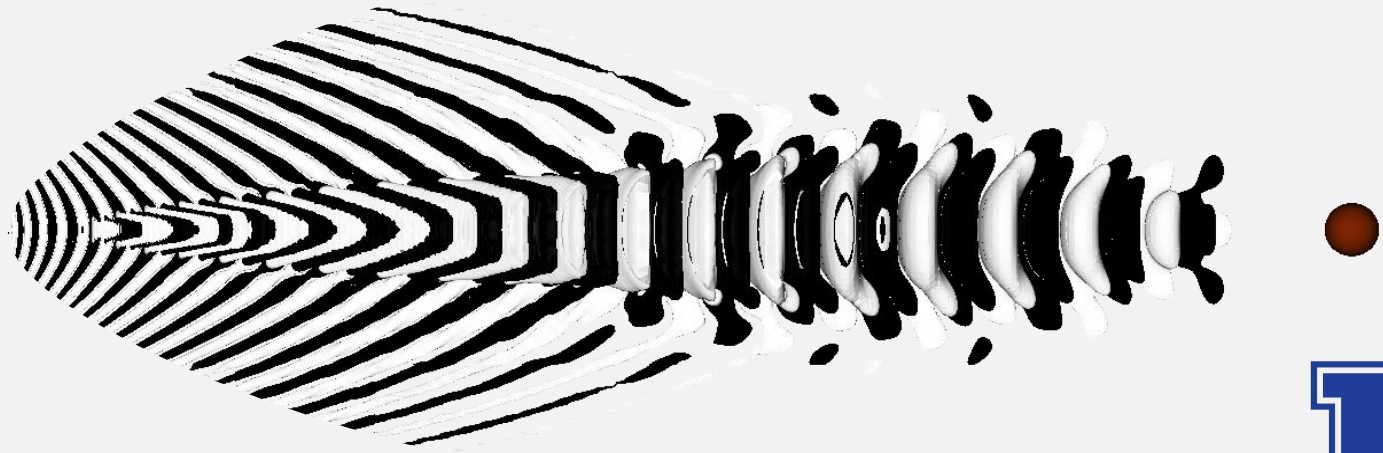
Advanced Modeling & Simulations (AMS) Seminar Series
NASA Ames Research Center, May 4th, 2023

Adaptive Mesh Refinement Disturbance Flow Tracking for Hypersonic Boundary Layer Transition Prediction



Vincenzo **RUSSO** (UKY)
Professor Christoph **BREHM** (UMD)

OUTLINE

- Introduction and Research Motivation

On the relevance of Hypersonic Transition

- Computational Approach

Disturbance Flow Formulation, Adaptive Mesh Refinement and Immersed Boundary Method

- Results

Validation, Disturbance Flow Simulations for Complex Geometries and Particle Impingement

- Conclusions and Outlook

Summary of Presented Research and Future Work

OUTLINE

- Introduction and Research Motivation

On the relevance of Hypersonic Transition

- Computational Approach

Disturbance Flow Formulation, Adaptive Mesh Refinement and Immersed Boundary Method

- Results

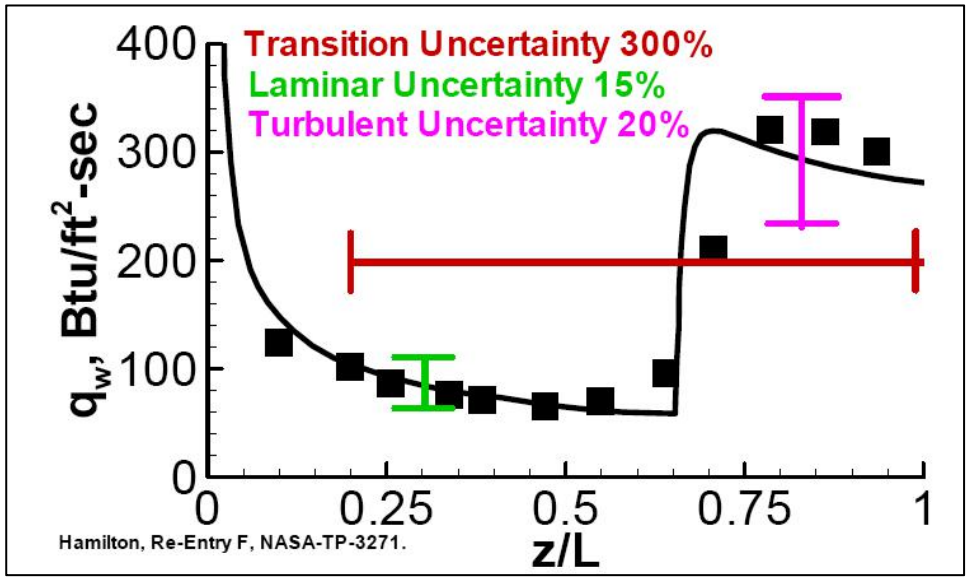
Validation, Disturbance Flow Simulations for Complex Geometries and Particle Impingement

- Conclusions and Outlook

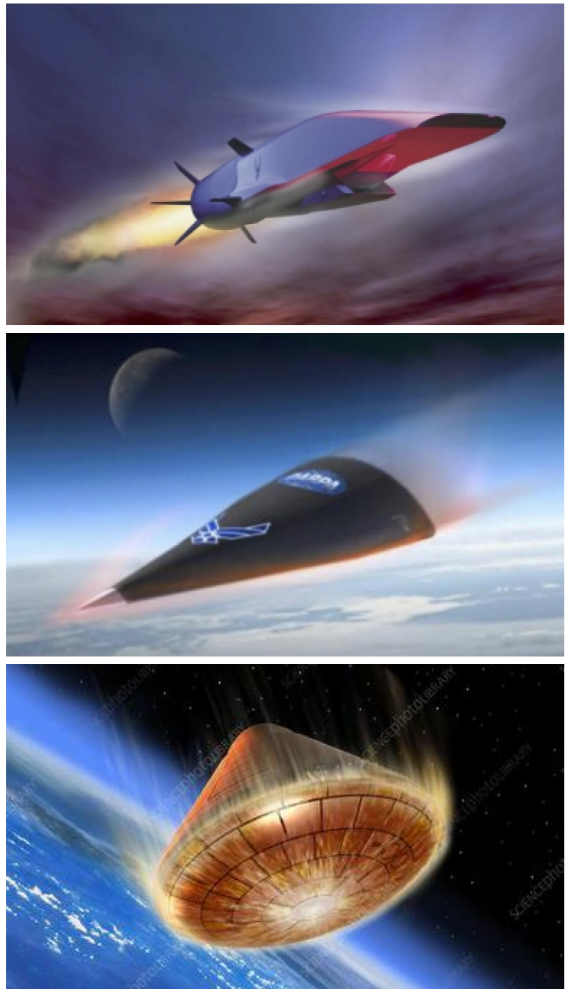
Summary of Presented Research and Future Work

RESEARCH MOTIVATION: HYPERSONIC TRANSITION

- Transition **increases** skin friction and heat transfer rates, thus producing higher **aerothermodynamic loads**



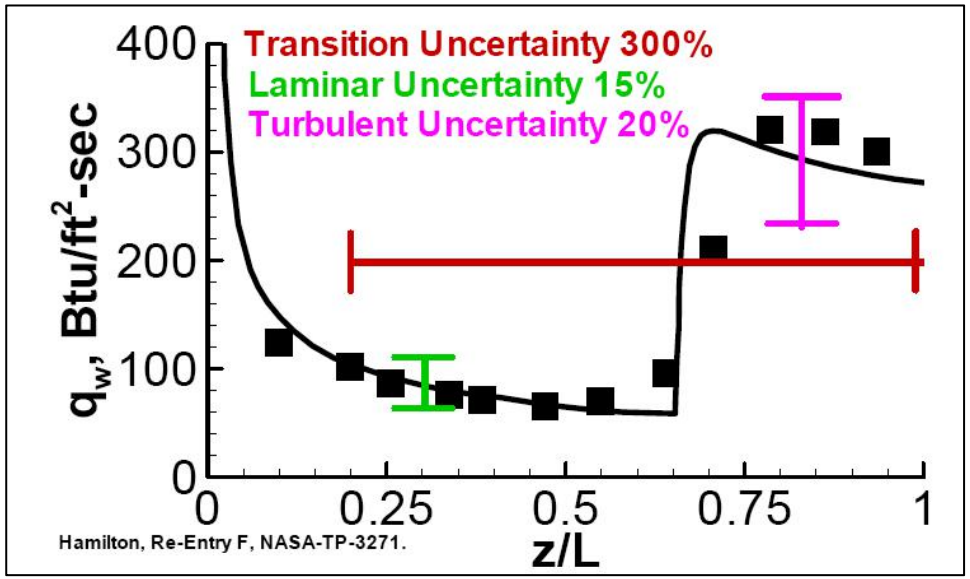
From Schneider (2002) and Hamilton (1992), Re-Entry F, NASA-TP-3271



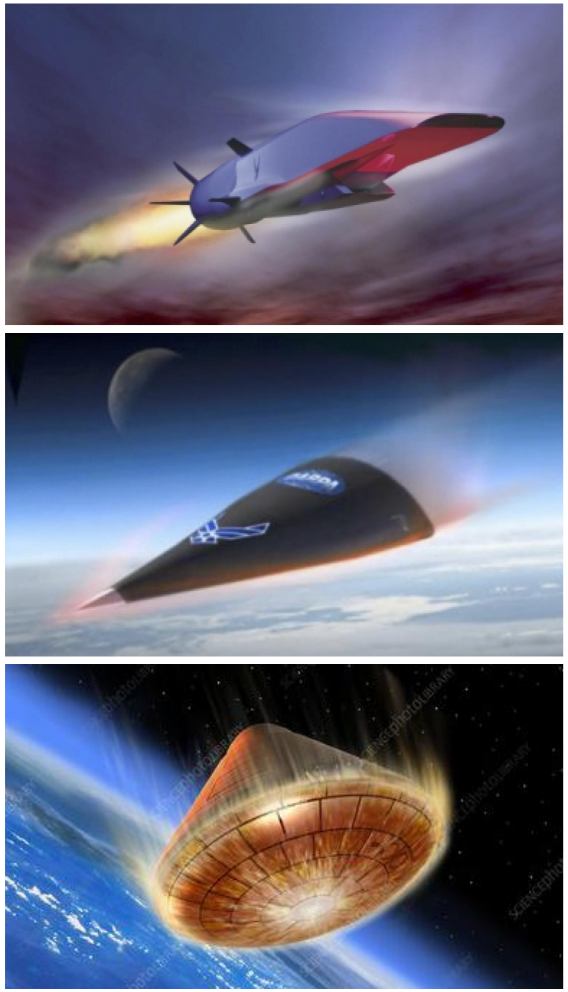
Artist's concepts of hypersonic vehicles

RESEARCH MOTIVATION: HYPERSONIC TRANSITION

- Transition **increases** skin friction and heat transfer rates, thus producing higher **aerothermodynamic loads**
- Understanding of the relevant physics is essential to **reduce design margins** and **systems uncertainties** and, ultimately, guide the development of improved hypersonic systems (e.g. TPS)



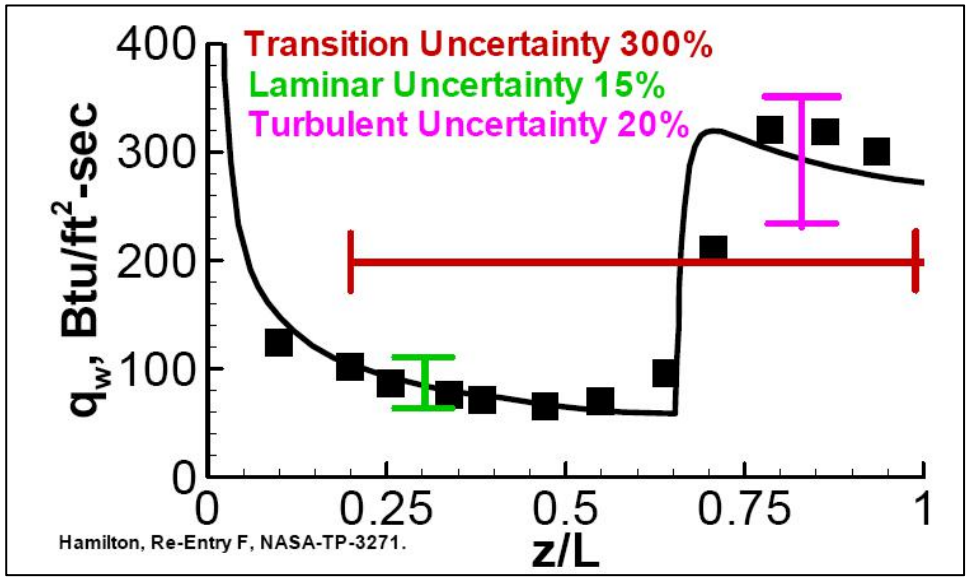
From Schneider (2002) and Hamilton (1992), Re-Entry F, NASA-TP-3271



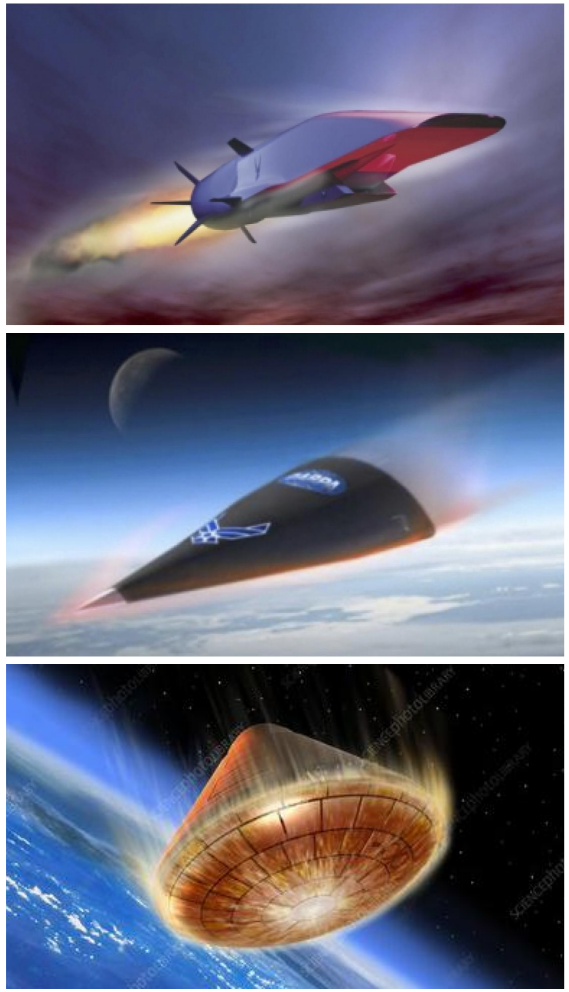
Artist's concepts of hypersonic vehicles

RESEARCH MOTIVATION: HYPERSONIC TRANSITION

- Transition **increases** skin friction and heat transfer rates, thus producing higher **aerothermodynamic loads**
- Understanding of the relevant physics is essential to **reduce design margins** and **systems uncertainties** and, ultimately, guide the development of improved hypersonic systems (e.g. TPS)
- Disturbance environment and its effects on the flow field need to be studied to provide **accurate predictions**



From Schneider (2002) and Hamilton (1992), Re-Entry F, NASA-TP-3271



Artist's concepts of hypersonic vehicles

RESEARCH MOTIVATION: HYPERSONIC TRANSITION

- Transition **increases** skin friction and heat transfer rates, thus producing higher **aerothermodynamic loads**
- Understanding of the relevant physics is essential to **reduce design margins** and **systems uncertainties** and, ultimately, guide the development of improved hypersonic systems (e.g. TPS)
- Disturbance environment and its effects on the flow field need to be studied to provide **accurate predictions**

Research Objectives

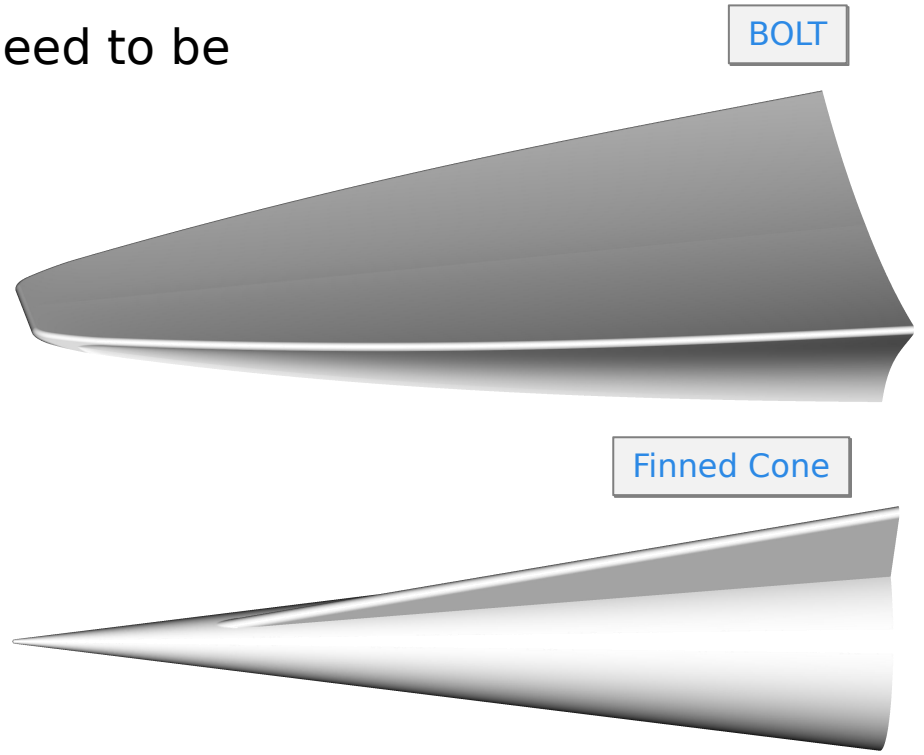
- Establish a **flexible** and **computationally efficient** framework to study complex geometries with highly 3D baseflows, for which traditional methods (e.g. LST) fail

RESEARCH MOTIVATION: HYPERSONIC TRANSITION

- Transition **increases** skin friction and heat transfer rates, thus producing higher **aerothermodynamic loads**
- Understanding of the relevant physics is essential to **reduce design margins** and **systems uncertainties** and, ultimately, guide the development of improved hypersonic systems (e.g. TPS)
- Disturbance environment and its effects on the flow field need to be studied to provide **accurate predictions**

Research Objectives

- Establish a **flexible** and **computationally efficient** framework to study complex geometries with highly 3D baseflows, for which traditional methods (e.g. LST) fail

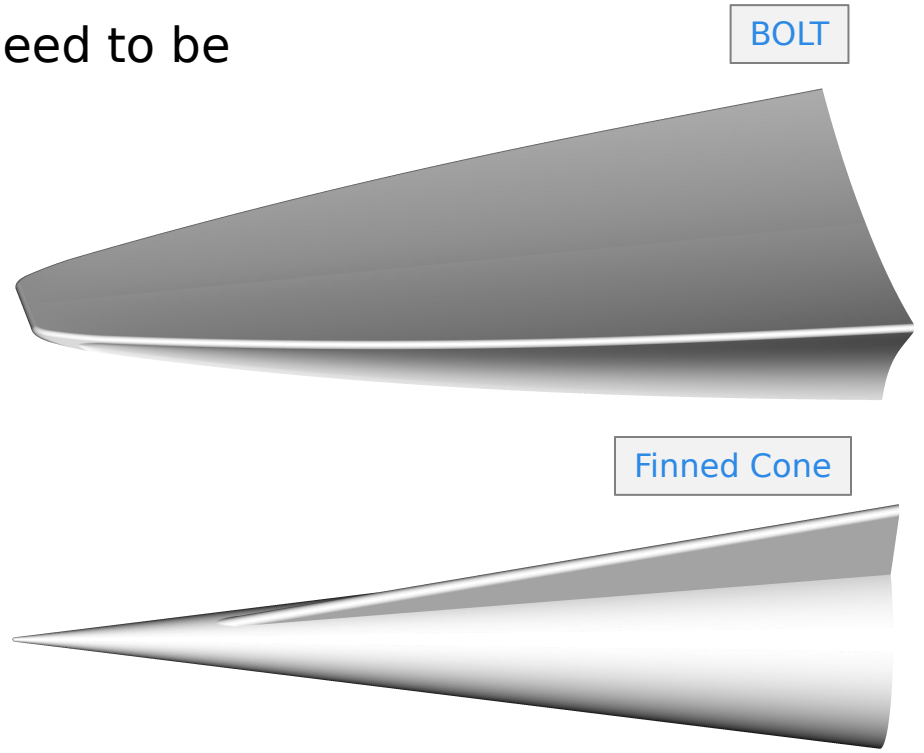


RESEARCH MOTIVATION: HYPERSONIC TRANSITION

- Transition **increases** skin friction and heat transfer rates, thus producing higher **aerothermodynamic loads**
- Understanding of the relevant physics is essential to **reduce design margins** and **systems uncertainties** and, ultimately, guide the development of improved hypersonic systems (e.g. TPS)
- Disturbance environment and its effects on the flow field need to be studied to provide **accurate predictions**

Research Objectives

- Establish a **flexible** and **computationally efficient** framework to study complex geometries with highly 3D baseflows, for which traditional methods (e.g. LST) fail
- Provide **physical insight** into the interaction of the disturbance environment, for scenarios relevant to realistic **hypersonic flows and configurations**



OUTLINE

- Introduction and Research Motivation

On the relevance of Hypersonic Transition

- Computational Approach

Disturbance Flow Formulation, Adaptive Mesh Refinement and Immersed Boundary Method

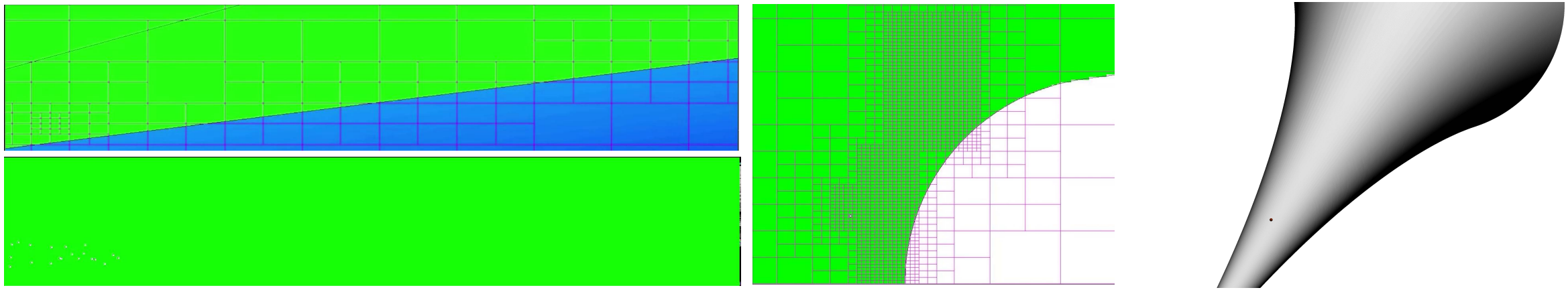
- Results

Validation, Disturbance Flow Simulations for Complex Geometries and Particle Impingement

- Conclusions and Outlook

Summary of Presented Research and Future Work

COMPUTATIONAL APPROACH - CHAMPS



*The presented studies were performed using **CHAMPS** (**Cartesian High-Order Adaptive Multi Physics Solver**), a in-house multi-physics solver developed at UMD (in collaboration with UKY and OX)*

- *Conservative FD scheme*
- *Higher-order shock capturing for convective terms (with characteristic variables transform)*
- *4th-order accurate treatment of viscous terms*
- *Higher-order explicit and implicit time-discretization*
- *Higher-order **Immersed Boundary** Method (IBM)*
- *Multi-species, gas chemistry, multi-phase capabilities.*
- *Fluid-Structure Interaction (FEM CSD solver)*
- ***Particle Solver***
- *Grid: generalized **Curvilinear** and **Adaptive Mesh Refinement (AMR) Cartesian***

OUTLINE

- Introduction and Research Motivation

On the relevance of Hypersonic Transition

- Computational Approach

Disturbance Flow Formulation, Adaptive Mesh Refinement and Immersed Boundary Method

- Results

Validation, Disturbance Flow Simulations for Complex Geometries and Particle Impingement

- Conclusions and Outlook

Summary of Presented Research and Future Work

OUTLINE

- Introduction and Research Motivation

On the relevance of Hypersonic Transition

- Computational Approach

Disturbance Flow Formulation, Adaptive Mesh Refinement and Immersed Boundary Method

- Results

Validation, Disturbance Flow Simulations for Complex Geometries and Particle Impingement

- Conclusions and Outlook

Summary of Presented Research and Future Work

Compressible N.S. in Vector Form

$$\frac{\partial \mathbf{W}}{\partial t} + \frac{\partial \mathbf{E}}{\partial x} + \frac{\partial \mathbf{F}}{\partial y} + \frac{\partial \mathbf{G}}{\partial z} = 0 \quad \text{where,} \quad \mathbf{W} = \bar{\mathbf{W}} + \tilde{\mathbf{W}}\,, \quad \mathbf{E} = \bar{\mathbf{E}} + \tilde{\mathbf{E}}, \qquad \mathbf{F} = \bar{\mathbf{F}} + \tilde{\mathbf{F}}, \quad \text{and} \quad \mathbf{G} = \bar{\mathbf{G}} + \tilde{\mathbf{G}}$$

Compressible N.S. in Vector Form

$$\frac{\partial \mathbf{W}}{\partial t} + \frac{\partial \mathbf{E}}{\partial x} + \frac{\partial \mathbf{F}}{\partial y} + \frac{\partial \mathbf{G}}{\partial z} = 0 \quad \text{where,} \quad \mathbf{W} = \bar{\mathbf{W}} + \tilde{\mathbf{W}}\,, \quad \mathbf{E} = \bar{\mathbf{E}} + \tilde{\mathbf{E}}, \qquad \mathbf{F} = \bar{\mathbf{F}} + \tilde{\mathbf{F}}, \quad \text{and} \quad \mathbf{G} = \bar{\mathbf{G}} + \tilde{\mathbf{G}}$$

the bar and tilde symbols refer to meanflow
and disturbance quantities, respectively

Compressible N.S. in Vector Form

$$\frac{\partial \mathbf{W}}{\partial t} + \frac{\partial \mathbf{E}}{\partial x} + \frac{\partial \mathbf{F}}{\partial y} + \frac{\partial \mathbf{G}}{\partial z} = 0 \quad \text{where,} \quad \mathbf{W} = \bar{\mathbf{W}} + \tilde{\mathbf{W}}\,, \quad \mathbf{E} = \bar{\mathbf{E}} + \tilde{\mathbf{E}}, \quad \mathbf{F} = \bar{\mathbf{F}} + \tilde{\mathbf{F}}, \quad \text{and} \quad \mathbf{G} = \bar{\mathbf{G}} + \tilde{\mathbf{G}}$$

the bar and tilde symbols refer to meanflow and disturbance quantities, respectively

Compressible N.S. in Vector Form

$$\frac{\partial \mathbf{W}}{\partial t} + \frac{\partial \mathbf{E}}{\partial x} + \frac{\partial \mathbf{F}}{\partial y} + \frac{\partial \mathbf{G}}{\partial z} = 0 \quad \text{where,} \quad \mathbf{W} = \bar{\mathbf{W}} + \tilde{\mathbf{W}}\,, \quad \mathbf{E} = \bar{\mathbf{E}} + \tilde{\mathbf{E}}, \quad \mathbf{F} = \bar{\mathbf{F}} + \tilde{\mathbf{F}}, \quad \text{and} \quad \mathbf{G} = \bar{\mathbf{G}} + \tilde{\mathbf{G}}$$

the bar and tilde symbols refer to meanflow and disturbance quantities, respectively

$$\mathbf{W} = \bar{\mathbf{W}} + \tilde{\mathbf{W}}$$

Compressible N.S. in Vector Form

$$\frac{\partial \mathbf{W}}{\partial t} + \frac{\partial \mathbf{E}}{\partial x} + \frac{\partial \mathbf{F}}{\partial y} + \frac{\partial \mathbf{G}}{\partial z} = 0 \quad \text{where,} \quad \mathbf{W} = \bar{\mathbf{W}} + \tilde{\mathbf{W}}\,, \quad \mathbf{E} = \bar{\mathbf{E}} + \tilde{\mathbf{E}}, \quad \mathbf{F} = \bar{\mathbf{F}} + \tilde{\mathbf{F}}, \quad \text{and} \quad \mathbf{G} = \bar{\mathbf{G}} + \tilde{\mathbf{G}}$$

the bar and tilde symbols refer to **meanflow** and **disturbance** quantities, respectively

$$\mathbf{W} = \bar{\mathbf{W}} + \tilde{\mathbf{W}} = \underbrace{\begin{bmatrix} \bar{\rho} \\ \bar{\rho}\bar{u} \\ \bar{\rho}\bar{v} \\ \bar{\rho}\bar{w} \\ \bar{\rho}\bar{E}_t \end{bmatrix}}_{\text{baseflow}} + \underbrace{\begin{bmatrix} \tilde{\rho} \\ \tilde{\rho}\bar{u} + \bar{\rho}\tilde{u} \\ \tilde{\rho}\bar{v} + \bar{\rho}\tilde{v} \\ \tilde{\rho}\bar{w} + \bar{\rho}\tilde{w} \\ \bar{\rho}\tilde{E}_t + \tilde{\rho}\bar{E}_t \end{bmatrix}}_{\text{linear disturbance}} + \underbrace{\begin{bmatrix} \\ \tilde{\rho}\tilde{u} \\ \tilde{\rho}\tilde{v} \\ \tilde{\rho}\tilde{w} \\ \tilde{\rho}\tilde{E}_t \end{bmatrix}}_{\text{nonlinear disturbance}}$$

Compressible N.S. in Vector Form

$$\frac{\partial \mathbf{W}}{\partial t}+\frac{\partial \mathbf{E}}{\partial x}+\frac{\partial \mathbf{F}}{\partial y}+\frac{\partial \mathbf{G}}{\partial z}=0 \quad \text{where,} \quad \mathbf{W}=\bar{\mathbf{W}}+\tilde{\mathbf{W}}\,, \quad \mathbf{E}=\bar{\mathbf{E}}+\tilde{\mathbf{E}}, \quad \mathbf{F}=\bar{\mathbf{F}}+\tilde{\mathbf{F}}, \quad \text{and} \quad \mathbf{G}=\bar{\mathbf{G}}+\tilde{\mathbf{G}}$$

the bar and tilde symbols refer to **meanflow** and **disturbance** quantities, respectively

$$\mathbf{W}=\bar{\mathbf{W}}+\tilde{\mathbf{W}}=\underbrace{\begin{bmatrix}\bar{\rho}\\ \bar{\rho}\bar{u}\\ \bar{\rho}\bar{v}\\ \bar{\rho}\bar{w}\\ \bar{\rho}\bar{E}_t\end{bmatrix}}_{\text{baseflow}}+\underbrace{\begin{bmatrix}\tilde{\rho}\\ \tilde{\rho}\bar{u}+\bar{\rho}\tilde{u}\\ \tilde{\rho}\bar{v}+\bar{\rho}\tilde{v}\\ \tilde{\rho}\bar{w}+\bar{\rho}\tilde{w}\\ \bar{\rho}\tilde{E}_t+\tilde{\rho}\bar{E}_t\end{bmatrix}}_{\text{linear disturbance}}+\underbrace{\begin{bmatrix}\\ \tilde{\rho}\tilde{u}\\ \tilde{\rho}\tilde{v}\\ \tilde{\rho}\tilde{w}\\ \tilde{\rho}\tilde{E}_t\end{bmatrix}}_{\text{nonlinear disturbance}}$$

$$\frac{\partial \tilde{\mathbf{W}}}{\partial t}+\frac{\partial \tilde{\mathbf{E}}}{\partial x}+\frac{\partial \tilde{\mathbf{F}}}{\partial y}+\frac{\partial \tilde{\mathbf{G}}}{\partial z}=-\left(\frac{\partial \bar{\mathbf{W}}}{\partial t}+\frac{\partial \bar{\mathbf{E}}}{\partial x}+\frac{\partial \bar{\mathbf{F}}}{\partial y}+\frac{\partial \bar{\mathbf{G}}}{\partial z}\right)$$

Compressible N.S. in Vector Form

$$\frac{\partial \mathbf{W}}{\partial t}+\frac{\partial \mathbf{E}}{\partial x}+\frac{\partial \mathbf{F}}{\partial y}+\frac{\partial \mathbf{G}}{\partial z}=0 \quad \text{where,} \quad \mathbf{W}=\bar{\mathbf{W}}+\tilde{\mathbf{W}}\,, \quad \mathbf{E}=\bar{\mathbf{E}}+\tilde{\mathbf{E}}, \quad \mathbf{F}=\bar{\mathbf{F}}+\tilde{\mathbf{F}}, \quad \text{and} \quad \mathbf{G}=\bar{\mathbf{G}}+\tilde{\mathbf{G}}$$

the bar and tilde symbols refer to **meanflow** and **disturbance** quantities, respectively

$$\mathbf{W}=\bar{\mathbf{W}}+\tilde{\mathbf{W}}=\underbrace{\begin{bmatrix}\bar{\rho}\\ \bar{\rho}\bar{u}\\ \bar{\rho}\bar{v}\\ \bar{\rho}\bar{w}\\ \bar{\rho}\bar{E}_t\end{bmatrix}}_{\text{baseflow}}+\underbrace{\begin{bmatrix}\tilde{\rho}\\ \tilde{\rho}\bar{u}+\bar{\rho}\tilde{u}\\ \tilde{\rho}\bar{v}+\bar{\rho}\tilde{v}\\ \tilde{\rho}\bar{w}+\bar{\rho}\tilde{w}\\ \bar{\rho}\tilde{E}_t+\tilde{\rho}\bar{E}_t\end{bmatrix}}_{\text{linear disturbance}}+\underbrace{\begin{bmatrix}\\ \tilde{\rho}\tilde{u}\\ \tilde{\rho}\tilde{v}\\ \tilde{\rho}\tilde{w}\\ \tilde{\rho}\tilde{E}_t\end{bmatrix}}_{\text{nonlinear disturbance}}$$

$$\frac{\partial \tilde{\mathbf{W}}}{\partial t}+\frac{\partial \tilde{\mathbf{E}}}{\partial x}+\frac{\partial \tilde{\mathbf{F}}}{\partial y}+\frac{\partial \tilde{\mathbf{G}}}{\partial z}=-\cancel{\left(\frac{\partial \bar{\mathbf{W}}}{\partial t}+\frac{\partial \bar{\mathbf{E}}}{\partial x}+\frac{\partial \bar{\mathbf{F}}}{\partial y}+\frac{\partial \bar{\mathbf{G}}}{\partial z}\right)}$$

Compressible N.S. in Vector Form

$$\frac{\partial \mathbf{W}}{\partial t}+\frac{\partial \mathbf{E}}{\partial x}+\frac{\partial \mathbf{F}}{\partial y}+\frac{\partial \mathbf{G}}{\partial z}=0 \quad \text{where,} \quad \mathbf{W}=\bar{\mathbf{W}}+\tilde{\mathbf{W}}\,, \quad \mathbf{E}=\bar{\mathbf{E}}+\tilde{\mathbf{E}}, \quad \mathbf{F}=\bar{\mathbf{F}}+\tilde{\mathbf{F}}, \quad \text{and} \quad \mathbf{G}=\bar{\mathbf{G}}+\tilde{\mathbf{G}}$$

the bar and tilde symbols refer to **meanflow** and **disturbance** quantities, respectively

$$\mathbf{W}=\bar{\mathbf{W}}+\tilde{\mathbf{W}}=\underbrace{\begin{bmatrix}\bar{\rho}\\ \bar{\rho}\bar{u}\\ \bar{\rho}\bar{v}\\ \bar{\rho}\bar{w}\\ \bar{\rho}\bar{E}_t\end{bmatrix}}_{\text{baseflow}}+\underbrace{\begin{bmatrix}\tilde{\rho}\\ \tilde{\rho}\bar{u}+\bar{\rho}\tilde{u}\\ \tilde{\rho}\bar{v}+\bar{\rho}\tilde{v}\\ \tilde{\rho}\bar{w}+\bar{\rho}\tilde{w}\\ \bar{\rho}\tilde{E}_t+\tilde{\rho}\bar{E}_t\end{bmatrix}}_{\text{linear disturbance}}+\underbrace{\begin{bmatrix}\\ \tilde{\rho}\tilde{u}\\ \tilde{\rho}\tilde{v}\\ \tilde{\rho}\tilde{w}\\ \tilde{\rho}\tilde{E}_t\end{bmatrix}}_{\text{nonlinear disturbance}}$$

$$\frac{\partial \tilde{\mathbf{W}}}{\partial t}+\frac{\partial \tilde{\mathbf{E}}}{\partial x}+\frac{\partial \tilde{\mathbf{F}}}{\partial y}+\frac{\partial \tilde{\mathbf{G}}}{\partial z}=-\left(\frac{\partial \bar{\mathbf{W}}}{\partial t}+\frac{\partial \bar{\mathbf{E}}}{\partial x}+\frac{\partial \bar{\mathbf{F}}}{\partial y}+\frac{\partial \bar{\mathbf{G}}}{\partial z}\right)$$

Finally, we obtain the
Compressible N.S. Disturbance Flow Equations:

$$\frac{\partial \tilde{\mathbf{W}}}{\partial t}+\frac{\partial \tilde{\mathbf{E}}}{\partial x}+\frac{\partial \tilde{\mathbf{F}}}{\partial y}+\frac{\partial \tilde{\mathbf{G}}}{\partial z}=0$$

Compressible N.S. in Vector Form

$$\frac{\partial \mathbf{W}}{\partial t}+\frac{\partial \mathbf{E}}{\partial x}+\frac{\partial \mathbf{F}}{\partial y}+\frac{\partial \mathbf{G}}{\partial z}=0 \quad \text{where,} \quad \mathbf{W}=\bar{\mathbf{W}}+\tilde{\mathbf{W}}\,, \quad \mathbf{E}=\bar{\mathbf{E}}+\tilde{\mathbf{E}}, \quad \mathbf{F}=\bar{\mathbf{F}}+\tilde{\mathbf{F}}, \quad \text{and} \quad \mathbf{G}=\bar{\mathbf{G}}+\tilde{\mathbf{G}}$$

the bar and tilde symbols refer to **meanflow** and **disturbance** quantities, respectively

$$\mathbf{W}=\bar{\mathbf{W}}+\tilde{\mathbf{W}}=\underbrace{\begin{bmatrix}\bar{\rho}\\ \bar{\rho}\bar{u}\\ \bar{\rho}\bar{v}\\ \bar{\rho}\bar{w}\\ \bar{\rho}\bar{E}_t\end{bmatrix}}_{\text{baseflow}}+\underbrace{\begin{bmatrix}\tilde{\rho}\\ \tilde{\rho}\bar{u}+\bar{\rho}\tilde{u}\\ \tilde{\rho}\bar{v}+\bar{\rho}\tilde{v}\\ \tilde{\rho}\bar{w}+\bar{\rho}\tilde{w}\\ \bar{\rho}\tilde{E}_t+\tilde{\rho}\bar{E}_t\end{bmatrix}}_{\text{linear disturbance}}+\underbrace{\begin{bmatrix}\\ \tilde{\rho}\tilde{u}\\ \tilde{\rho}\tilde{v}\\ \tilde{\rho}\tilde{w}\\ \tilde{\rho}\tilde{E}_t\end{bmatrix}}_{\text{nonlinear disturbance}}$$

$$\frac{\partial \tilde{\mathbf{W}}}{\partial t}+\frac{\partial \tilde{\mathbf{E}}}{\partial x}+\frac{\partial \tilde{\mathbf{F}}}{\partial y}+\frac{\partial \tilde{\mathbf{G}}}{\partial z}=-\left(\frac{\partial \bar{\mathbf{W}}}{\partial t}+\frac{\partial \bar{\mathbf{E}}}{\partial x}+\frac{\partial \bar{\mathbf{F}}}{\partial y}+\frac{\partial \bar{\mathbf{G}}}{\partial z}\right)$$

(1) *An efficient linear wavepacket tracking method for hypersonic boundary-layer stability prediction*, Oliver M.F. **Browne**, Anthony P. Haas, Herman F. Fasel, Christoph Brehm, *Journal of Computational Physics*

Finally, we obtain the
Compressible N.S. Disturbance Flow Equations:[1]

$$\frac{\partial \tilde{\mathbf{W}}}{\partial t}+\frac{\partial \tilde{\mathbf{E}}}{\partial x}+\frac{\partial \tilde{\mathbf{F}}}{\partial y}+\frac{\partial \tilde{\mathbf{G}}}{\partial z}=0$$

OUTLINE

- Introduction and Research Motivation

On the relevance of Hypersonic Transition

- Computational Approach

Disturbance Flow Formulation, Adaptive Mesh Refinement and Immersed Boundary Method

- Results

Validation, Disturbance Flow Simulations for Complex Geometries and Particle Impingement

- Conclusions and Outlook

Summary of Presented Research and Future Work

OUTLINE

- Introduction and Research Motivation

On the relevance of Hypersonic Transition

- Computational Approach

Disturbance Flow Formulation, **Adaptive Mesh Refinement** and **Immersed Boundary Method**

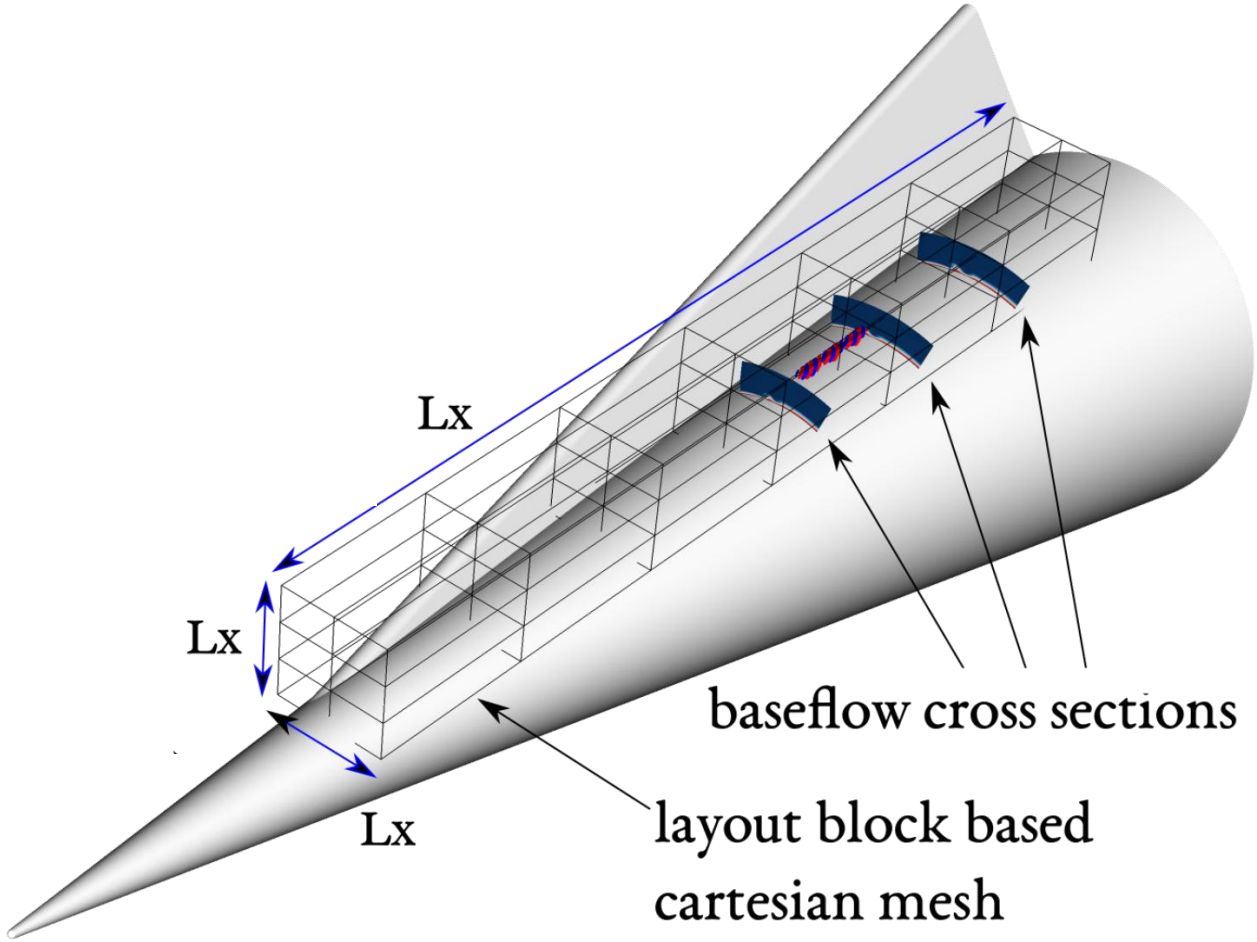
- Results

Validation, Disturbance Flow Simulations for Complex Geometries and Particle Impingement

- Conclusions and Outlook

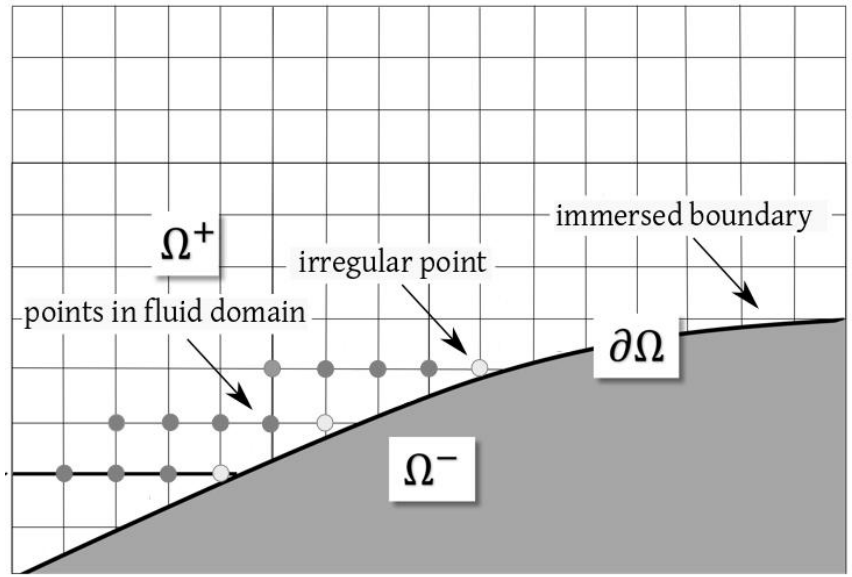
Summary of Presented Research and Future Work

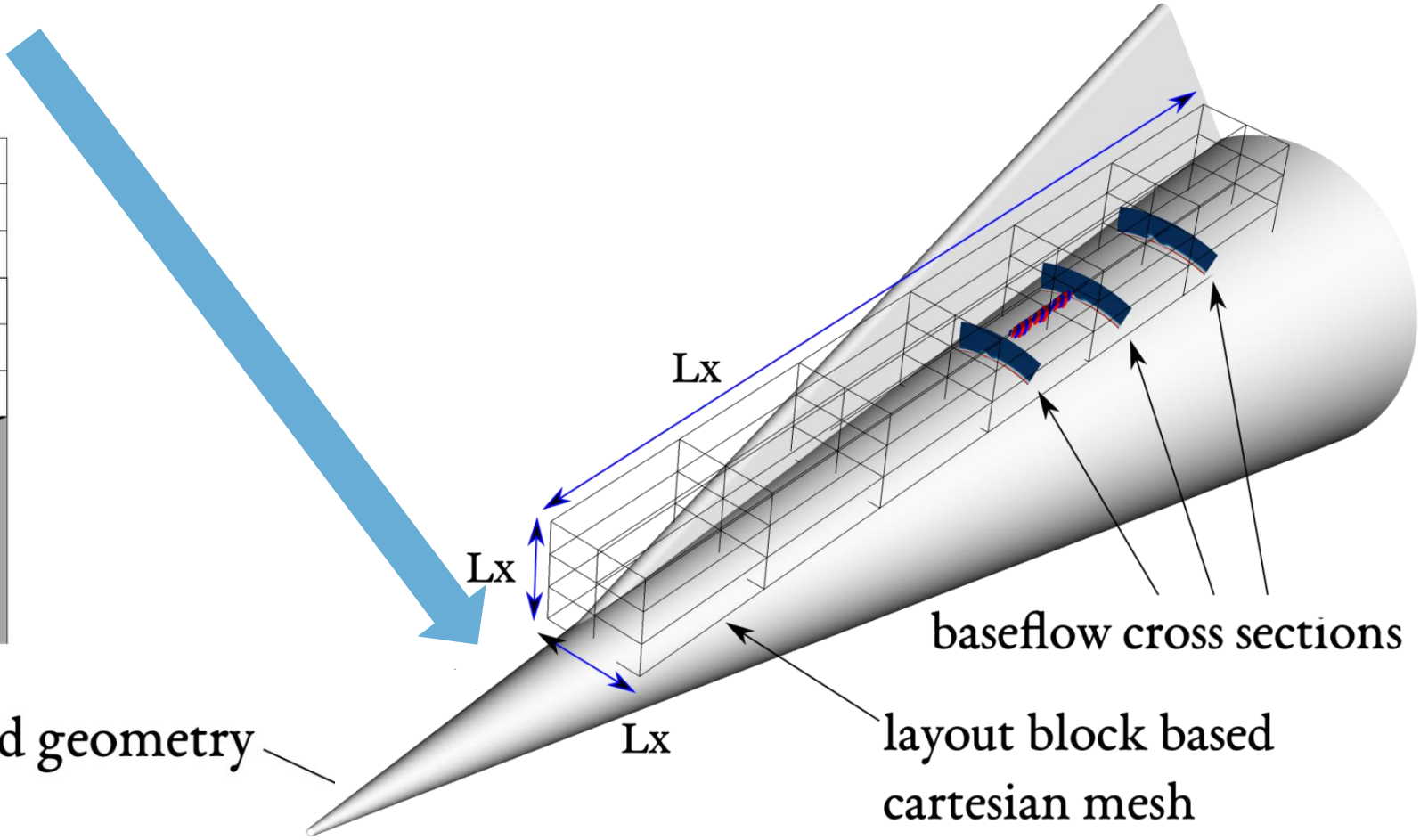
SIMULATION STRATEGY: AMR & IBM



SIMULATION STRATEGY: AMR & IBM

- Geometry is treated as an Immersed Boundary and placed in a cartesian box

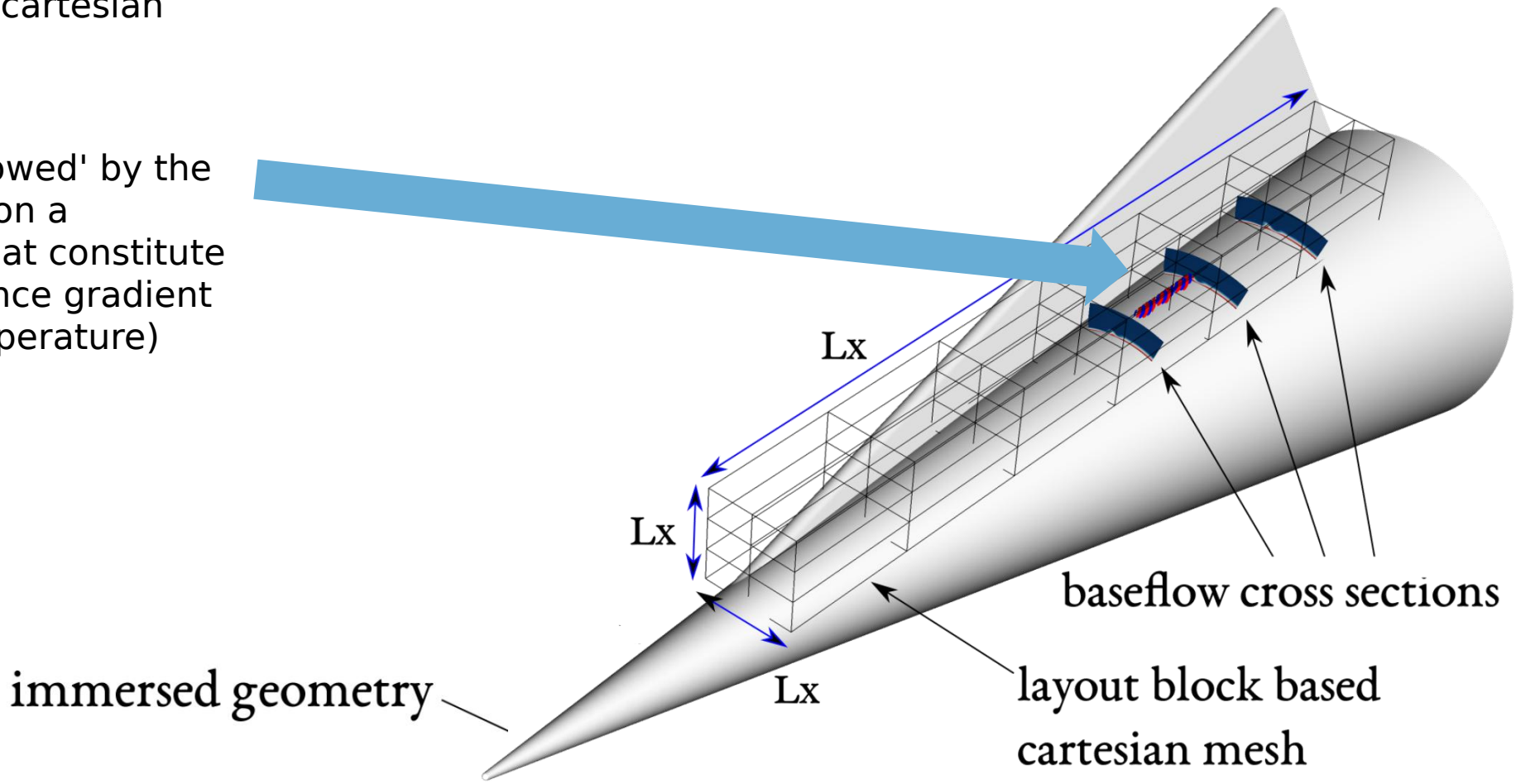




SIMULATION STRATEGY: AMR & IBM

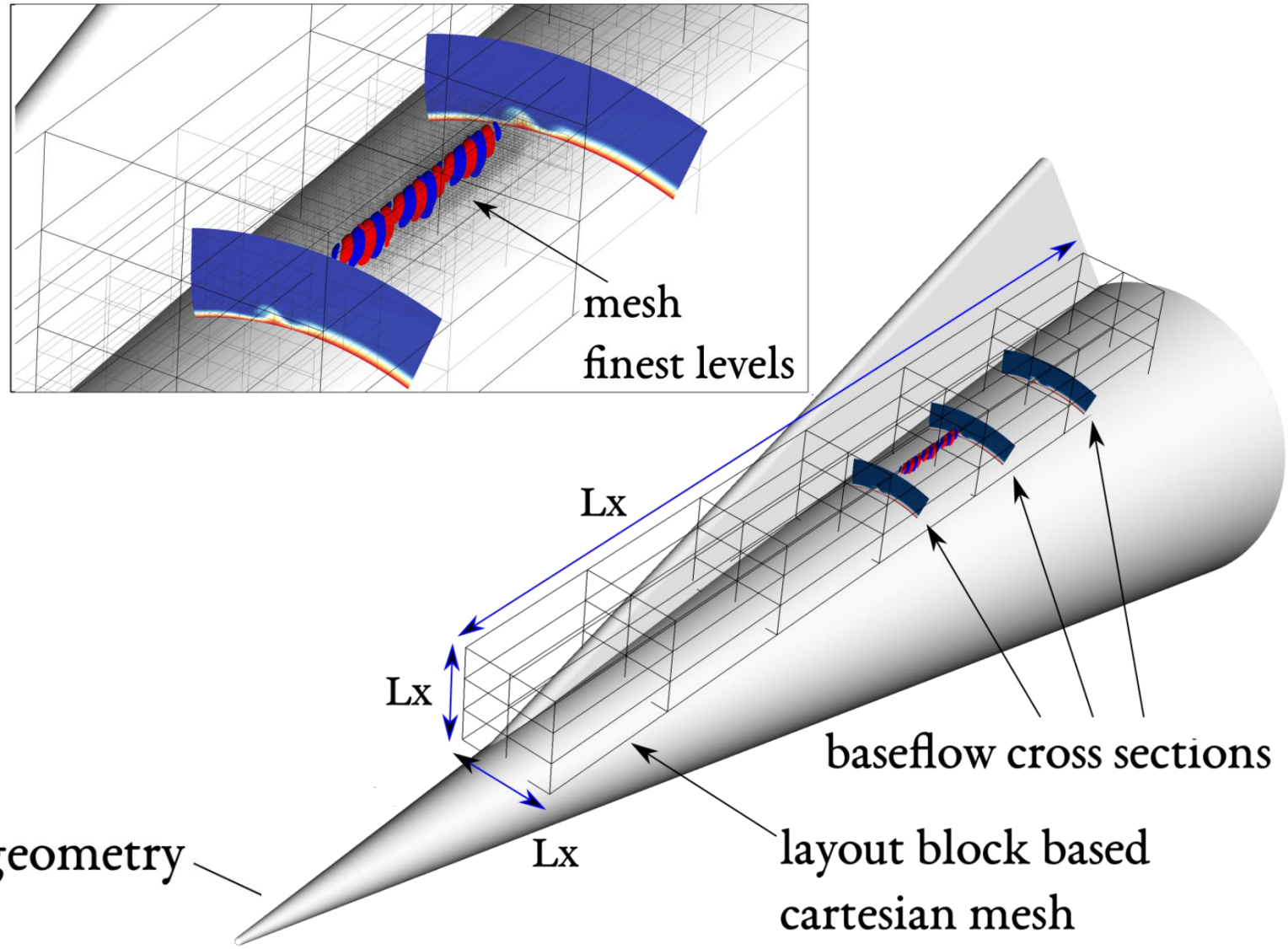
- Geometry is treated as an Immersed Boundary and placed in a cartesian box

- The disturbances are 'followed' by the tracking algorithm based on a 'mixture' of parameters that constitute tracking criteria (for instance gradient of pressure, vorticity, temperature)

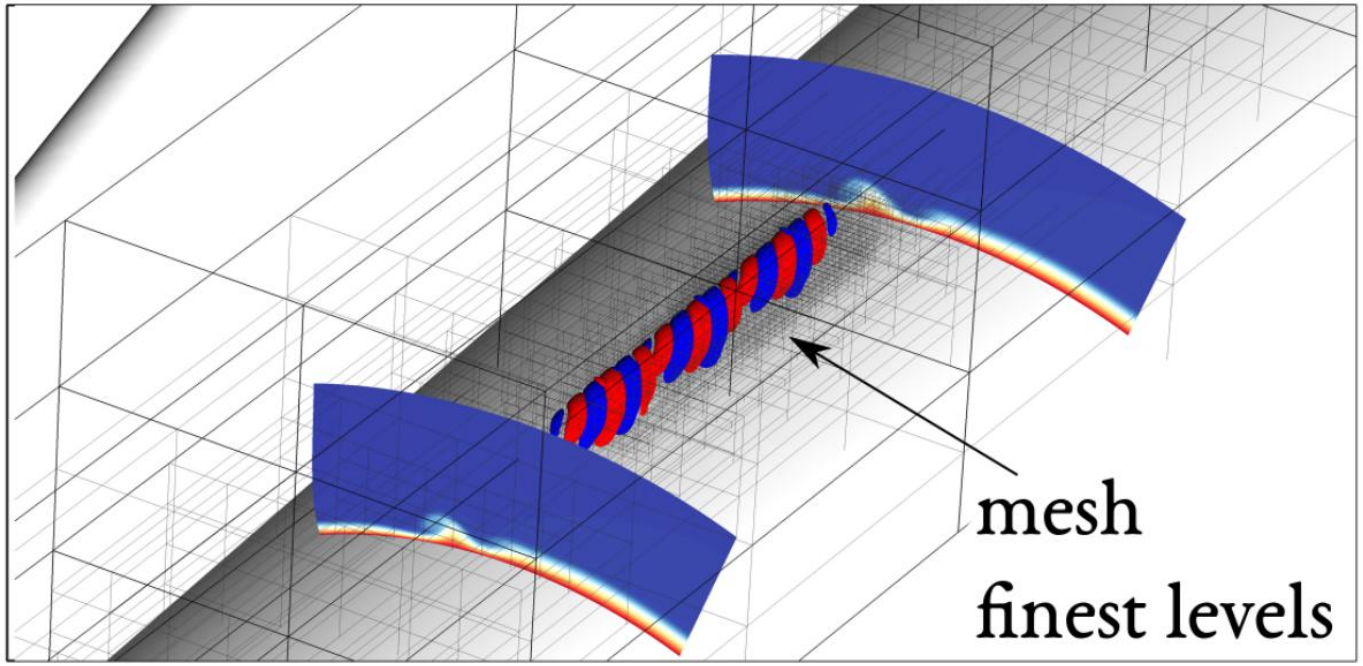


SIMULATION STRATEGY: AMR & IBM

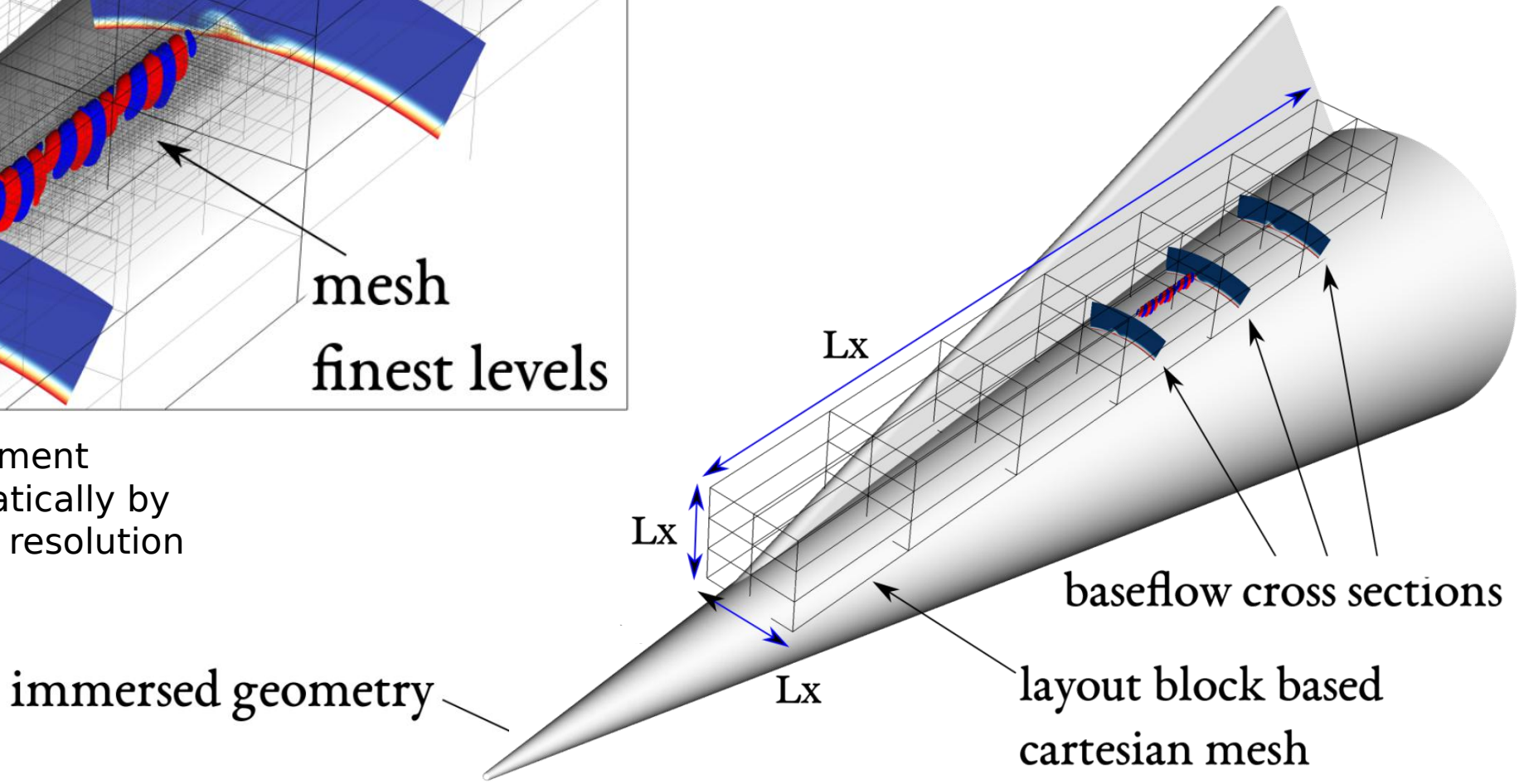
- Geometry is treated as an Immersed Boundary and placed in a cartesian box
- The disturbances are 'followed' by the tracking algorithm based on a 'mixture' of parameters that constitute tracking criteria (for instance gradient of pressure, vorticity, temperature)
- The Adaptive Mesh Refinement algorithm re-mesh automatically by only locally increasing the resolution where required



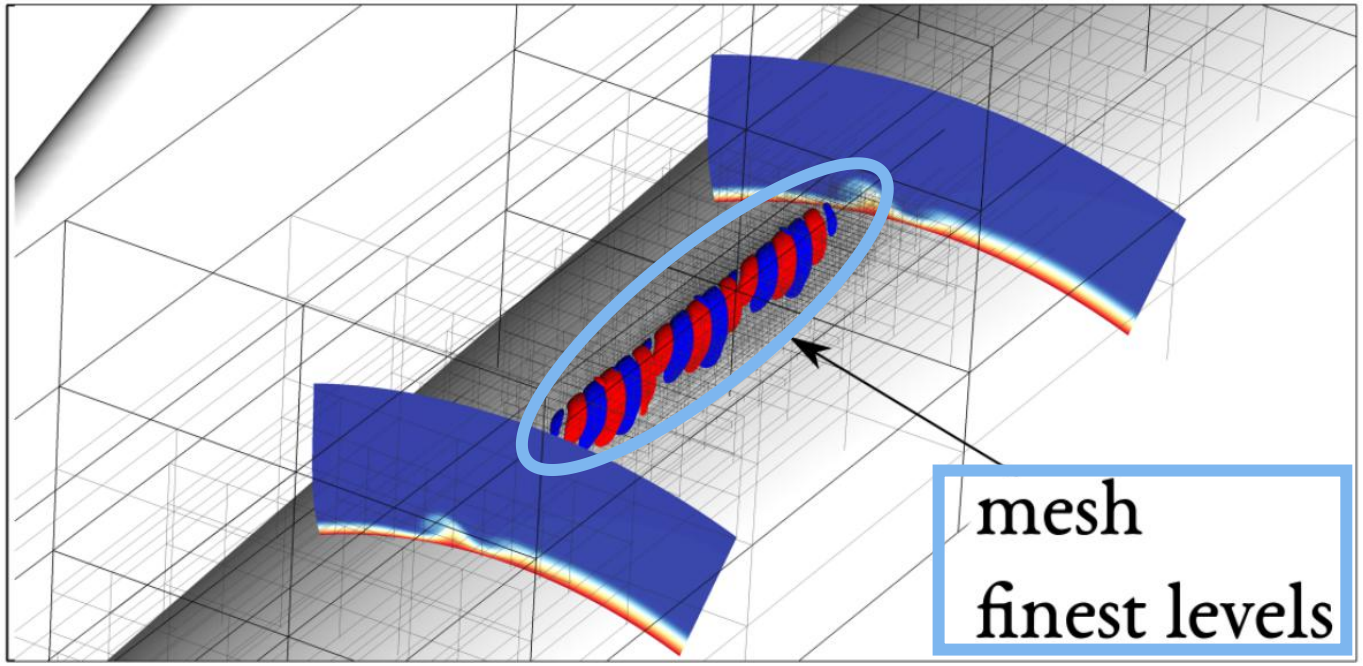
SIMULATION STRATEGY: AMR & IBM



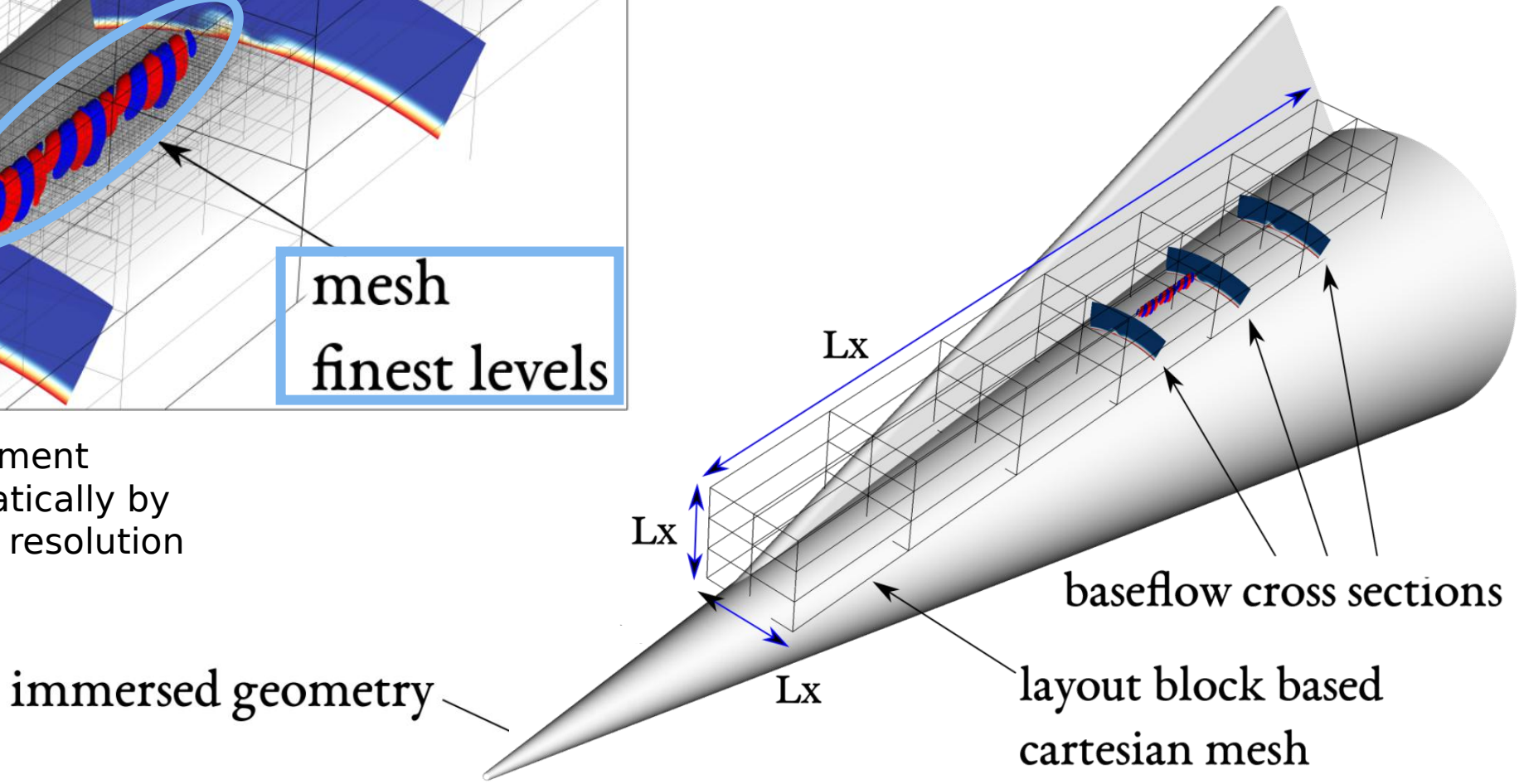
- The Adaptive Mesh Refinement algorithm re-mesh automatically by only locally increasing the resolution where required



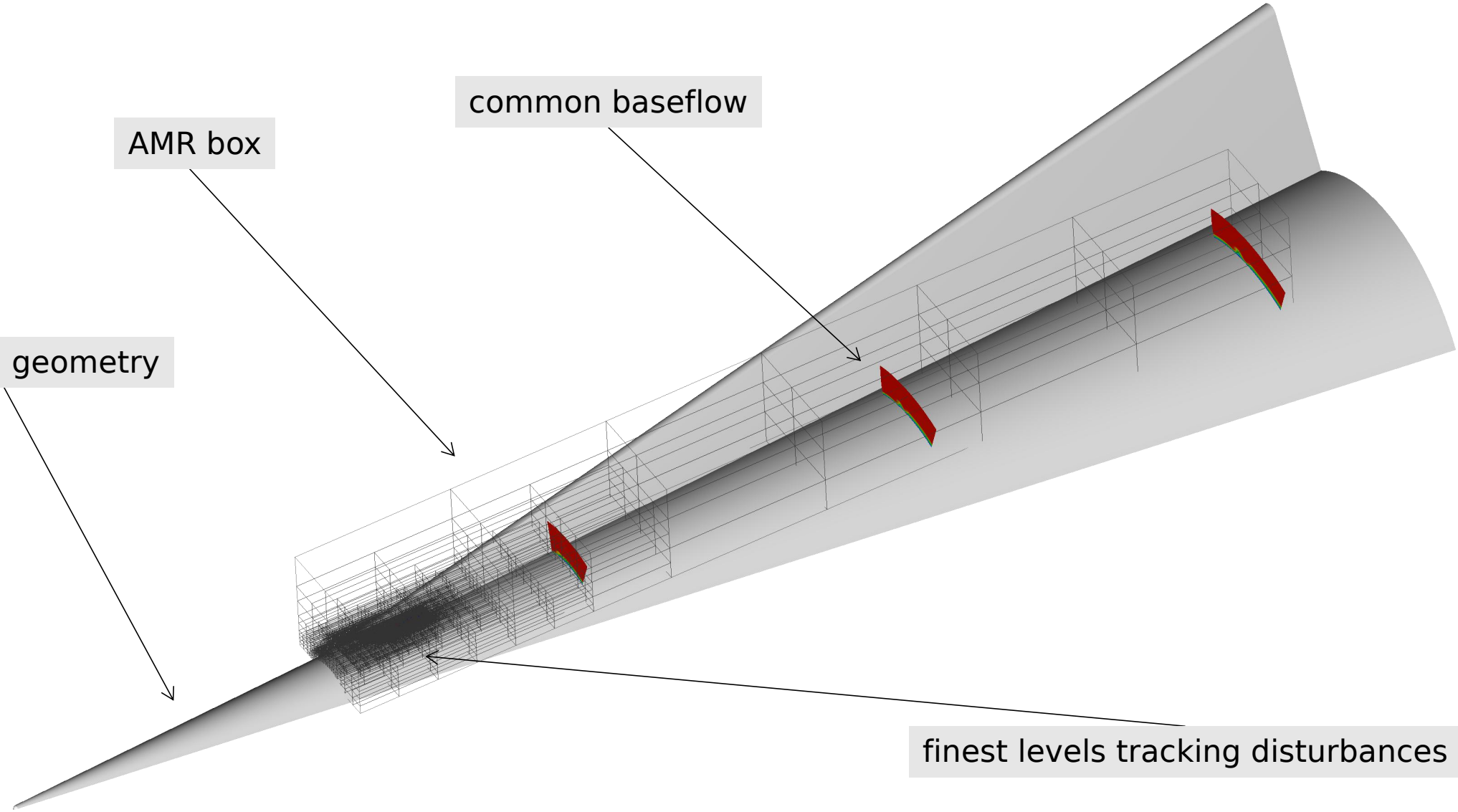
SIMULATION STRATEGY: AMR & IBM



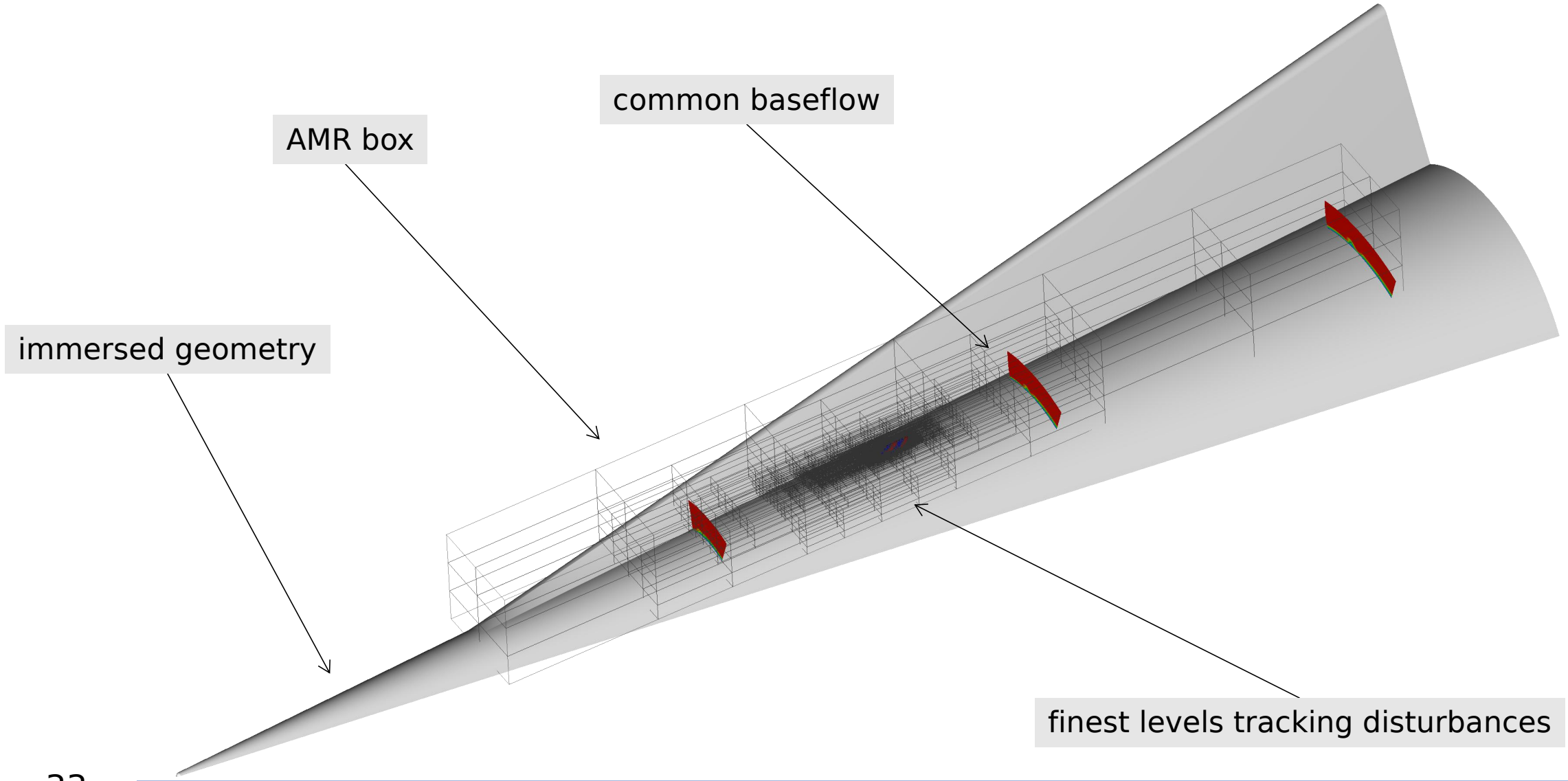
- The Adaptive Mesh Refinement algorithm re-mesh automatically by only locally increasing the resolution where required



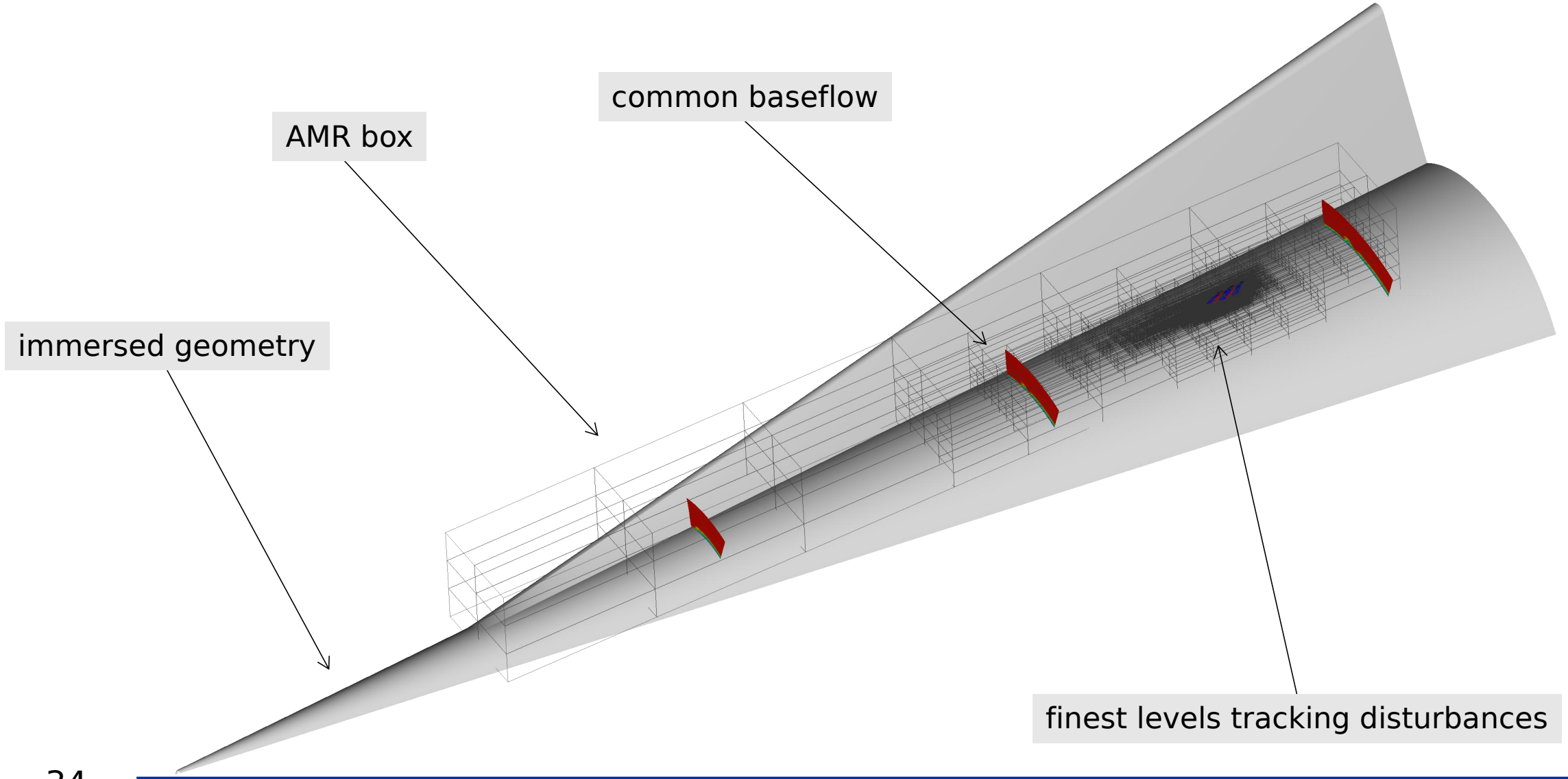
SIMULATION STRATEGY: AMR & IBM



SIMULATION STRATEGY: AMR & IBM



SIMULATION STRATEGY: AMR & IBM



OUTLINE

- Introduction and Research Motivation

On the relevance of Hypersonic Transition

- Computational Approach

Disturbance Flow Formulation, Adaptive Mesh Refinement and Immersed Boundary Method

- Results

Validation, Disturbance Flow Simulations for Complex Geometries and Particle Impingement

- Conclusions and Outlook

Summary of Presented Research and Future Work

OUTLINE

- Introduction and Research Motivation

On the relevance of Hypersonic Transition

- Computational Approach

Disturbance Flow Formulation, Adaptive Mesh Refinement and Immersed Boundary Method

- Results

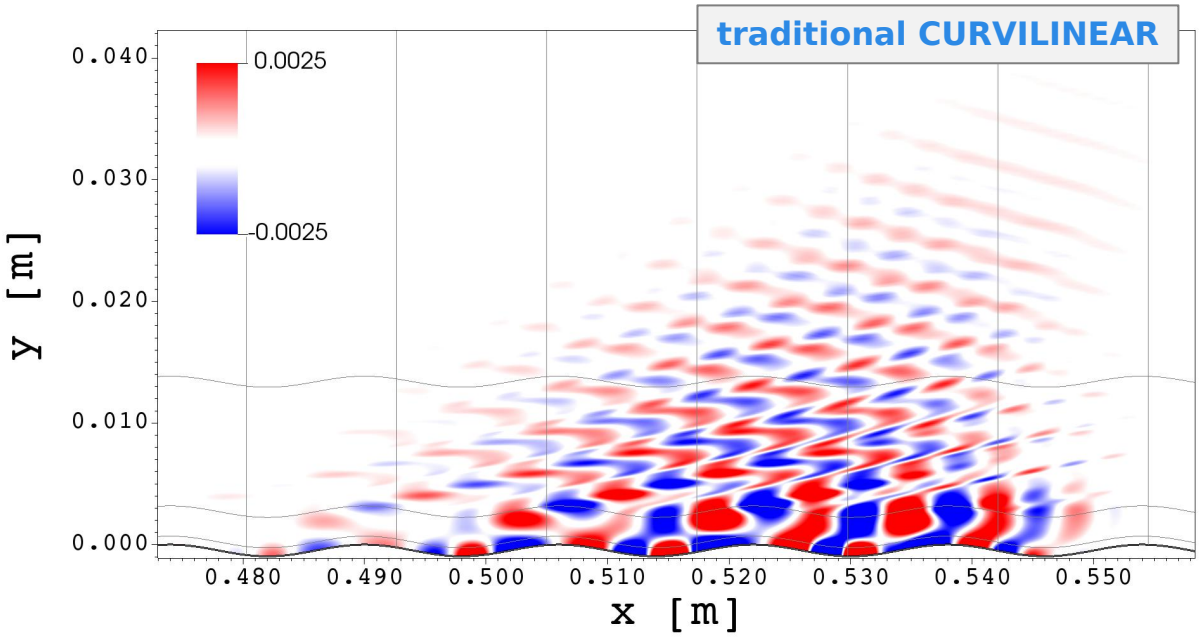
Validation, Disturbance Flow Simulations for Complex Geometries and Particle Impingement

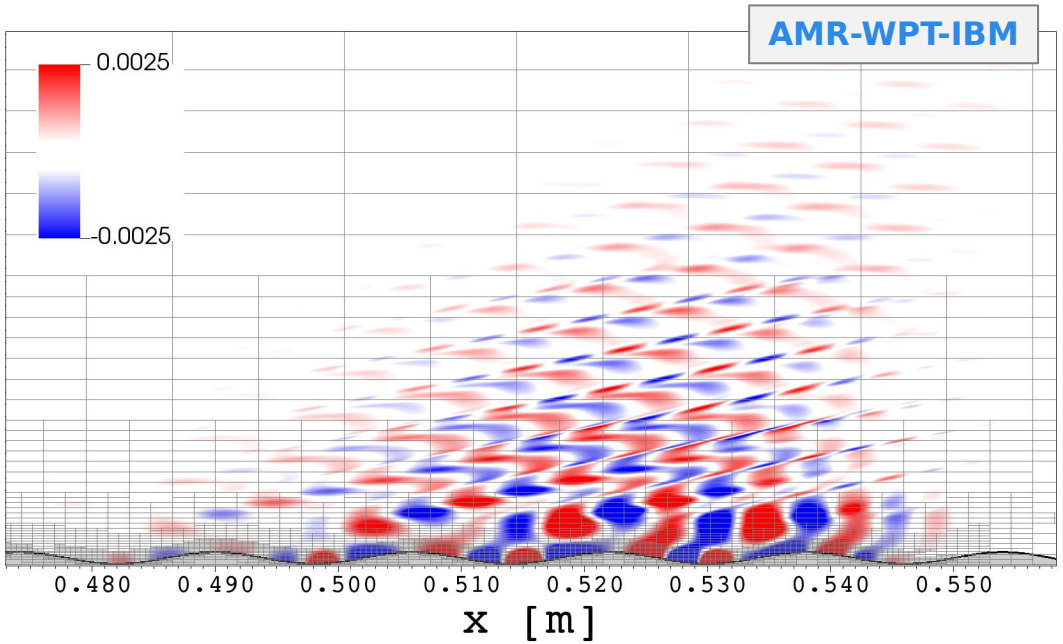
- Conclusions and Outlook

Summary of Presented Research and Future Work

RESULTS: SELECT VALIDATION CASES

Validation case 1: Mach 5.35 planar wavy wall with unit Reynolds number of 14.356 × 10^6 m −1 (free stream temperature 64.316 K and adiabatic wall)

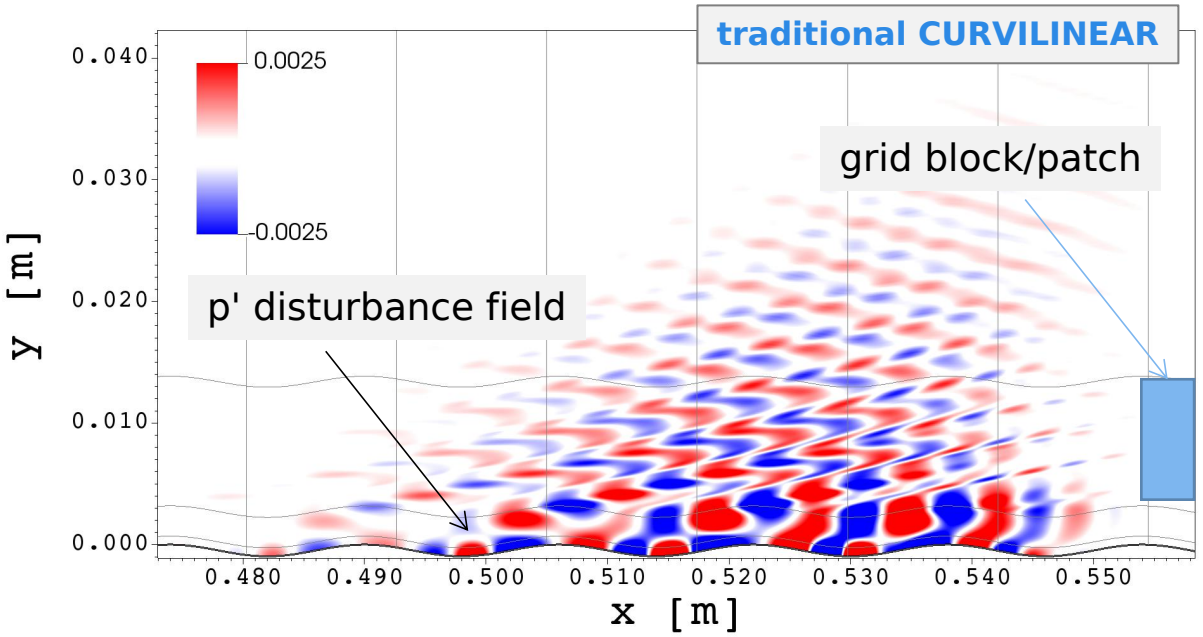


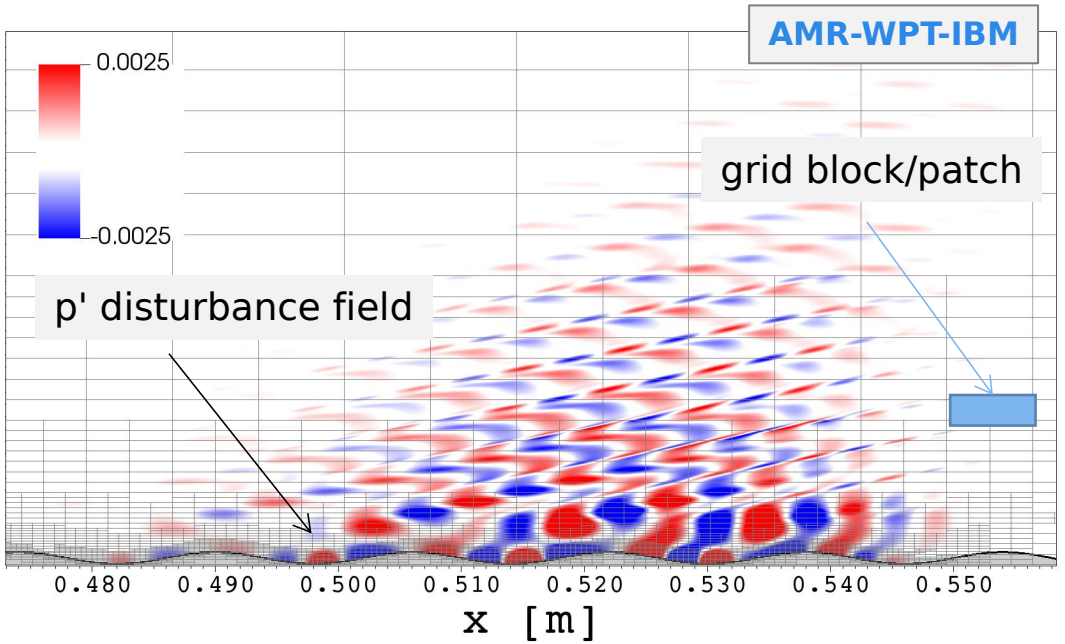


- differences between curvilinear and AMR-WPT-IBM are almost negligible close to the wall
- minor differences can be noticed only away from the wall, where the curvilinear grid stretching is much 'faster' then the cartesian adaptive grid

RESULTS: SELECT VALIDATION CASES

Validation case 1: Mach 5.35 planar wavy wall with unit Reynolds number of 14.356 × 10^6 m −1 (free stream temperature 64.316 K and adiabatic wall)

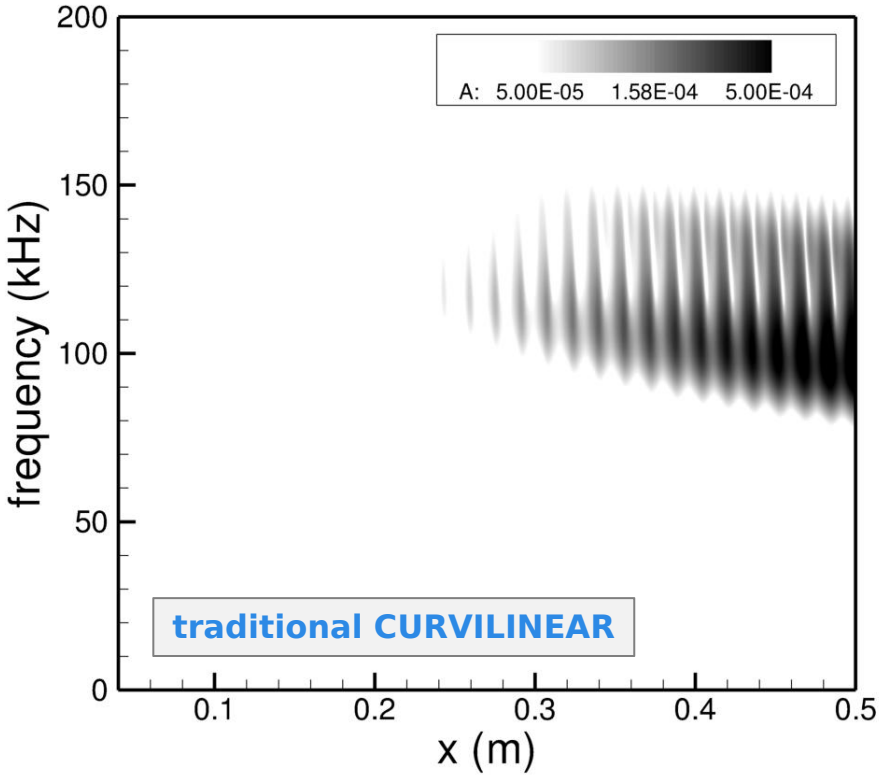


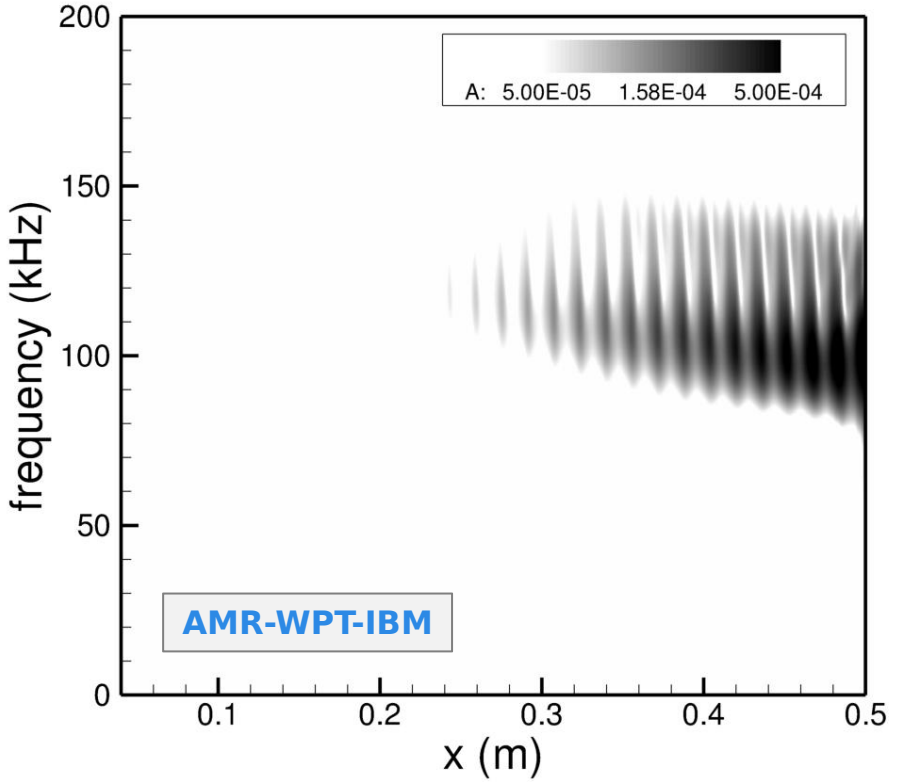


- differences between curvilinear and AMR-WPT-IBM are almost negligible close to the wall
- minor differences can be noticed only away from the wall, where the curvilinear grid stretching is much 'faster' then the cartesian adaptive grid

RESULTS: SELECT VALIDATION CASES

Validation case 1: Mach 5.35 planar wavy wall with unit Reynolds number of 14.356 × 10^6 m −1 (free stream temperature 64.316 K and adiabatic wall)

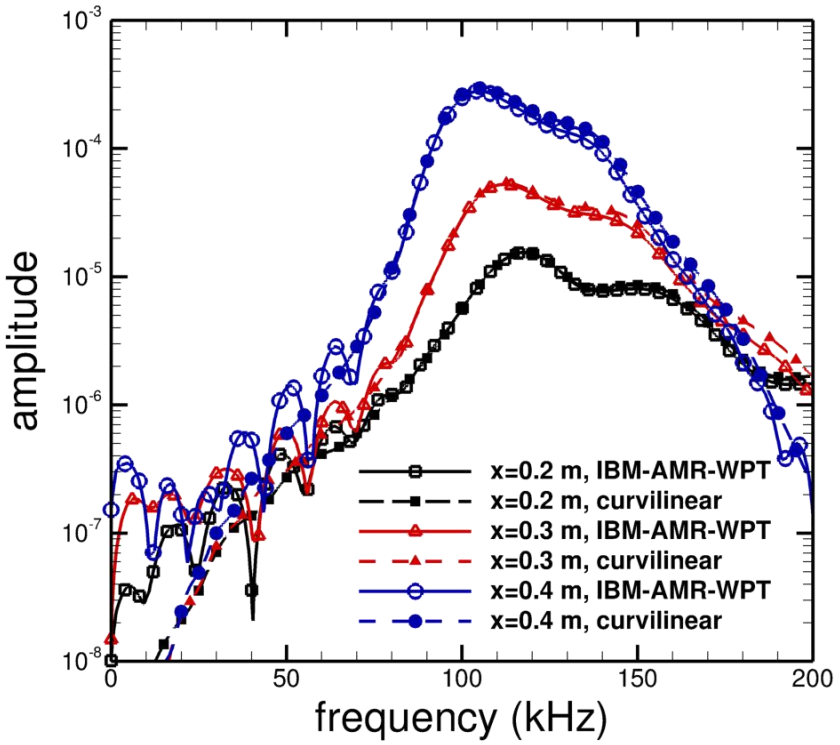


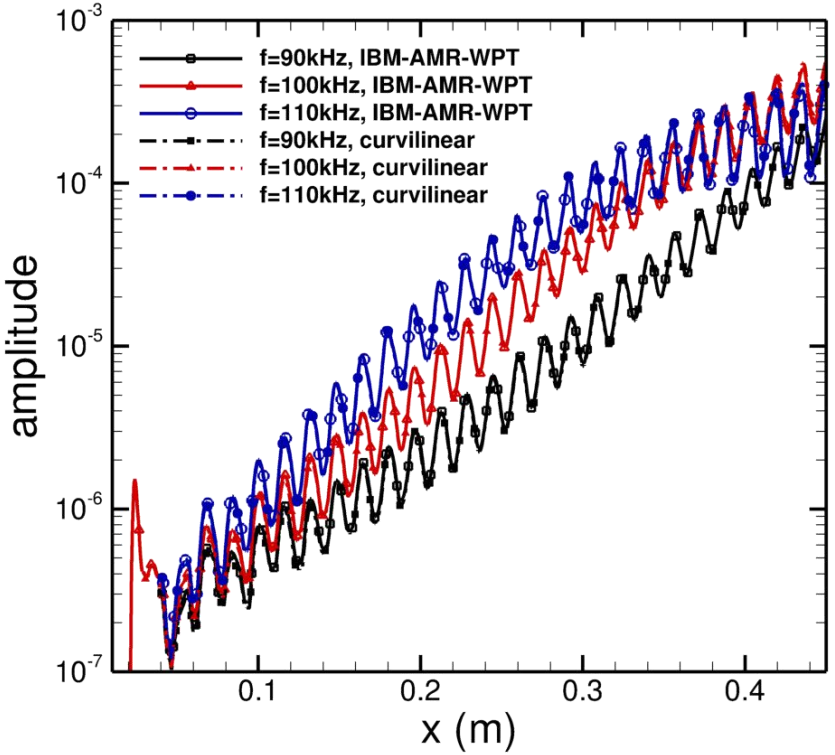


- amplitude diagrams display an almost perfect match
- amplitude curves for different frequencies and at select streamwise location display a good match between curvilinear and AMR-IBM-WPT

RESULTS: SELECT VALIDATION CASES

Validation case 1: Mach 5.35 planar wavy wall with unit Reynolds number of 14.356 × 10^6 m −1 (free stream temperature 64.316 K and adiabatic wall)



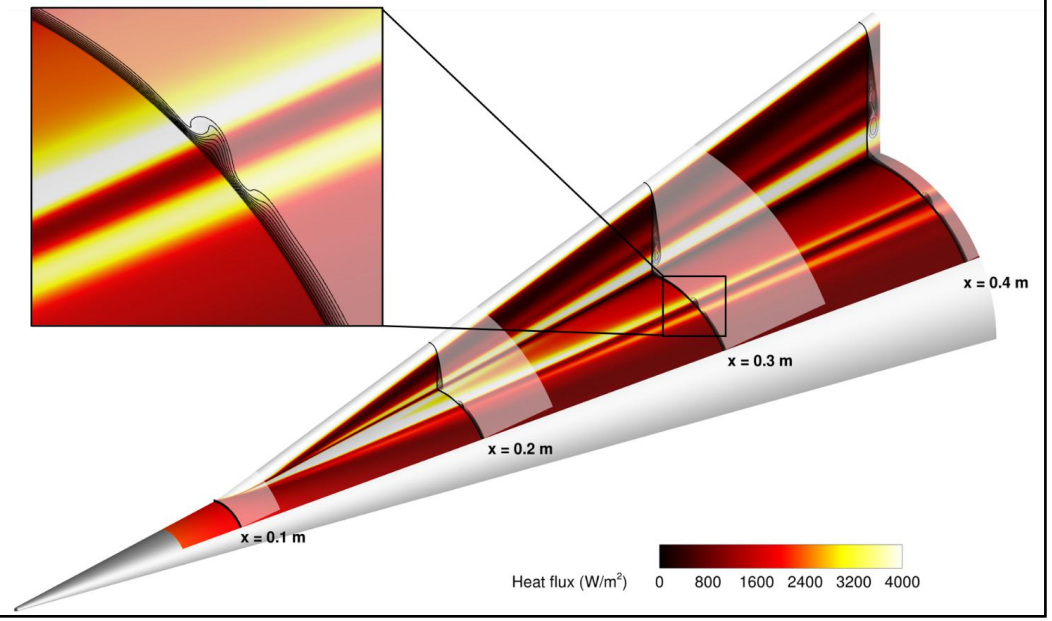


- amplitude diagrams display an almost perfect match
- amplitude curves for different frequencies and at select streamwise location display a good match between curvilinear and AMR-IBM-WPT

RESULTS: SELECT VALIDATION CASES

Validation case 2: BAM6QT finned-cone model (7° cone with 1mm nose and 75° swept fin) at Mach = 6 and Re=8.4e6/m

baseflow surface heat flux — US3D (Araya et al., 2022)



Why this is an important validation case?

1. complex and highly 3D baseflow, which represents a significant challenge and good benchmark for codes

2. classical 1D linear stability methods fail

3. the geometry is a good approximation of realistic hypersonic configurations

4. experimental data is available

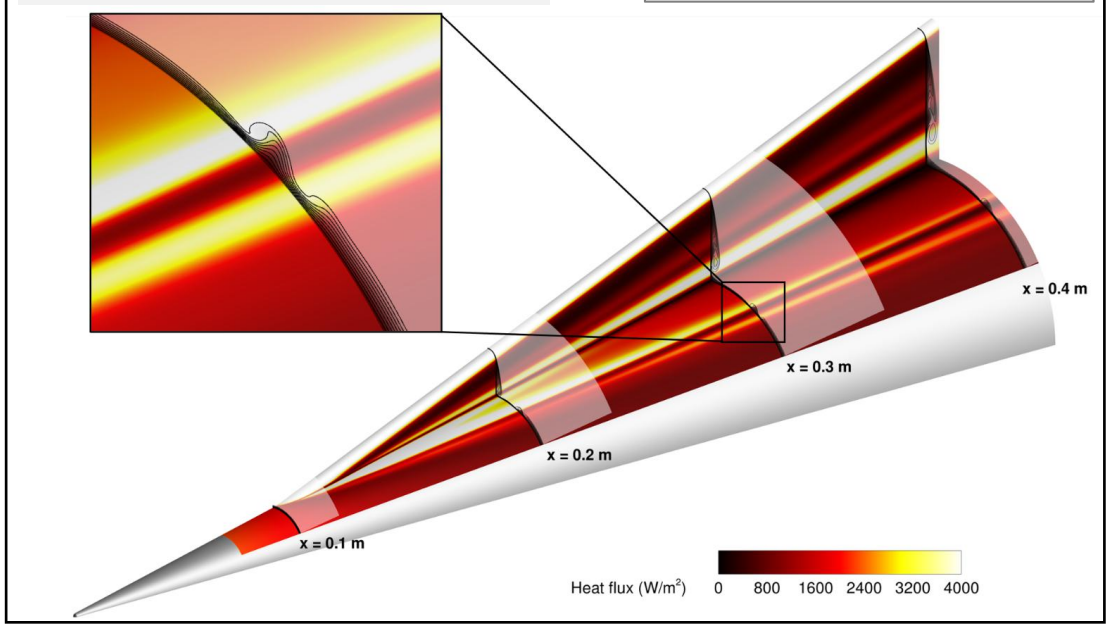
Assessment of linear methods for analysis of boundary layer instabilities on a finned cone at Mach 6, D. B. Araya, N. P. Bitter, B. M. Wheaton., O. Kamal, T. Colonius, A. Knutson, H. Johnson, J. Nichols, G. V. Candler, V. Russo, C. Brehm, AIAA Aviation 2022, National Harbor

- validation results used US3D baseflows (provided by Dr. Araya at JHU-APL and Dr. Knutson at UMN)
- the disturbance field for this configuration is expected to exhibit velocity fluctuations close to the fin with highest amplitudes at frequencies of 247 kHz

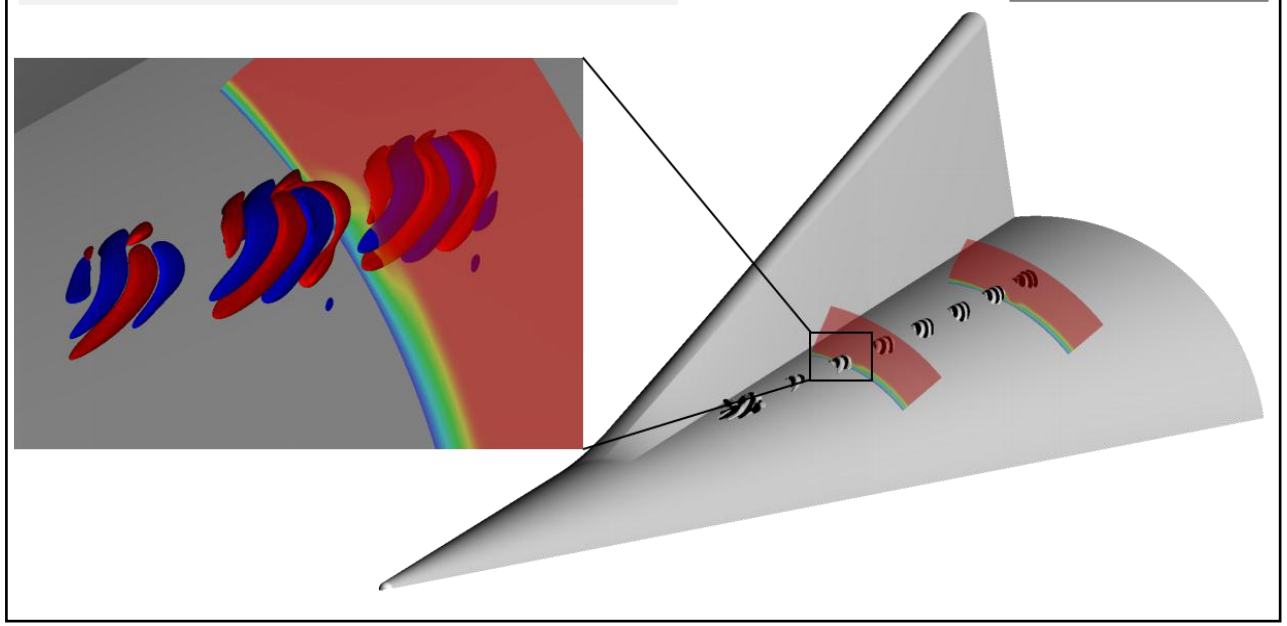
RESULTS: SELECT VALIDATION CASES

Validation case 2: BAM6QT finned-cone model (7° cone with 1mm nose and 75° swept fin) at Mach = 6 and Re=8.4e6/m

baseflow surface heat flux — US3D (Araya et al., 2022)



isovolumes velocity disturbances — AMR-WPT-IBM



Assessment of linear methods for analysis of boundary layer instabilities on a finned cone at Mach 6, D. B. Araya, N. P. Bitter, B. M. Wheaton., O. Kamal, T. Colonius, A. Knutson, H. Johnson, J. Nichols, G. V. Candler, V. Russo, C. Brehm, AIAA Aviation 2022, National Harbor

- validation results used US3D baseflows (provided by Dr. Araya at JHU-APL and Dr. Knutson at UMN)
- the disturbance field for this configuration is expected to exhibit velocity fluctuations close to the fin with highest amplitudes at frequencies of 247 kHz

RESULTS: SELECT VALIDATION CASES

Validation case 2: BAM6QT finned-cone model (7° cone with 1mm nose and 75° swept fin) at Mach = 6 and Re=8.4e6/m

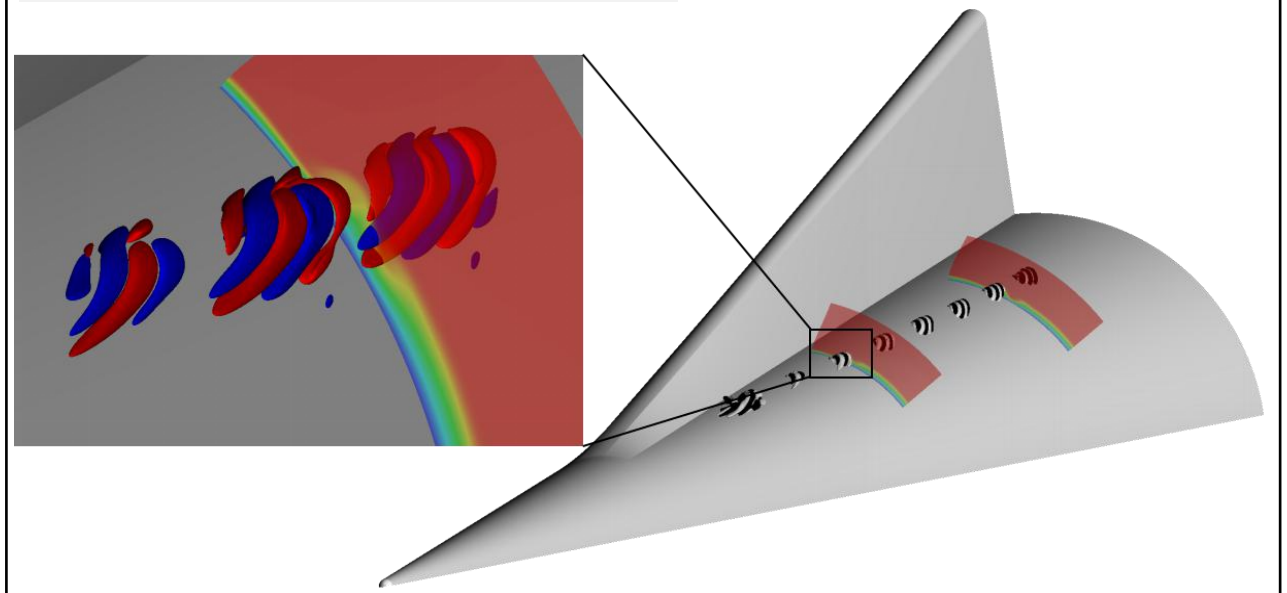
Which instability mechanism will be them main focus of validation and/or code to code comparison?

1. a vortical mode is predicted by PSE as the disturbance with large N-factors showing in proximity of the laminar vortex detached from the swept fin

2. eigenfunctions shapes and N-factors for this specific instability wave will be compared with other codes

isovolumes velocity disturbances

AMR-WPT-IBM

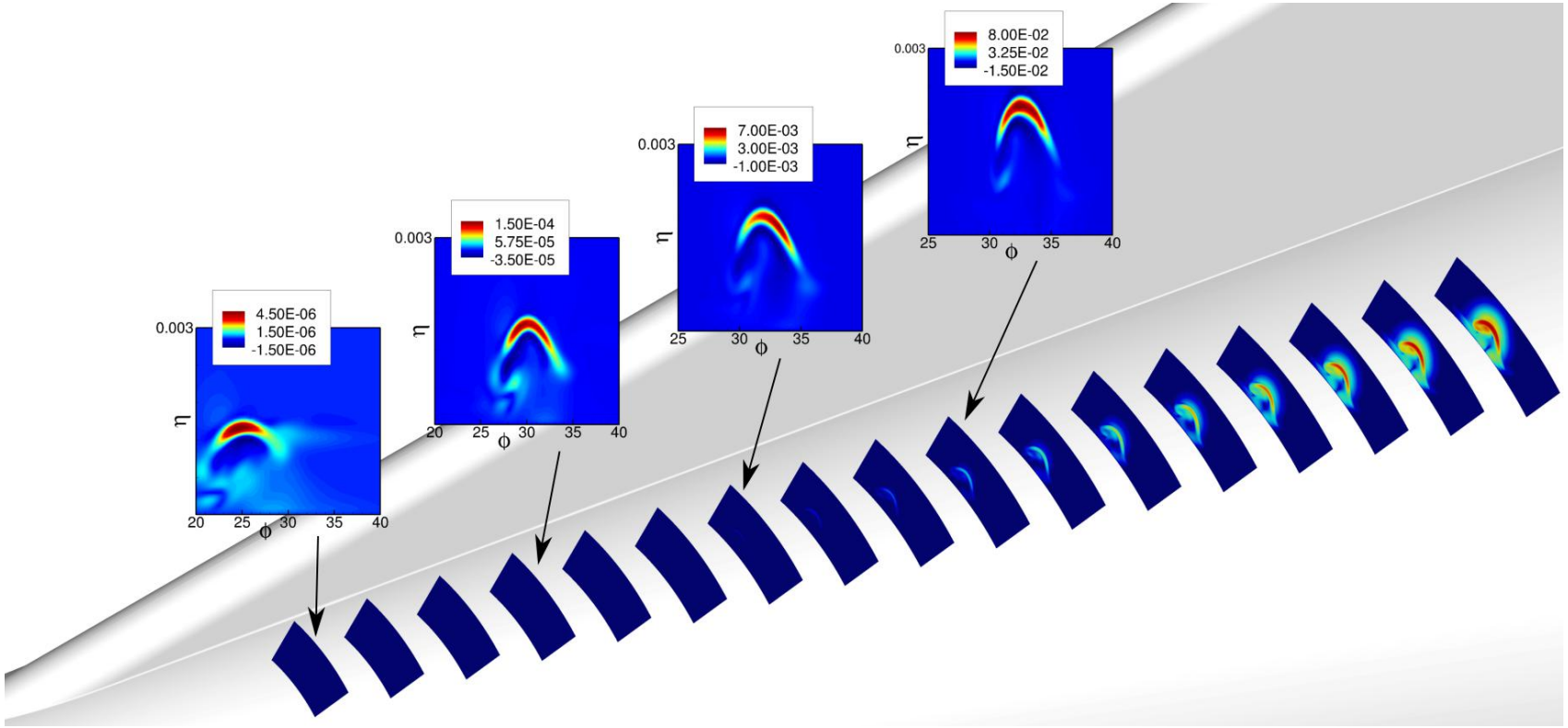


Assessment of linear methods for analysis of boundary layer instabilities on a finned cone at Mach 6, D. B. Araya, N. P. Bitter, B. M. Wheaton., O. Kamal, T. Colonius, A. Knutson, H. Johnson, J. Nichols, G. V. Candler, V. Russo, C. Brehm, AIAA Aviation 2022, National Harbor

- validation results used US3D baseflows (provided by Dr. Araya at JHU-APL and Dr. Knutson at UMN)
- the disturbance field for this configuration is expected to exhibit velocity fluctuations close to the fin with highest amplitudes at frequencies of 247 kHz

RESULTS: SELECT VALIDATION CASES

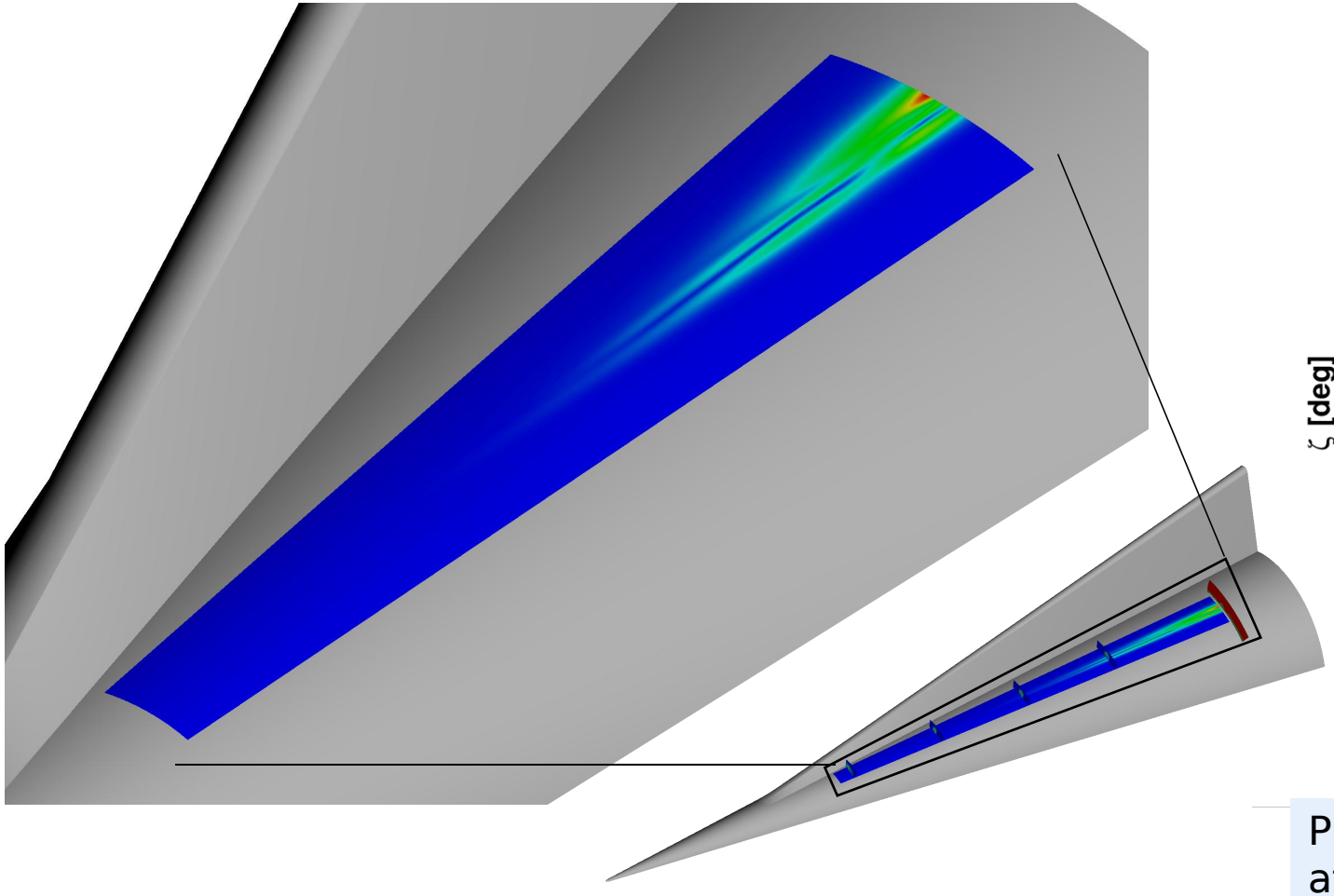
Validation case 2: BAM6QT finned-cone model (7° cone with 1mm nose and 75° swept fin) at Mach = 6 and Re=8.4e6/m

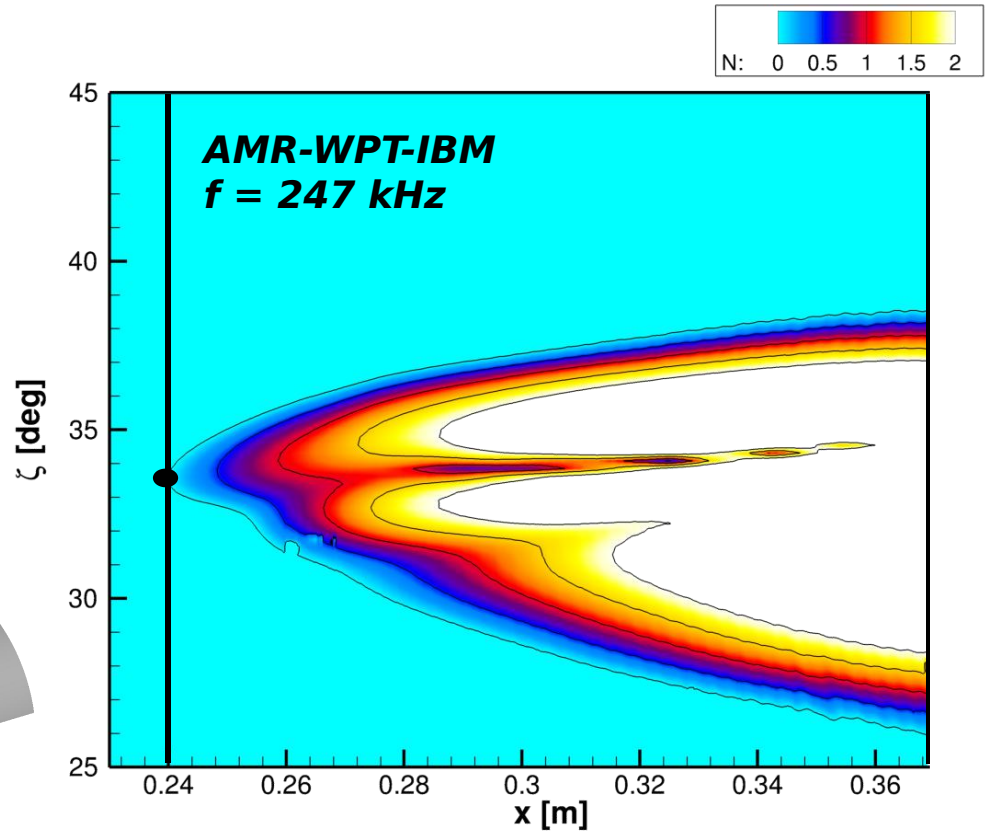


- the disturbance field for this configuration is expected to exhibit velocity fluctuations close to the fin with highest amplitudes at frequencies of 247 kHz
- **results from AMR-WPT-IBM confirm the presence of the aforementioned disturbance waves**

RESULTS: SELECT VALIDATION CASES

Validation case 2: BAM6QT finned-cone model (7° cone with 1mm nose and 75° swept fin) at Mach = 6 and Re=8.4e6/m

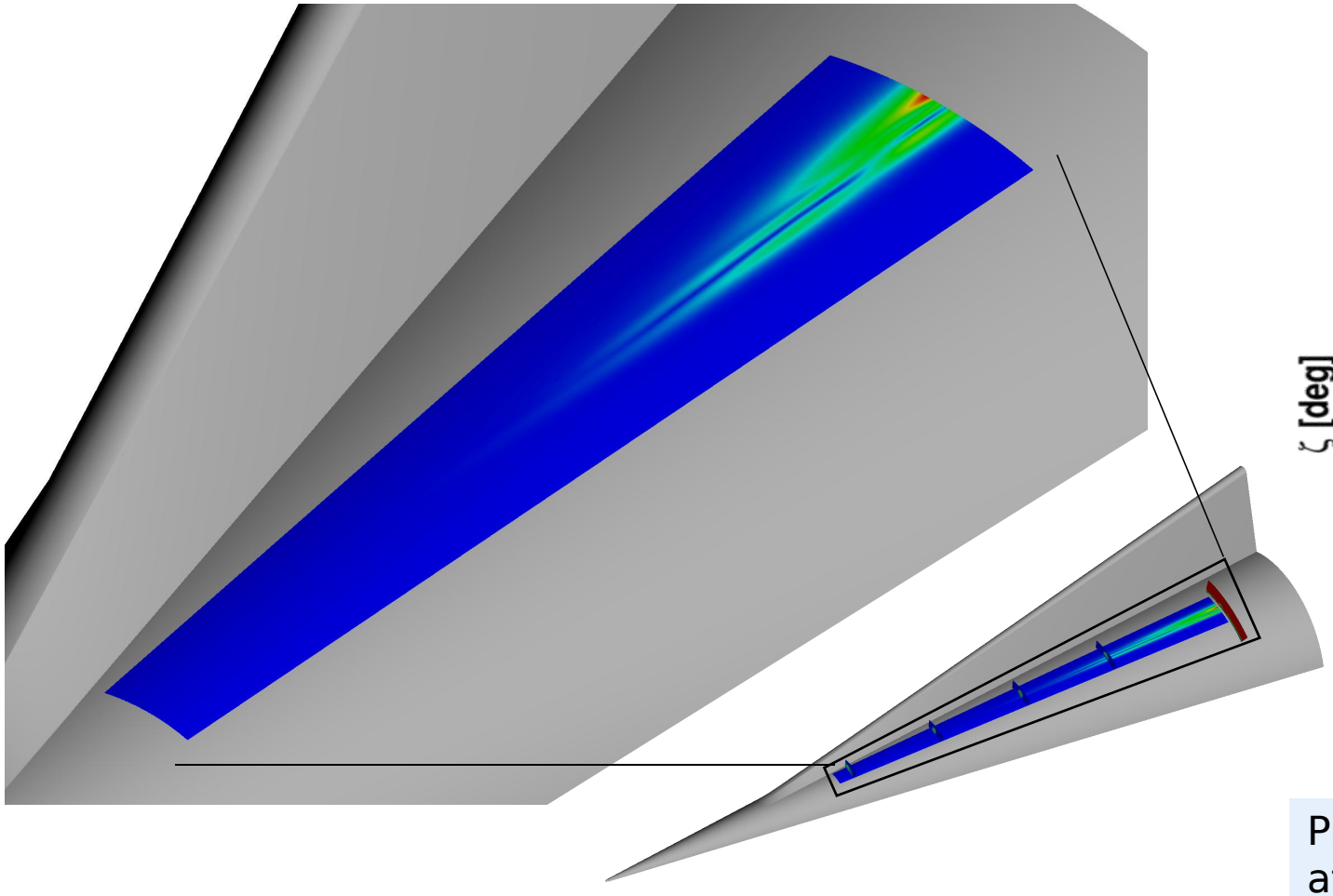


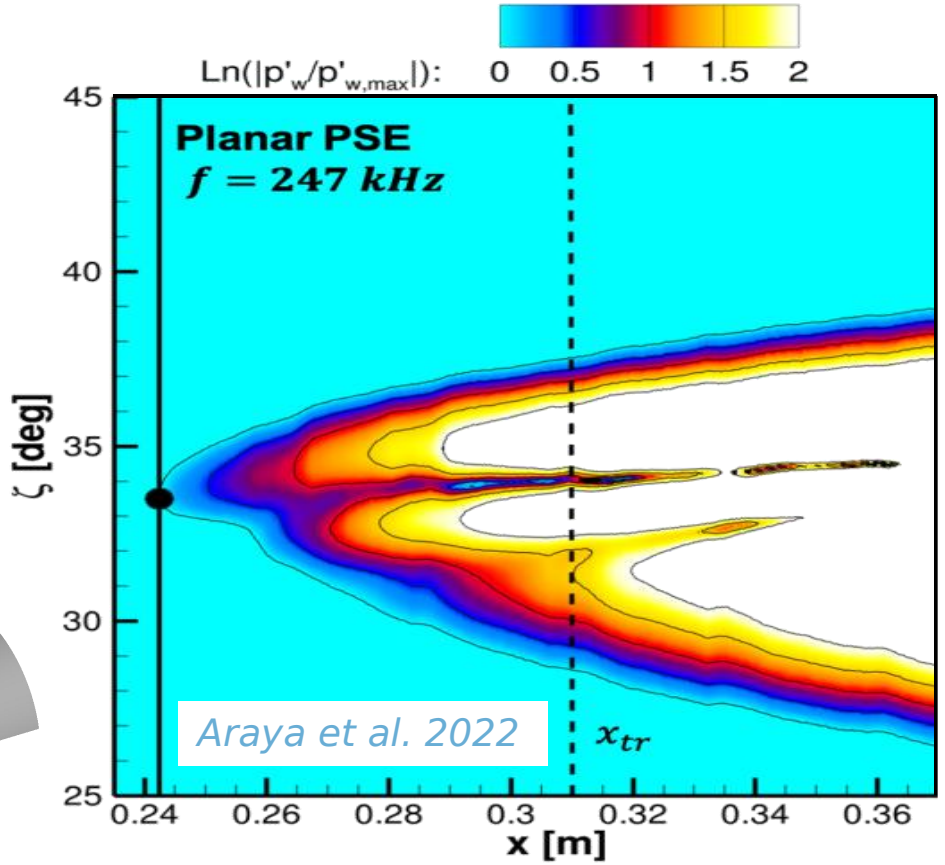


Pressure fluctuations (normalized by local max at x=0.24m (PCB sensor location) on the ground

RESULTS: SELECT VALIDATION CASES

Validation case 2: BAM6QT finned-cone model (7° cone with 1mm nose and 75° swept fin) at Mach = 6 and Re=8.4e6/m

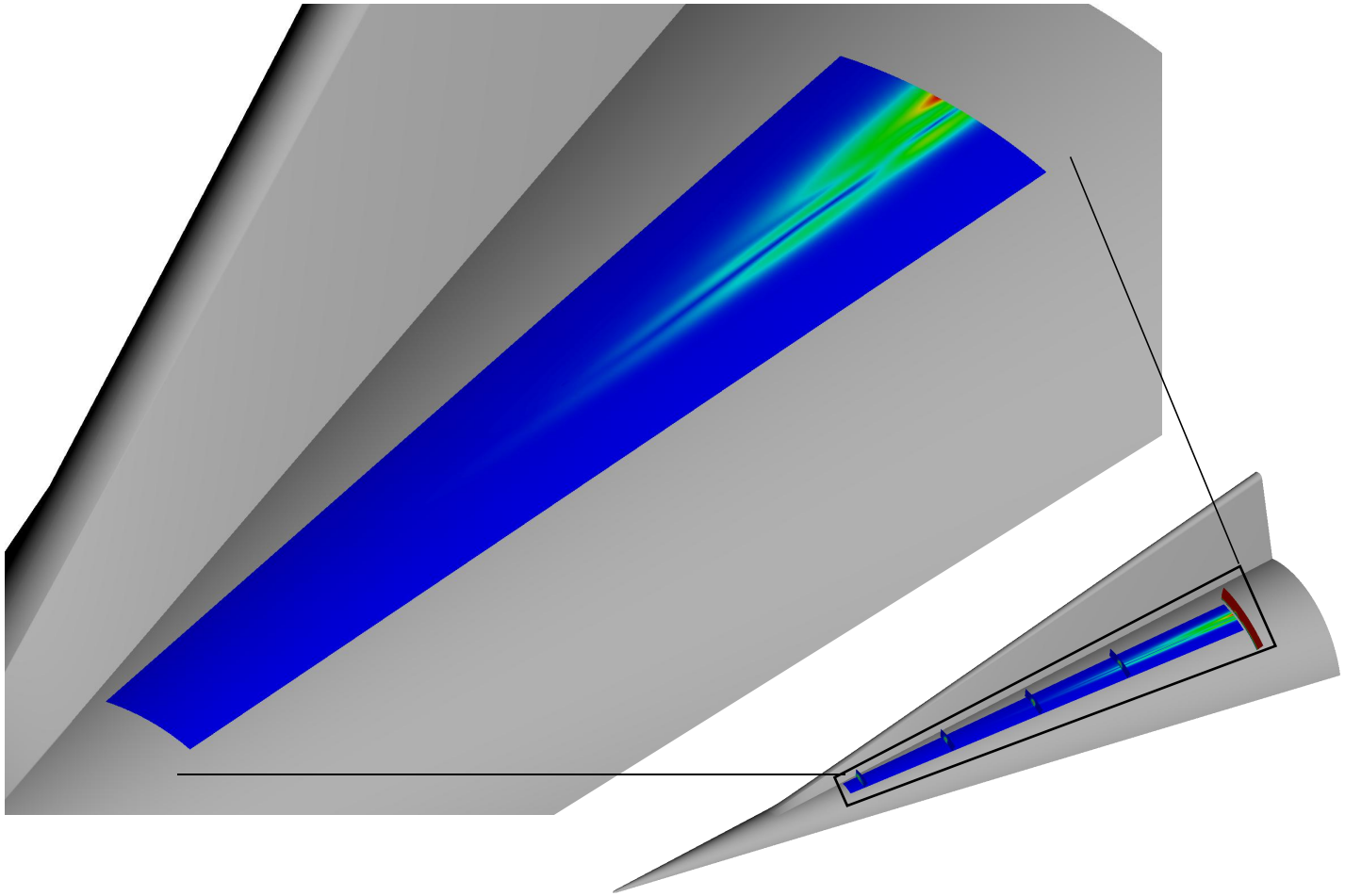


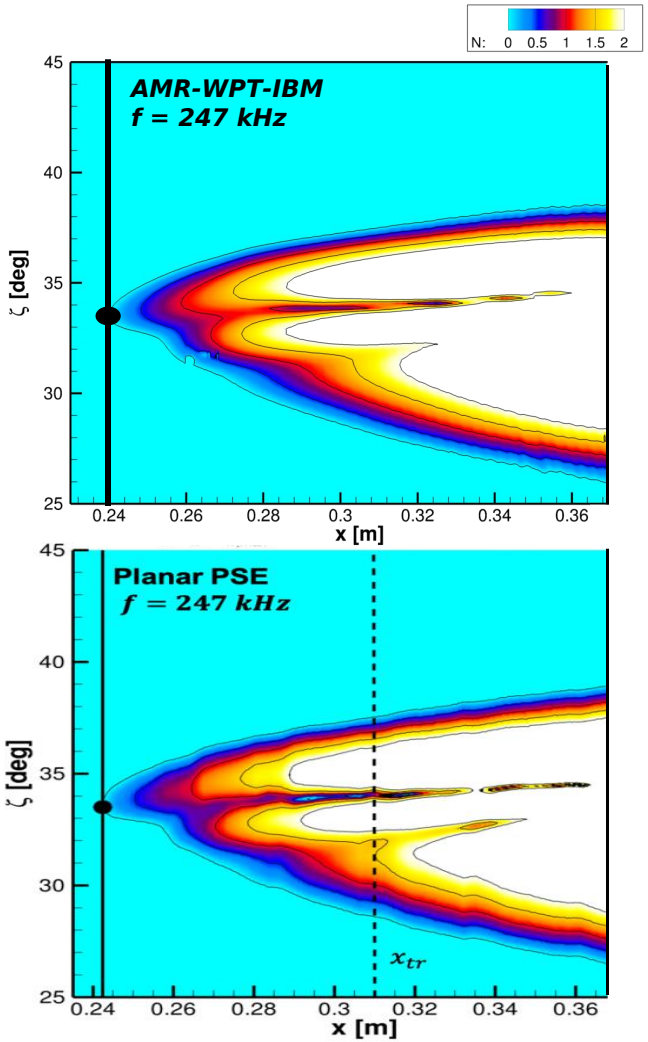


Pressure fluctuations (normalized by local max at x=0.24m (PCB sensor location) on the ground

RESULTS: SELECT VALIDATION CASES

Validation case 2: BAM6QT finned-cone model (7° cone with 1mm nose and 75° swept fin) at Mach = 6 and Re=8.4e6/m



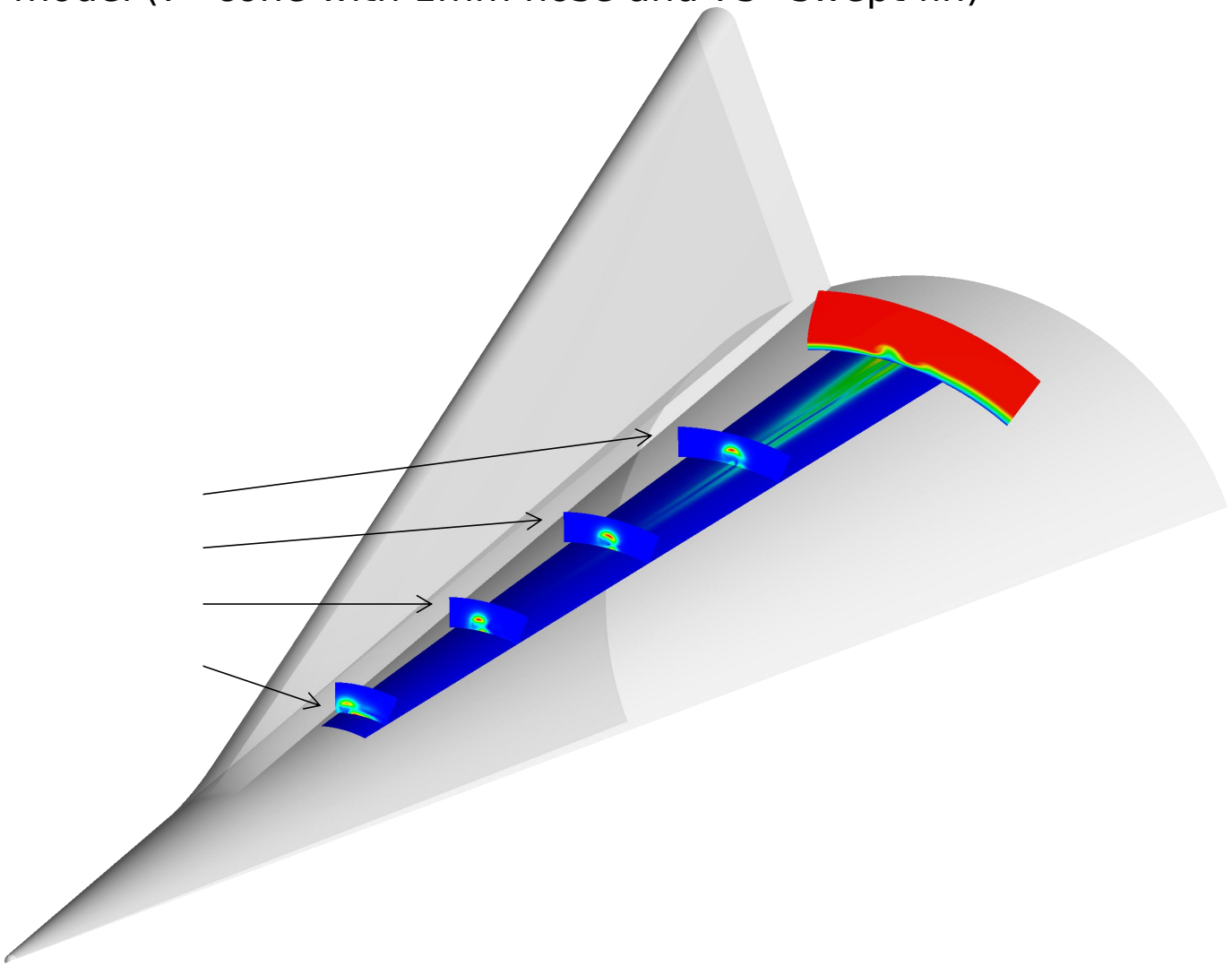


RESULTS: SELECT VALIDATION CASES

Validation case 2: BAM6QT finned-cone model (7° cone with 1mm nose and 75° swept fin) at Mach = 6 and Re=8.4e6/m

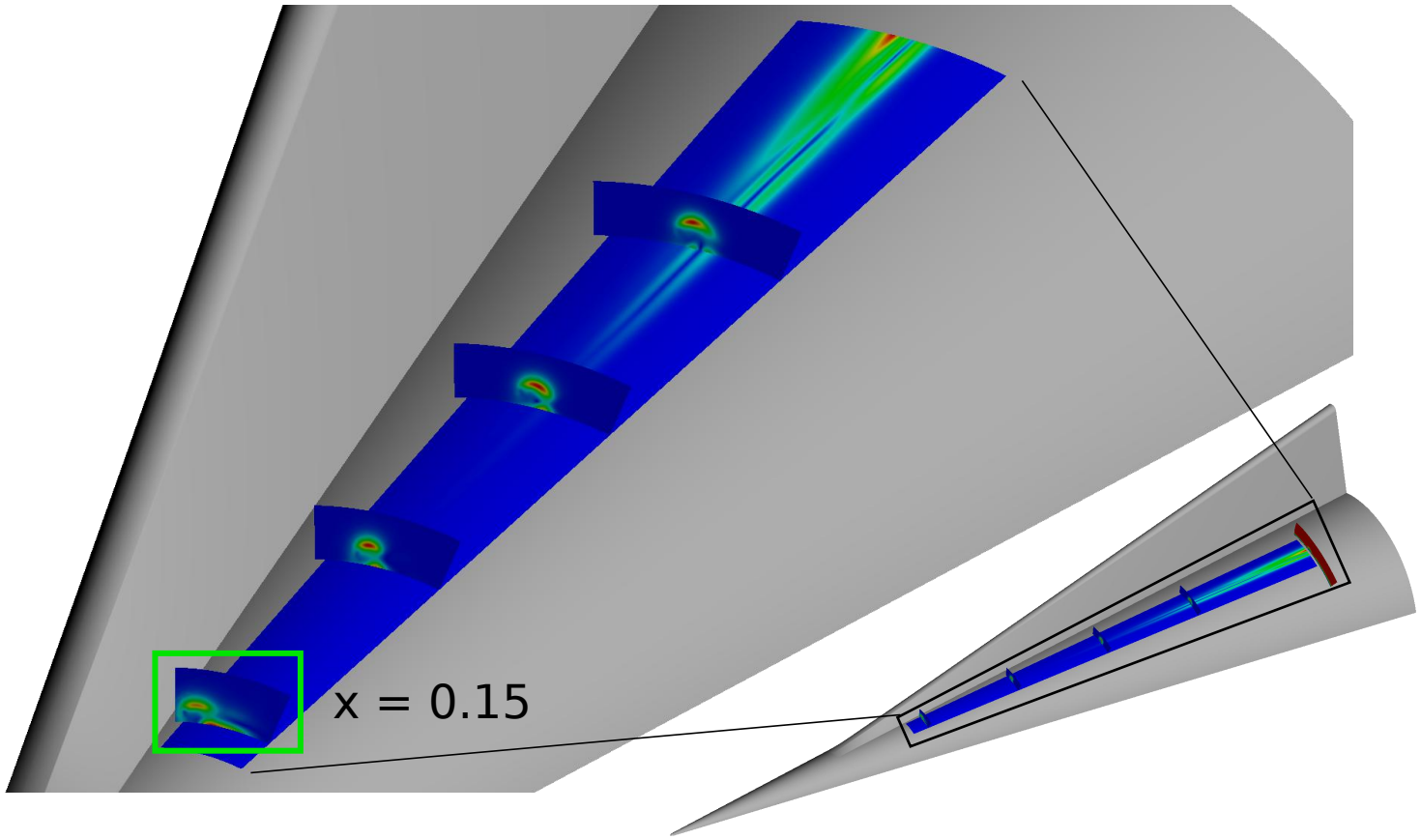
- In order to obtain quantitative comparisons of the DNS calculations and the PSE results, FFT of the point probes was performed on the surface and cross planes

- More specifically, the 4 'chosen' axial locations were *densely* probed/sampled for a thorough comparison of the pressure eigenfunctions with the other methods

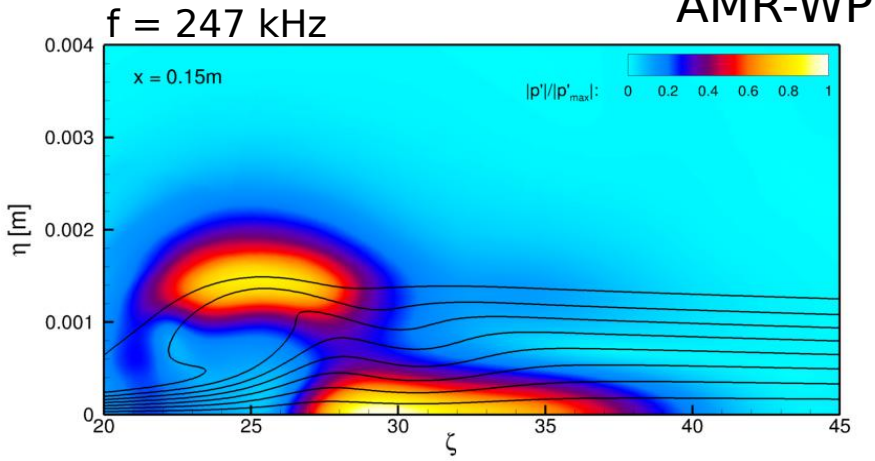


RESULTS: SELECT VALIDATION CASES

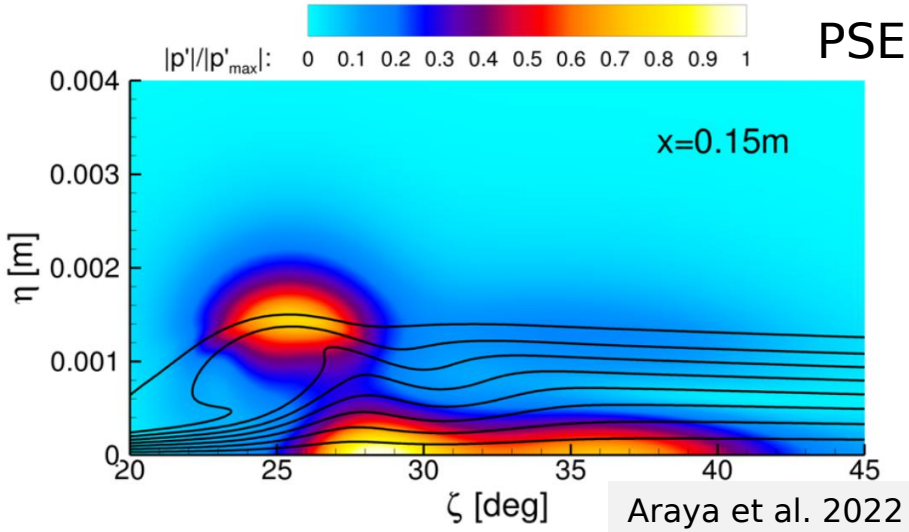
Validation case 2: BAM6QT finned-cone model (7° cone with 1mm nose and 75° swept fin) at Mach = 6 and Re=8.4e6/m



AMR-WPT



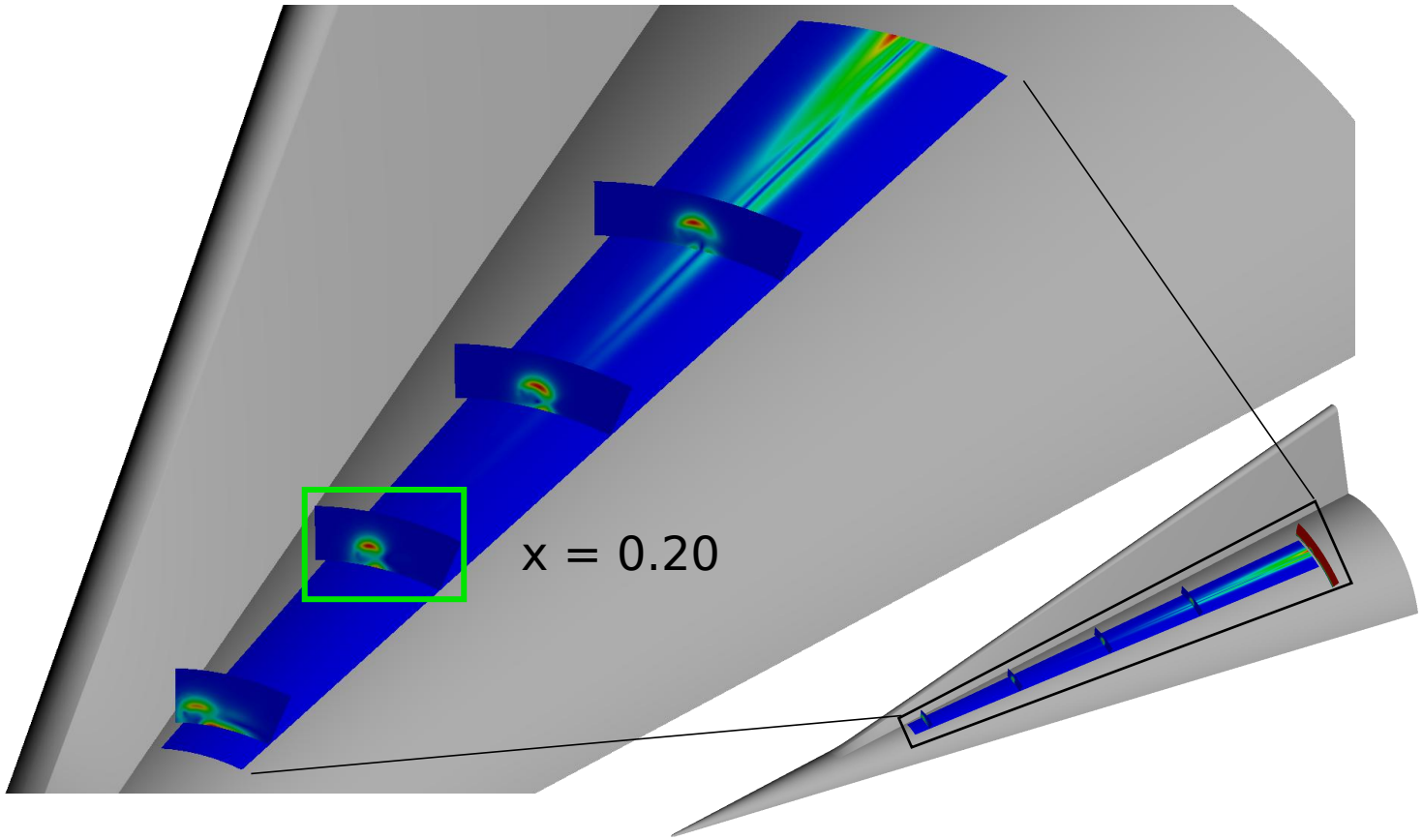
PSE



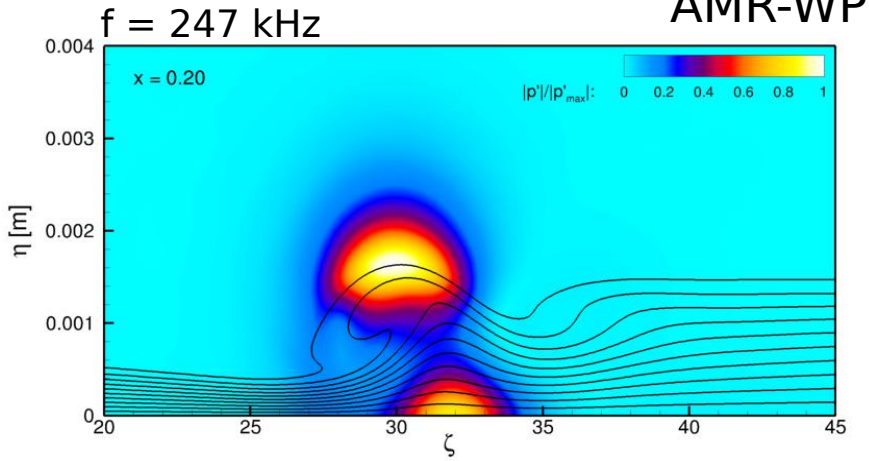
Araya et al. 2022

RESULTS: SELECT VALIDATION CASES

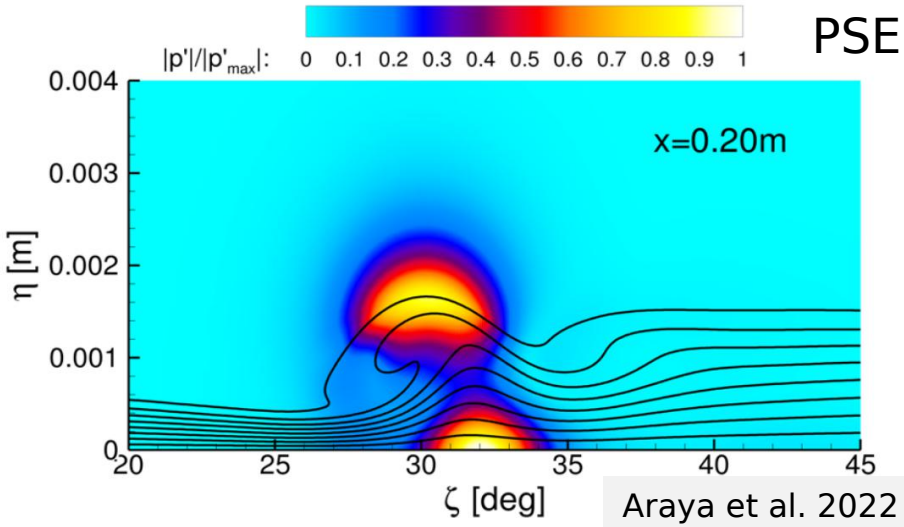
Validation case 2: BAM6QT finned-cone model (7° cone with 1mm nose and 75° swept fin) at Mach = 6 and Re=8.4e6/m



AMR-WPT



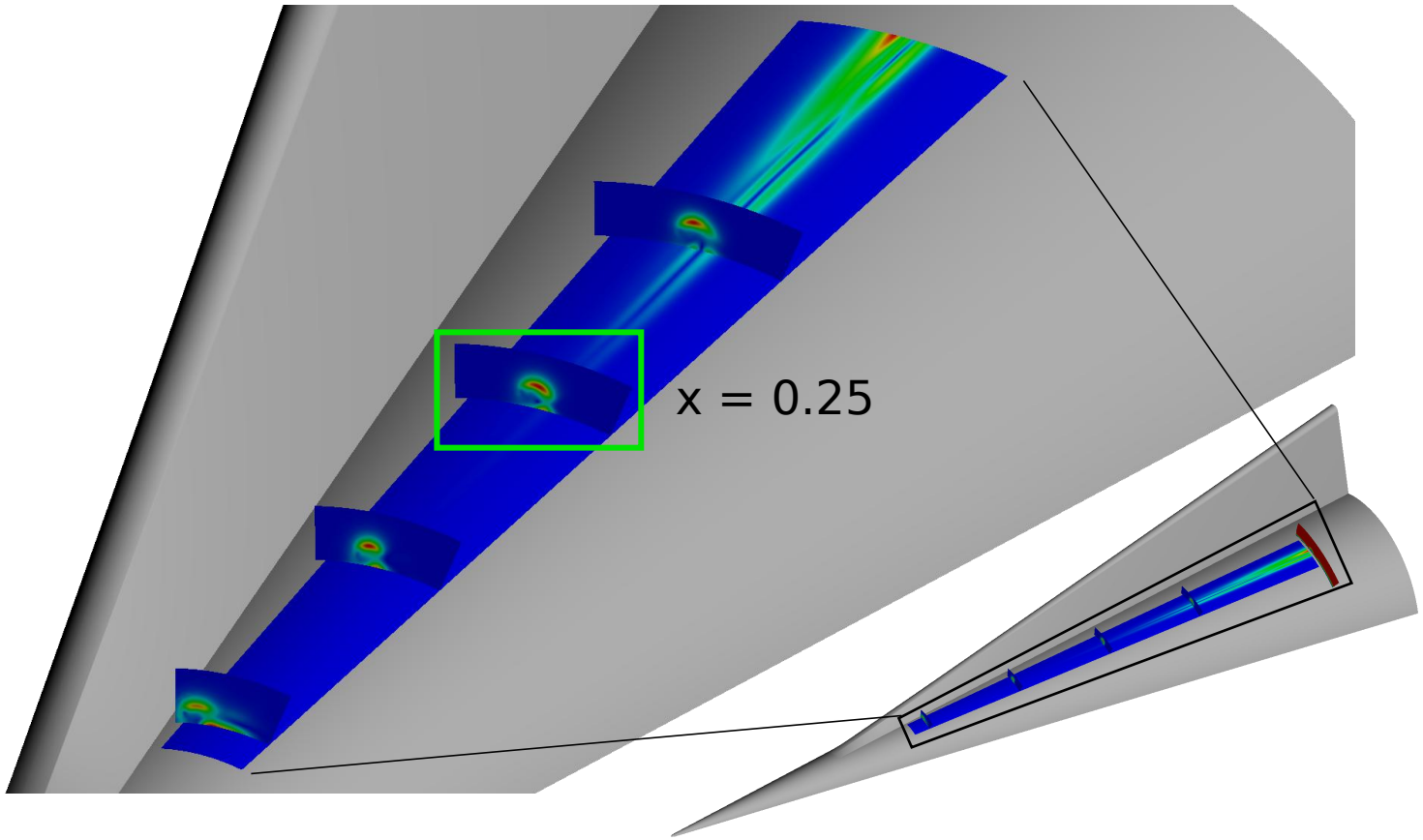
PSE



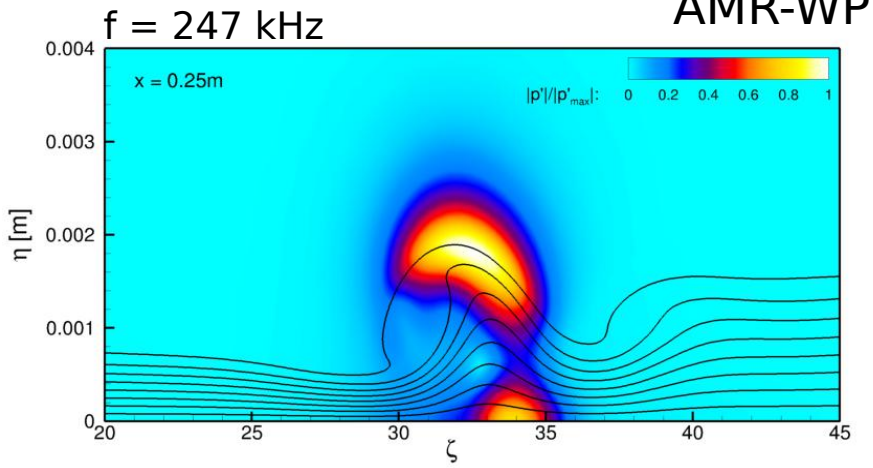
Araya et al. 2022

RESULTS: SELECT VALIDATION CASES

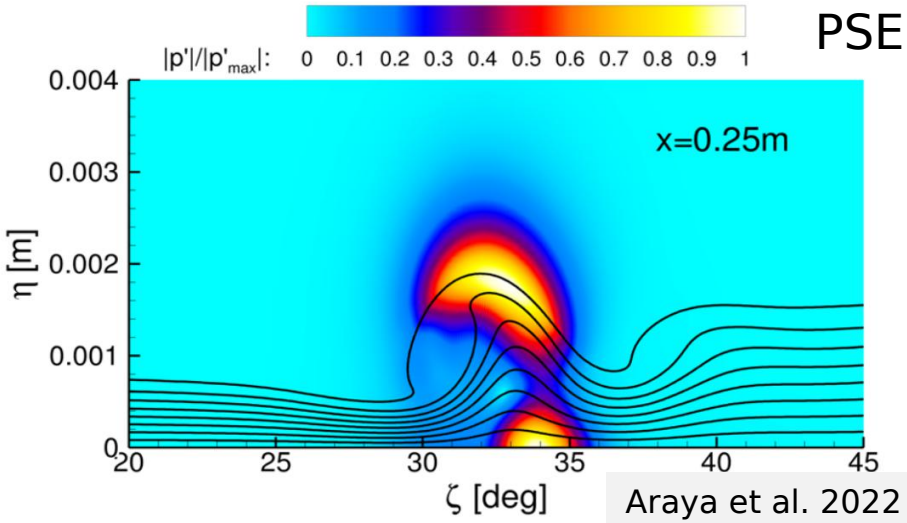
Validation case 2: BAM6QT finned-cone model (7° cone with 1mm nose and 75° swept fin) at Mach = 6 and Re=8.4e6/m



AMR-WPT



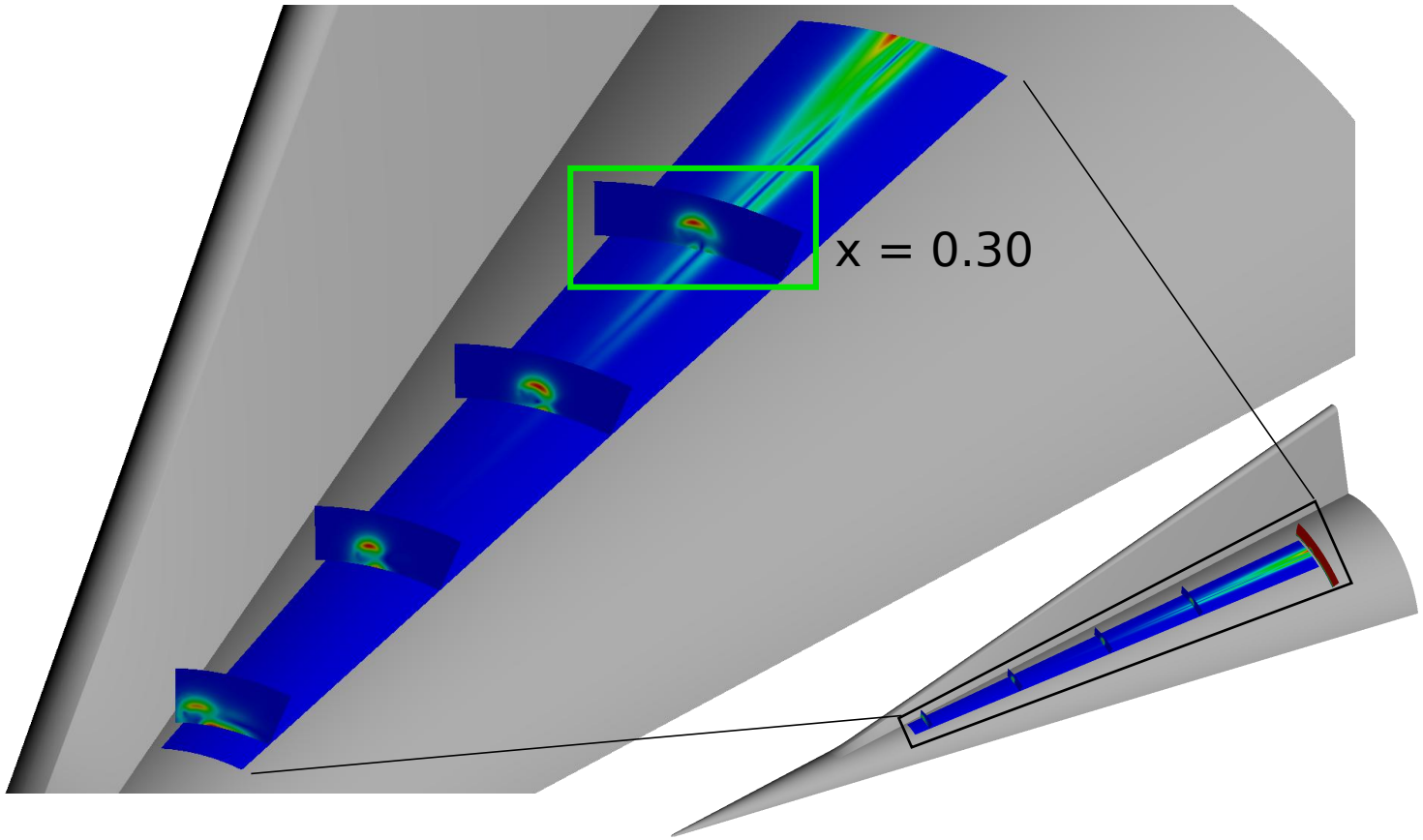
PSE



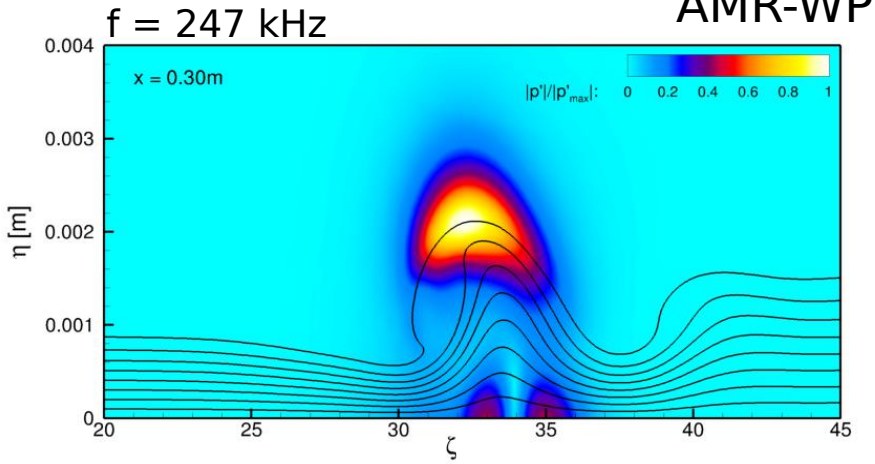
Araya et al. 2022

RESULTS: SELECT VALIDATION CASES

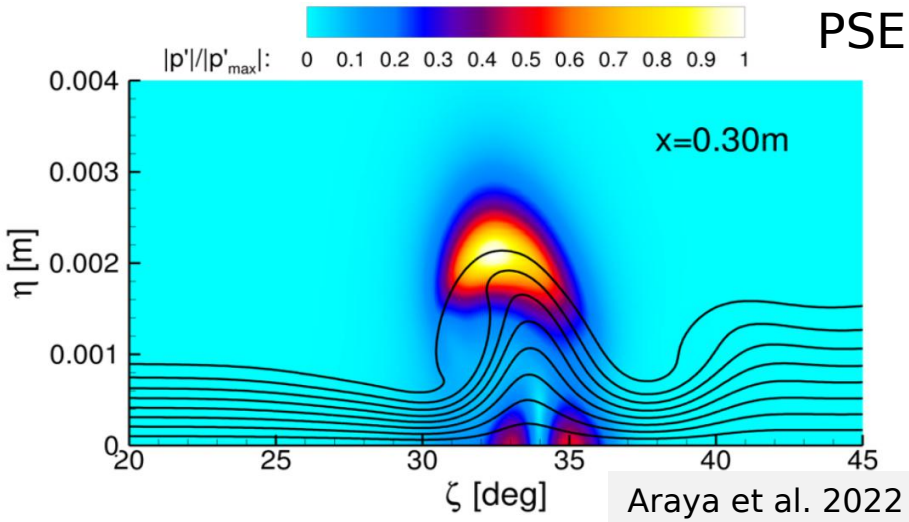
Validation case 2: BAM6QT finned-cone model (7° cone with 1mm nose and 75° swept fin) at Mach = 6 and Re=8.4e6/m



AMR-WPT



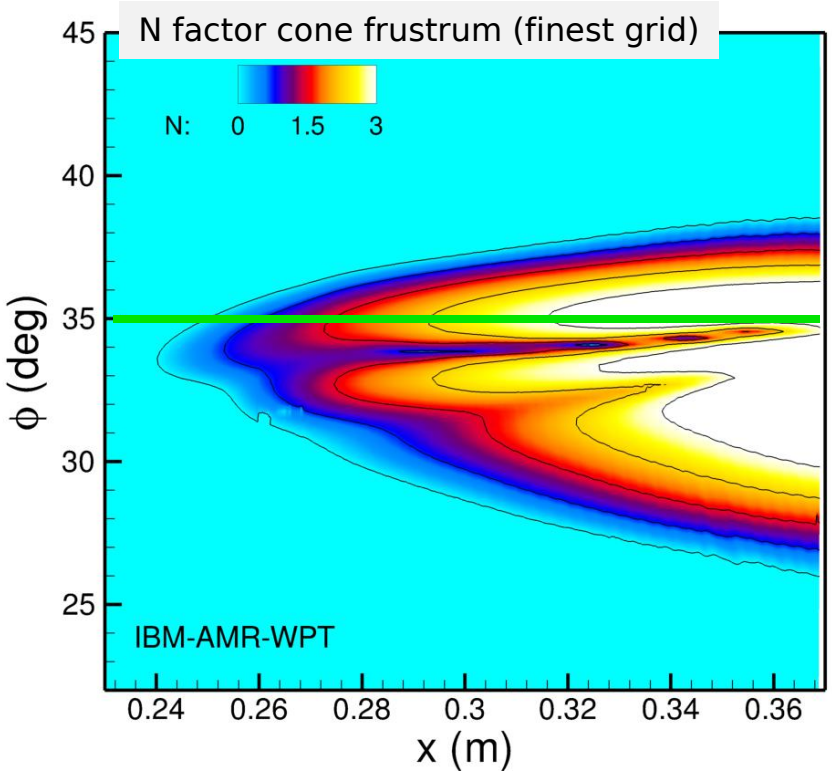
PSE

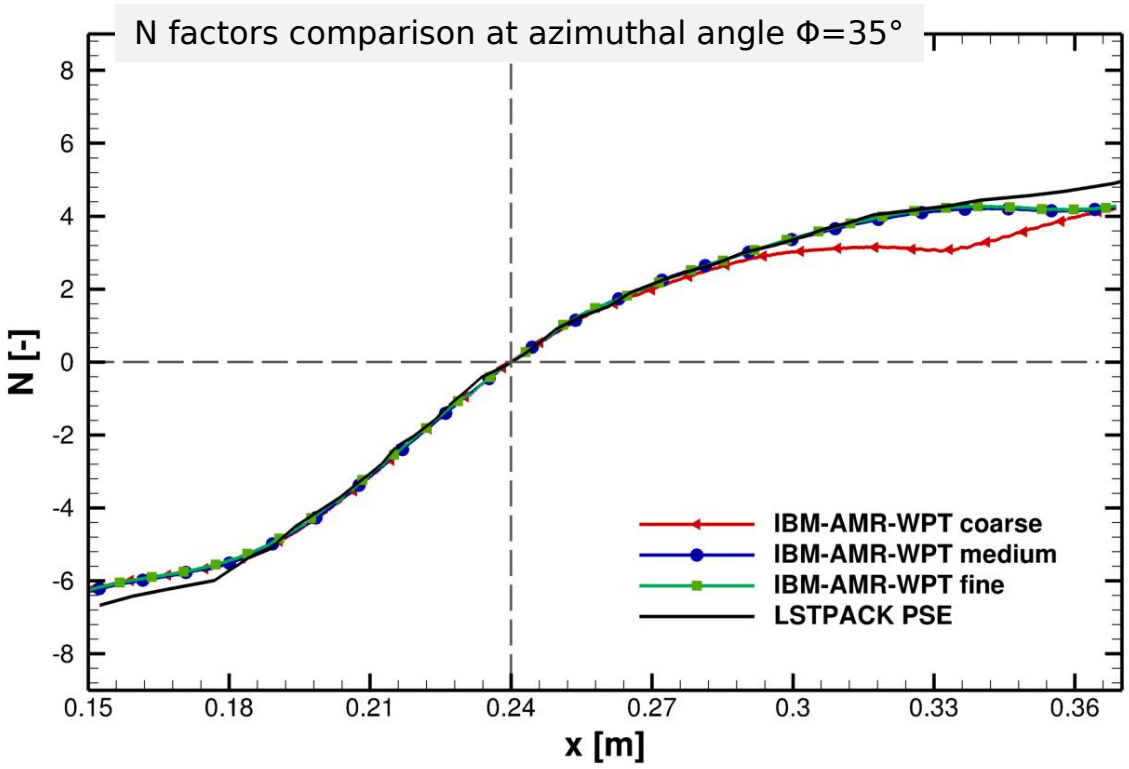


Araya et al. 2022

RESULTS: SELECT VALIDATION CASES

Validation case 2: BAM6QT finned-cone model (7° cone with 1mm nose and 75° swept fin) at Mach = 6 and Re=8.4e6/m

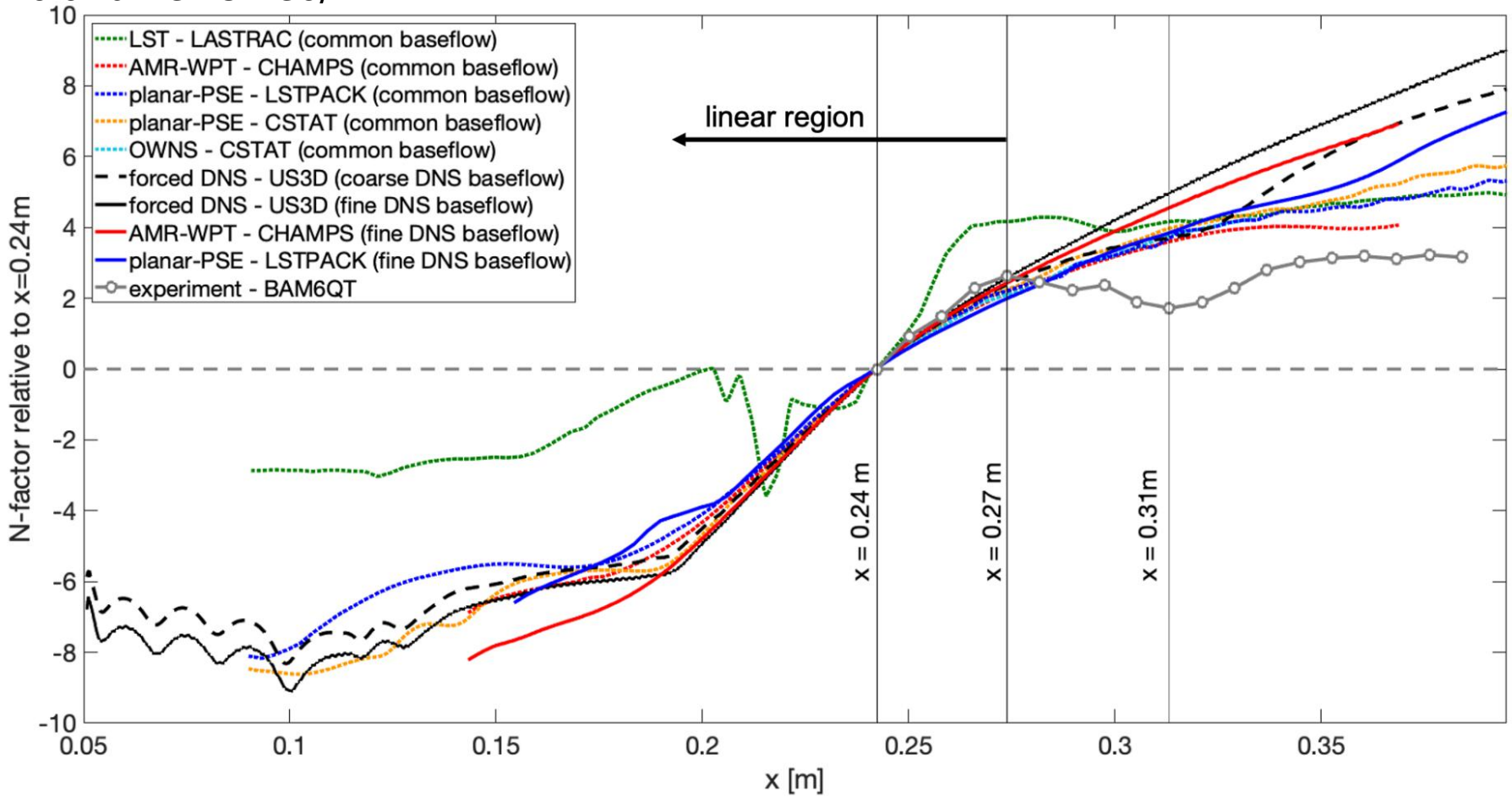




- a grid sensitivity study was also performed and results where considered grid converged
- **results display a very good match with PSE analysis**

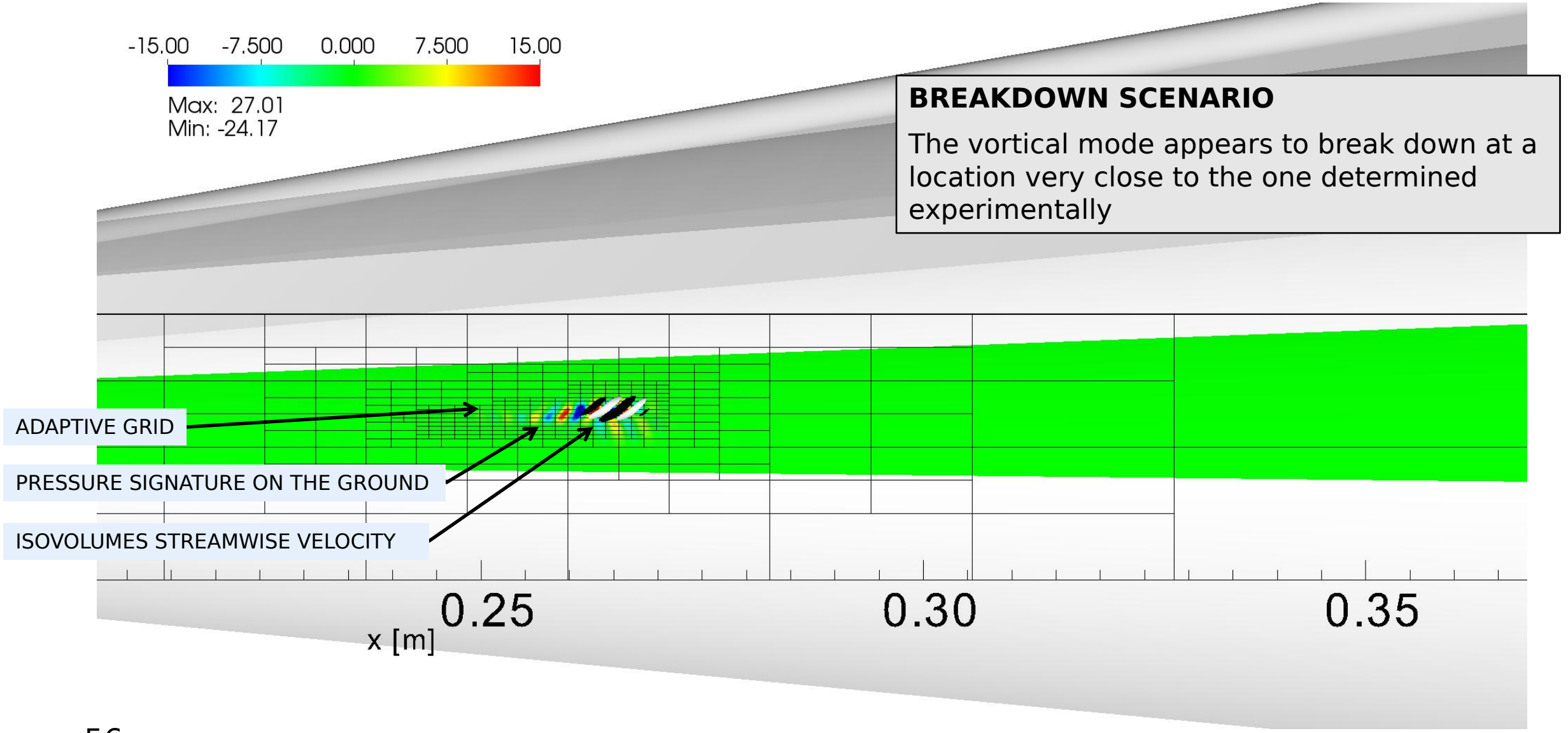
RESULTS: SELECT VALIDATION CASES

Validation case 2: BAM6QT finned-cone model (7° cone with 1mm nose and 75° swept fin) at Mach = 6 and Re=8.4e6/m



Assessment of linear methods for analysis of boundary layer instabilities on a finned cone at Mach 6, D. B. Araya, N. P. Bitter, B. M. Wheaton., O. Kamal, T. Colonius, A. Knutson, H. Johnson, J. Nichols, G. V. Candler, V. Russo, C. Brehm, AIAA Aviation 2022, National Harbor

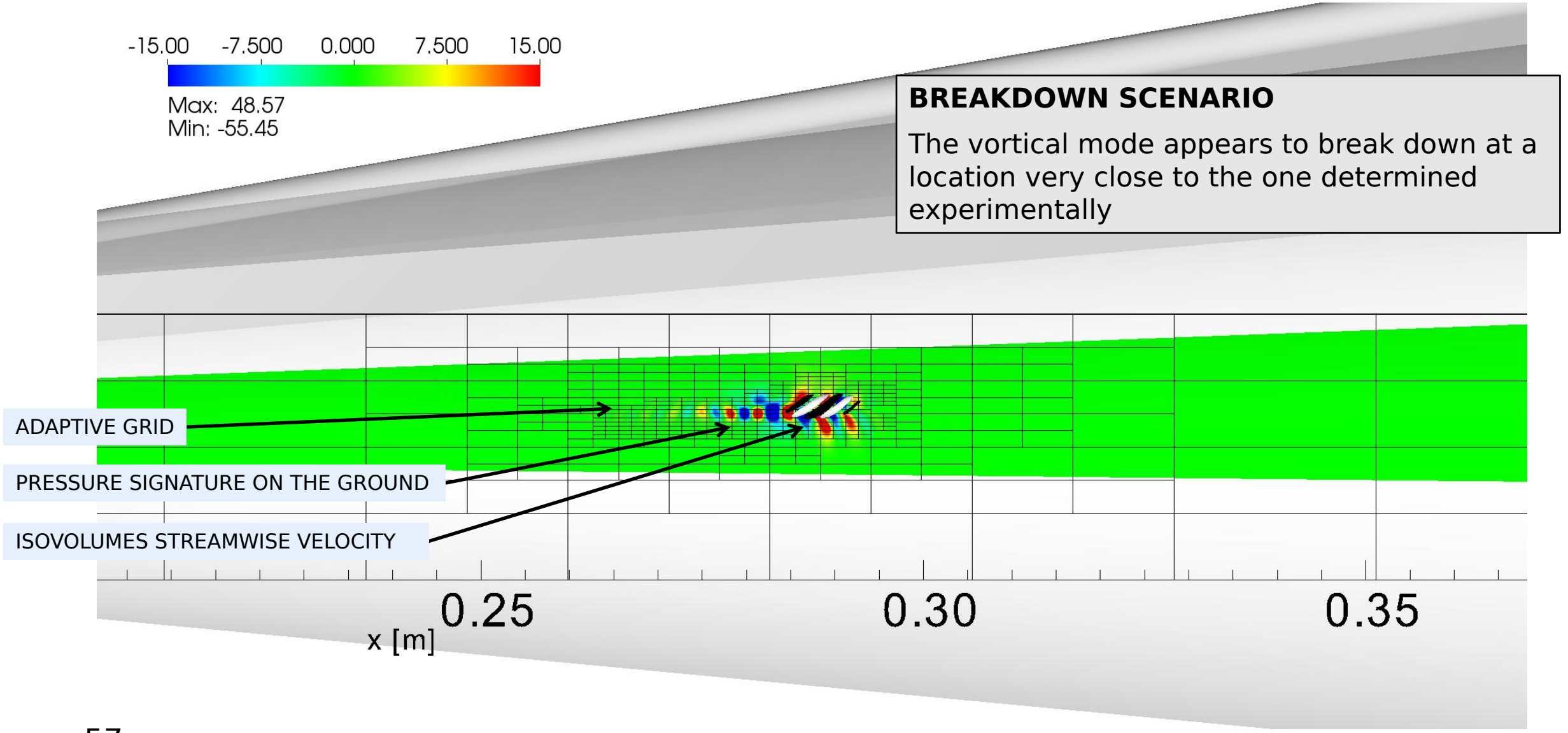
RESULTS: SELECT VALIDATION CASES



BREAKDOWN SCENARIO

The vortical mode appears to break down at a location very close to the one determined experimentally

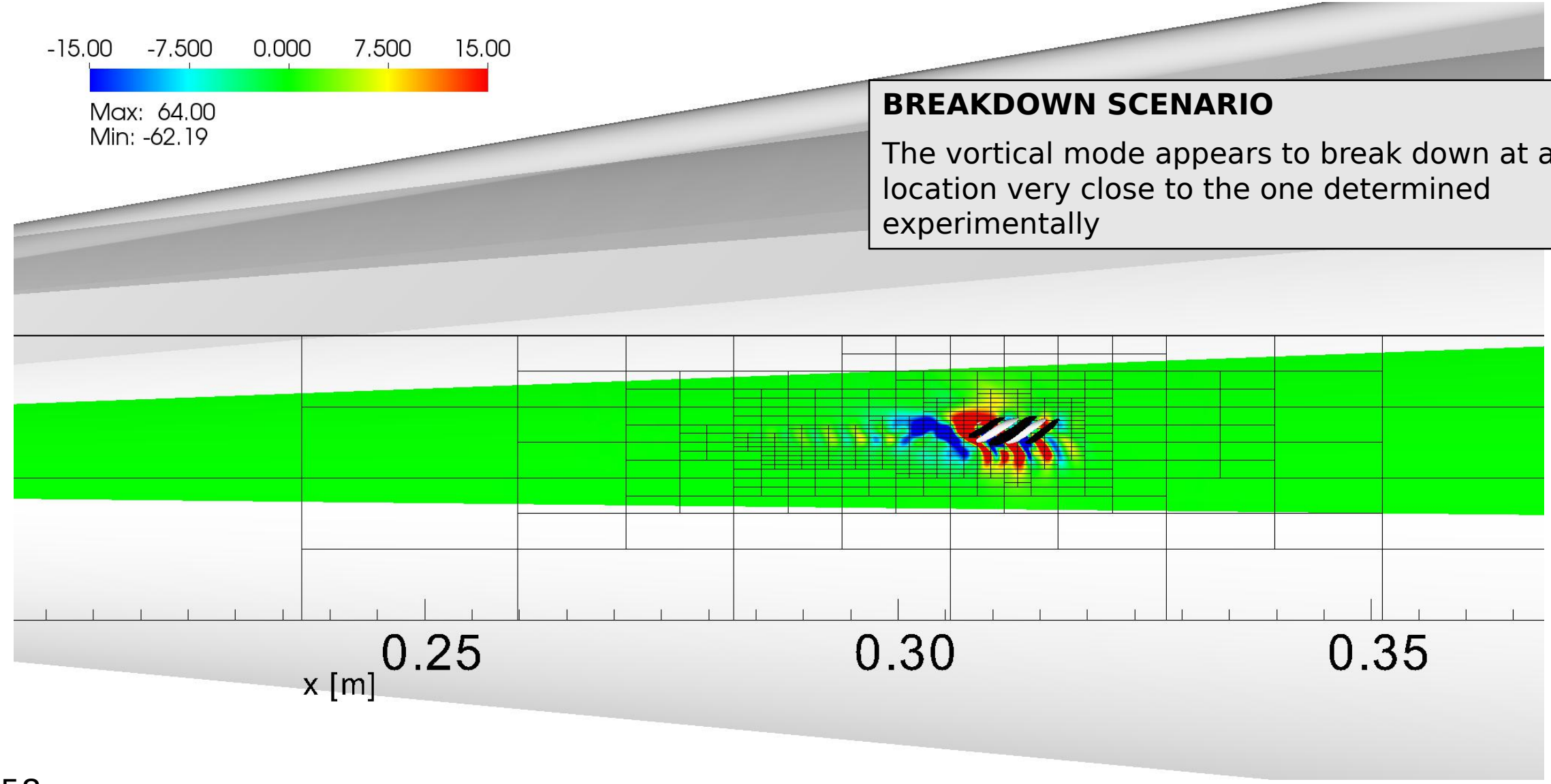
RESULTS: SELECT VALIDATION CASES



BREAKDOWN SCENARIO

The vortical mode appears to break down at a location very close to the one determined experimentally

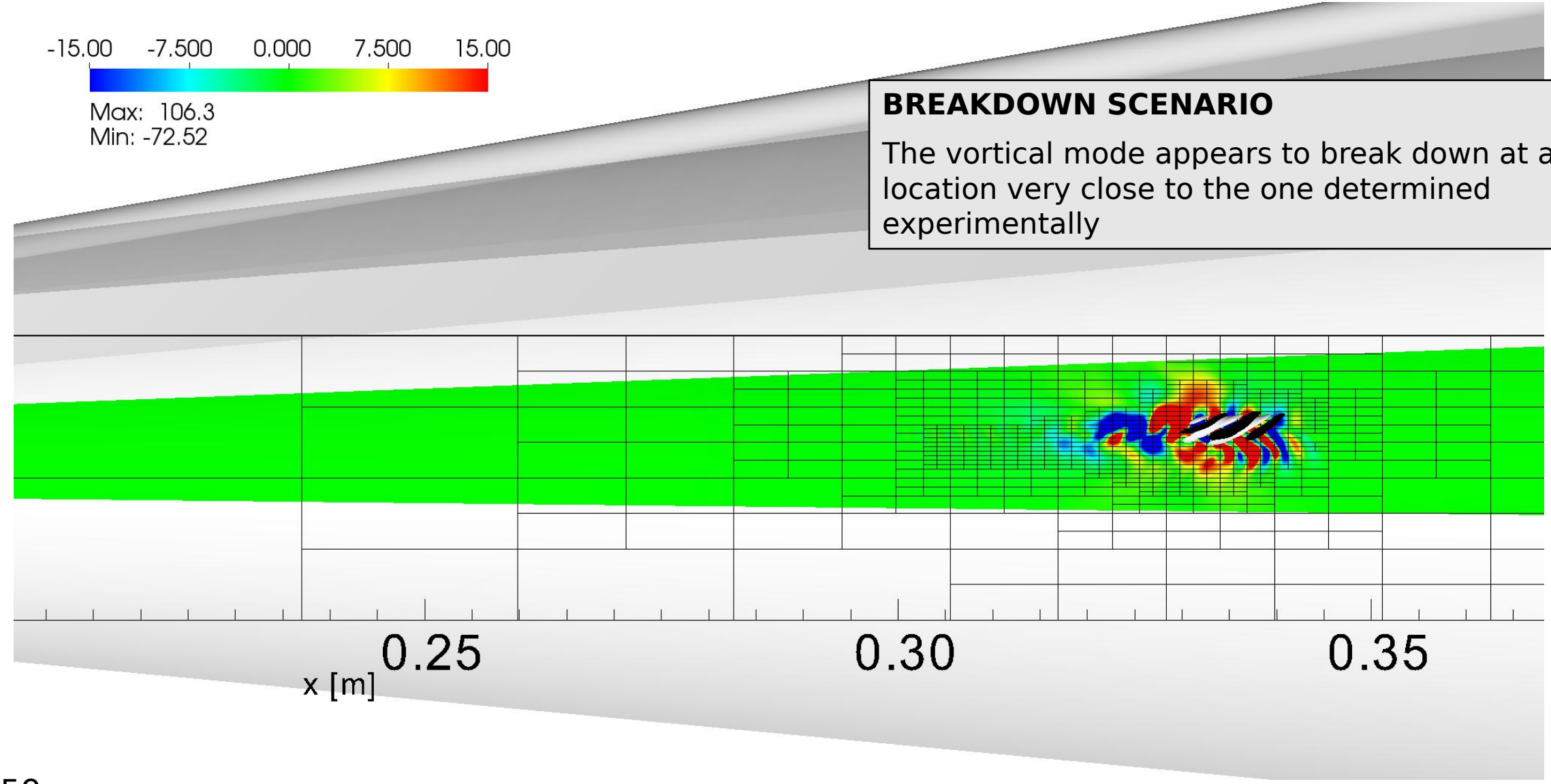
RESULTS: SELECT VALIDATION CASES



BREAKDOWN SCENARIO

The vortical mode appears to break down at a location very close to the one determined experimentally

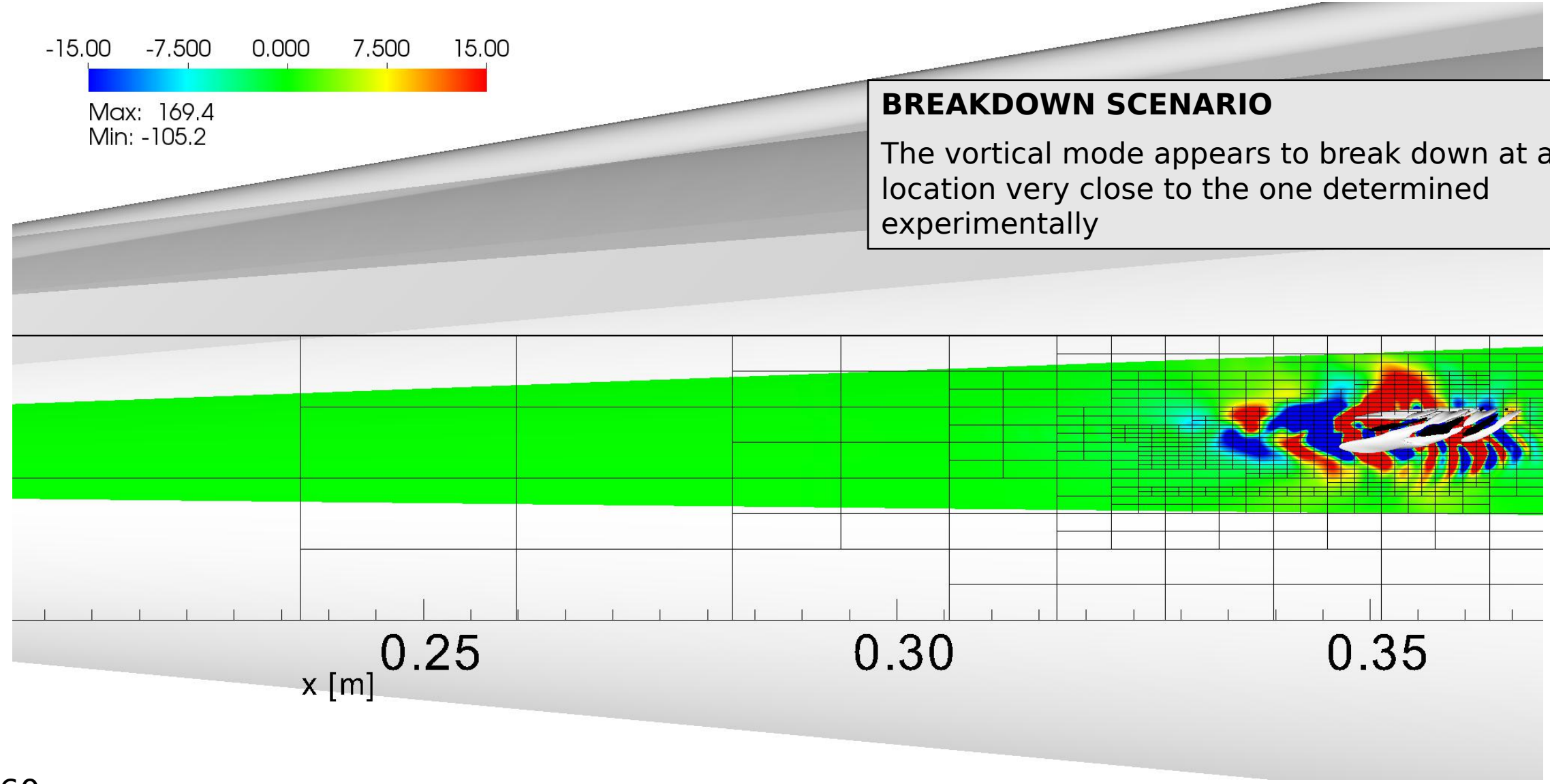
RESULTS: SELECT VALIDATION CASES



BREAKDOWN SCENARIO

The vortical mode appears to break down at a location very close to the one determined experimentally

RESULTS: SELECT VALIDATION CASES



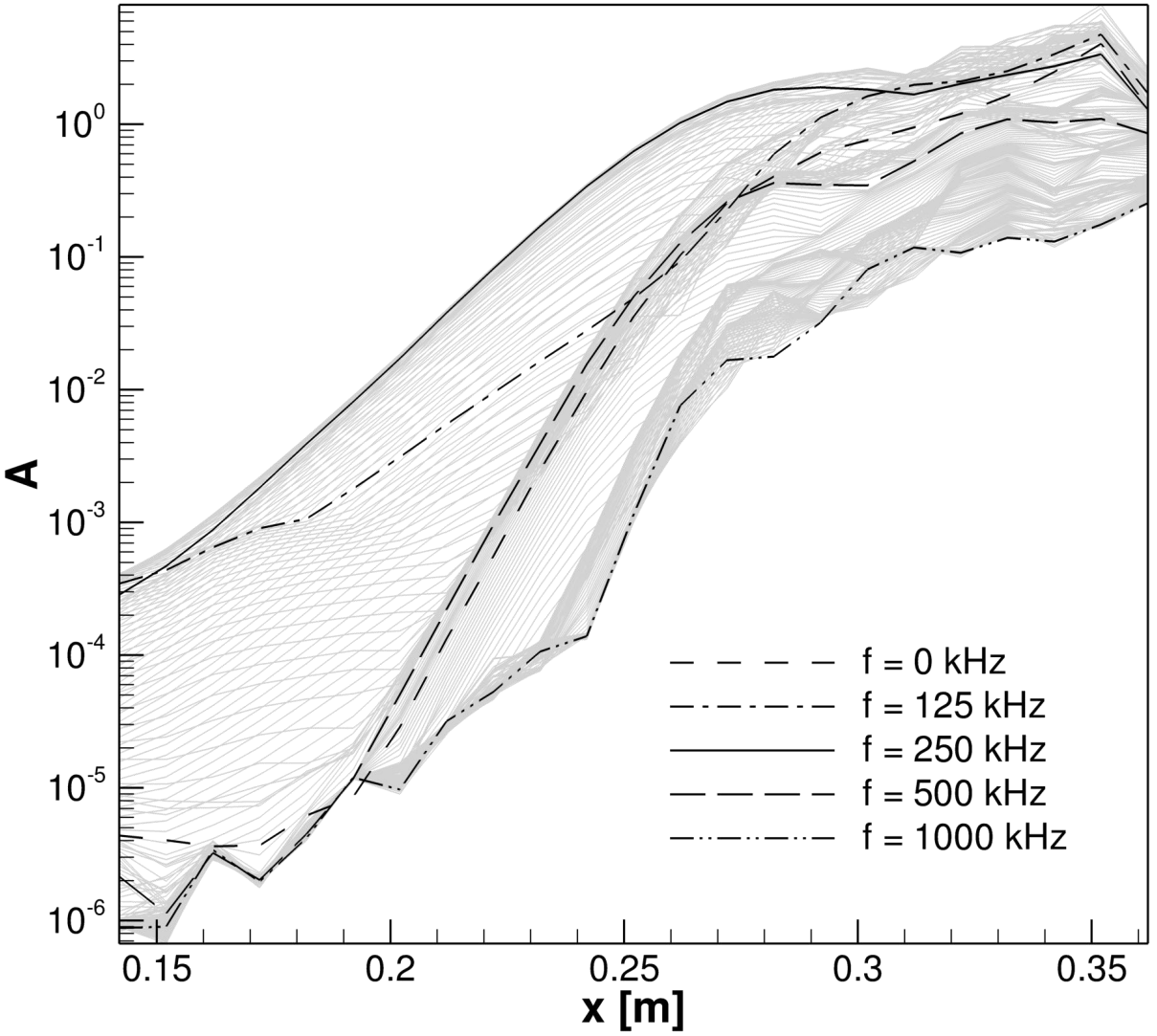
BREAKDOWN SCENARIO

The vortical mode appears to break down at a location very close to the one determined experimentally

RESULTS: SELECT VALIDATION CASES

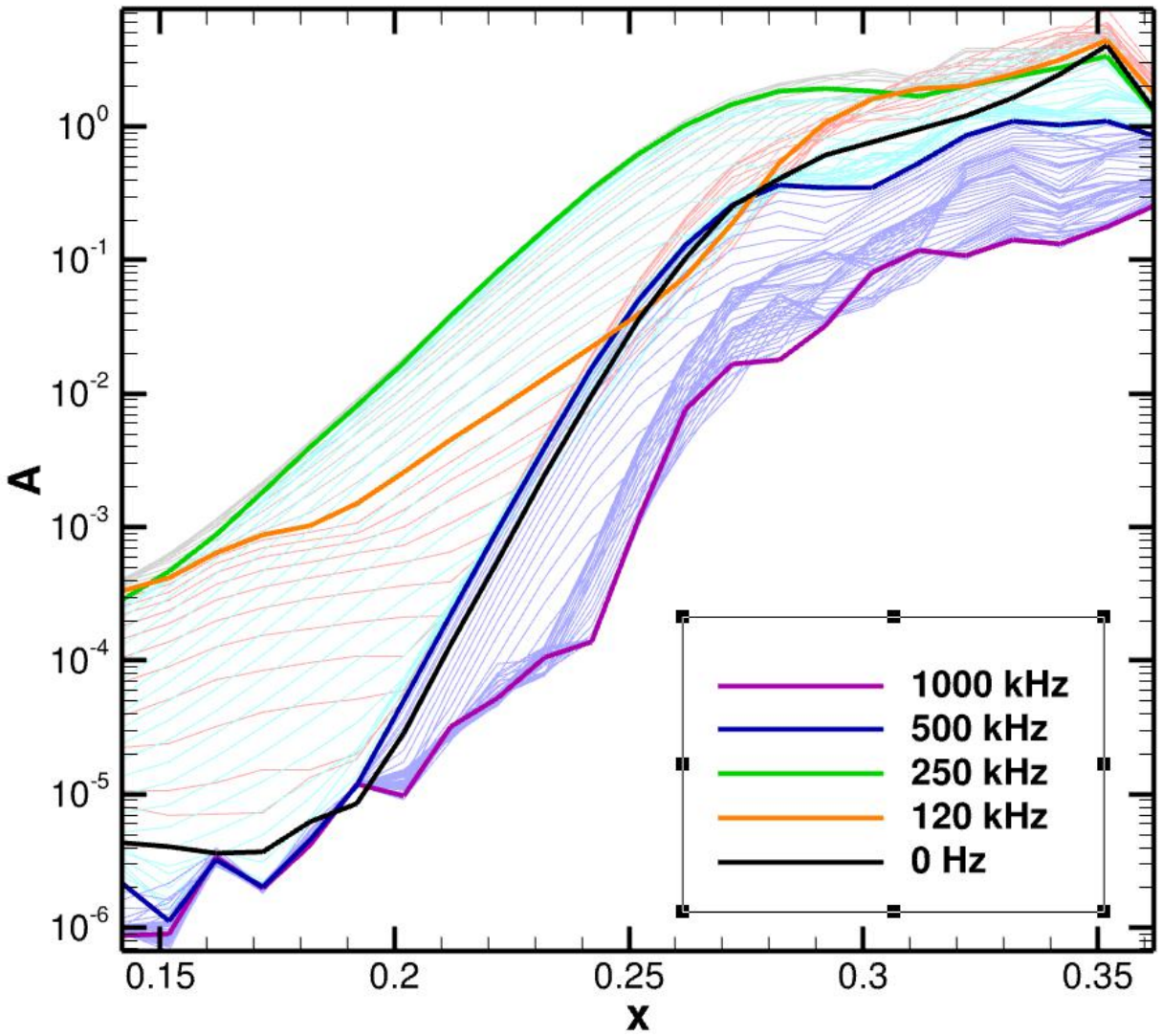
DOWNSTREAM DEVELOPMENT OF DISTURBANCES (breakdown scenario)

- Downstream development of pressure disturbance amplitudes has been computed for 400 discrete frequencies (from f1=0kHz to f2=1000kHz)
- The most amplified disturbances correspond to waves with frequencies in the range f=200kHz to f=280kHz
- Results confirm PSE results: the abomentioned range of frequencies dominate for almost the entirety of the computational domain considered



DOWNSTREAM DEVELOPMENT OF DISTURBANCES (breakdown scenario)

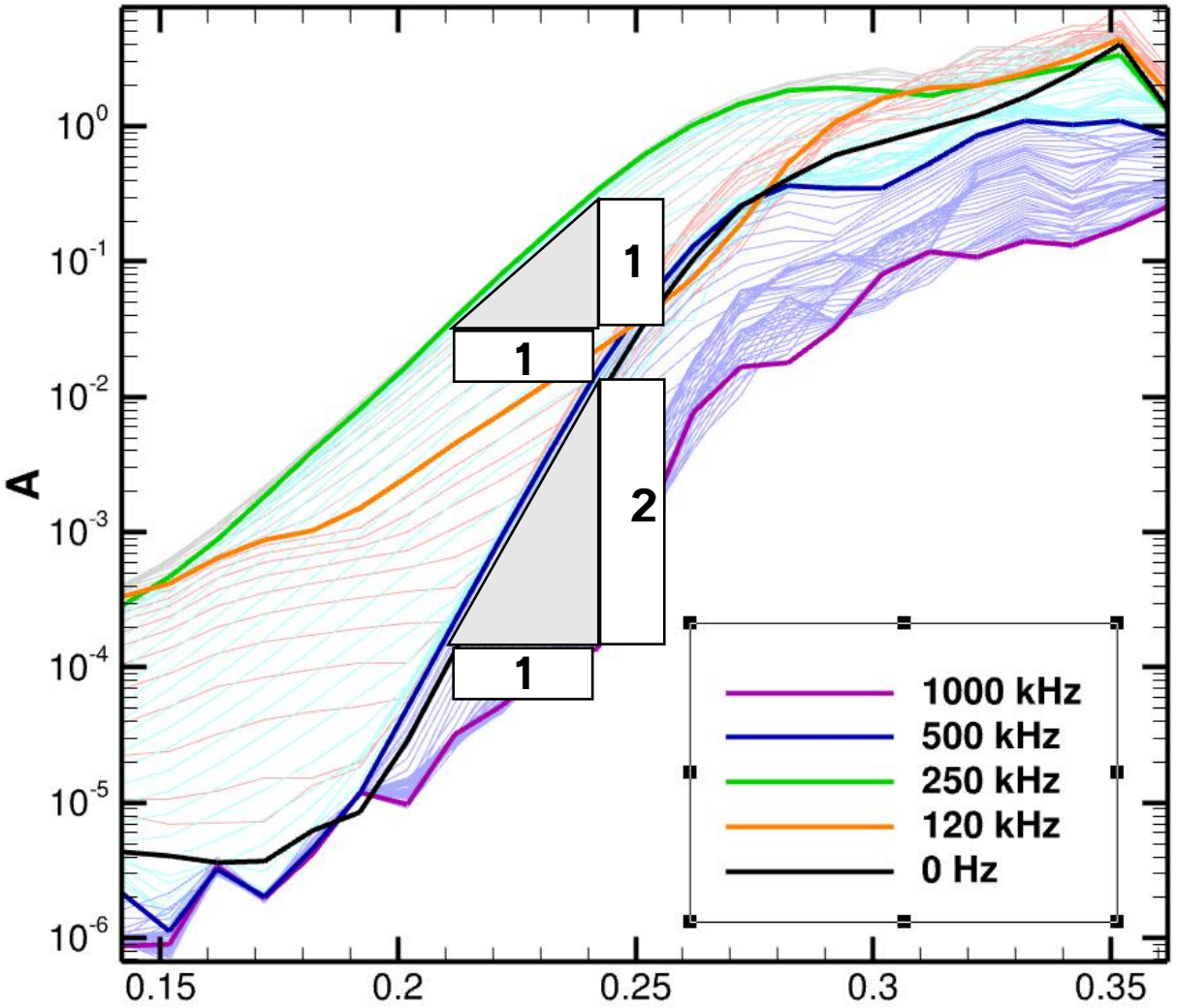
- Downstream development of pressure disturbance amplitudes has been computed for 400 discrete frequencies (from f1=0kHz to f2=1000kHz)
- The most amplified disturbances correspond to waves with frequencies in the range f=200kHz to f=280kHz
- Results confirm PSE results: the abomentioned range of frequencies dominate for almost the entirety of the computational domain considered



RESULTS: SELECT VALIDATION CASES

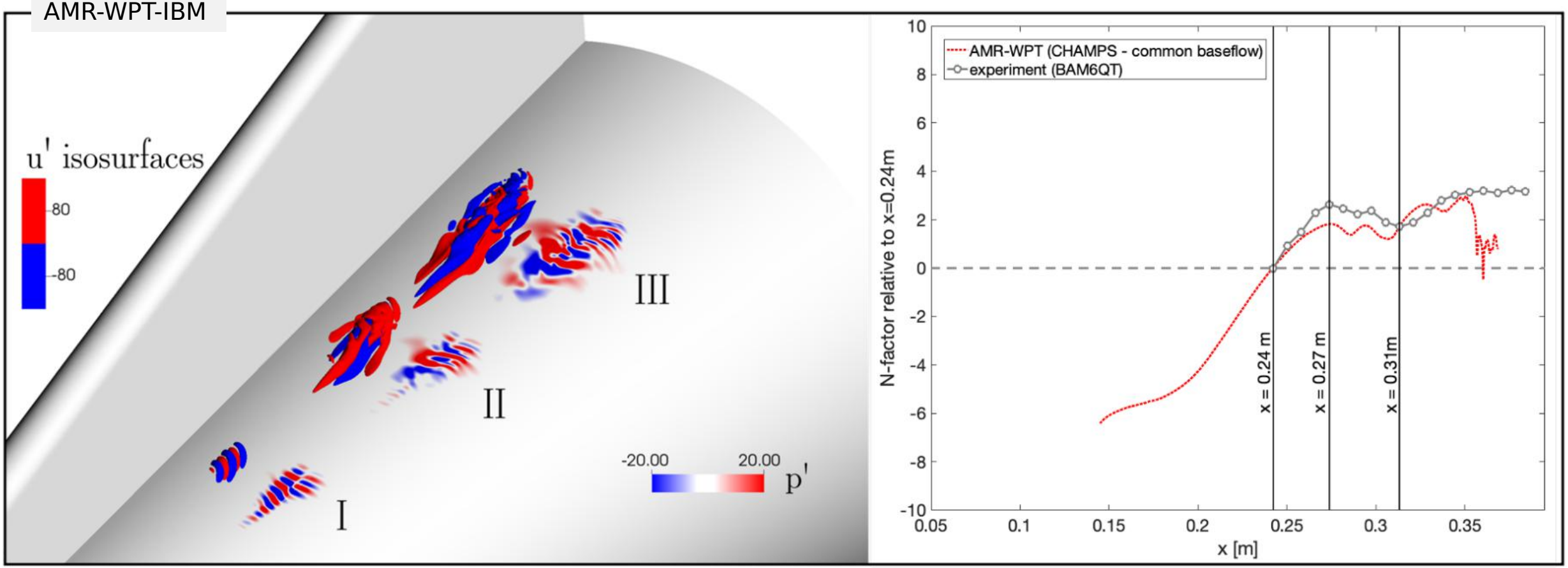
DOWNSTREAM DEVELOPMENT OF DISTURBANCES (breakdown scenario)

- Downstream development of pressure disturbance amplitudes has been computed for 400 discrete frequencies (from f1=0kHz to f2=1000kHz)
- The most amplified disturbances correspond to waves with frequencies in the range f=200kHz to f=280kHz
- Results confirm PSE results: the abomentioned range of frequencies dominate for almost the entirety of the computational domain considered



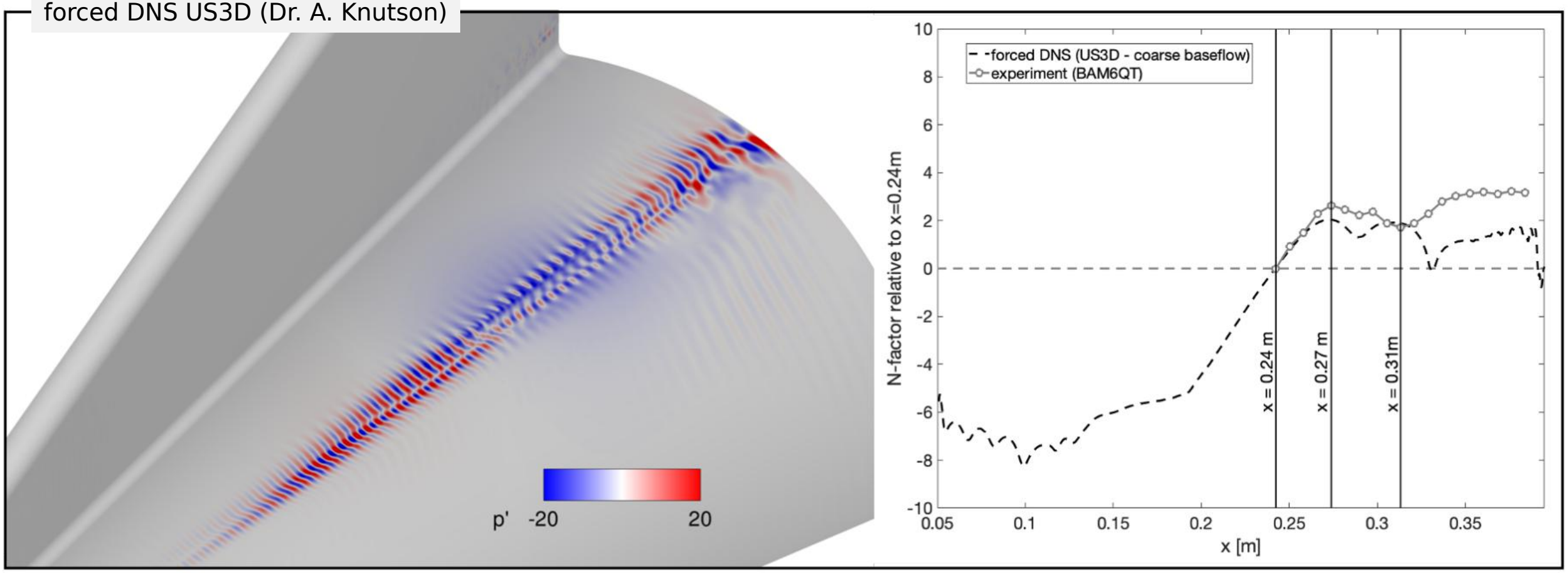
RESULTS: SELECT VALIDATION CASES

AMR-WPT-IBM



Assessment of linear methods for analysis of boundary layer instabilities on a finned cone at Mach 6, D. B. Araya, N. P. Bitter, B. M. Wheaton., O. Kamal, T. Colonius, A. Knutson, H. Johnson, J. Nichols, G. V. Candler, V. Russo, C. Brehm, AIAA Journal, submitted and currently under review.

forced DNS US3D (Dr. A. Knutson)

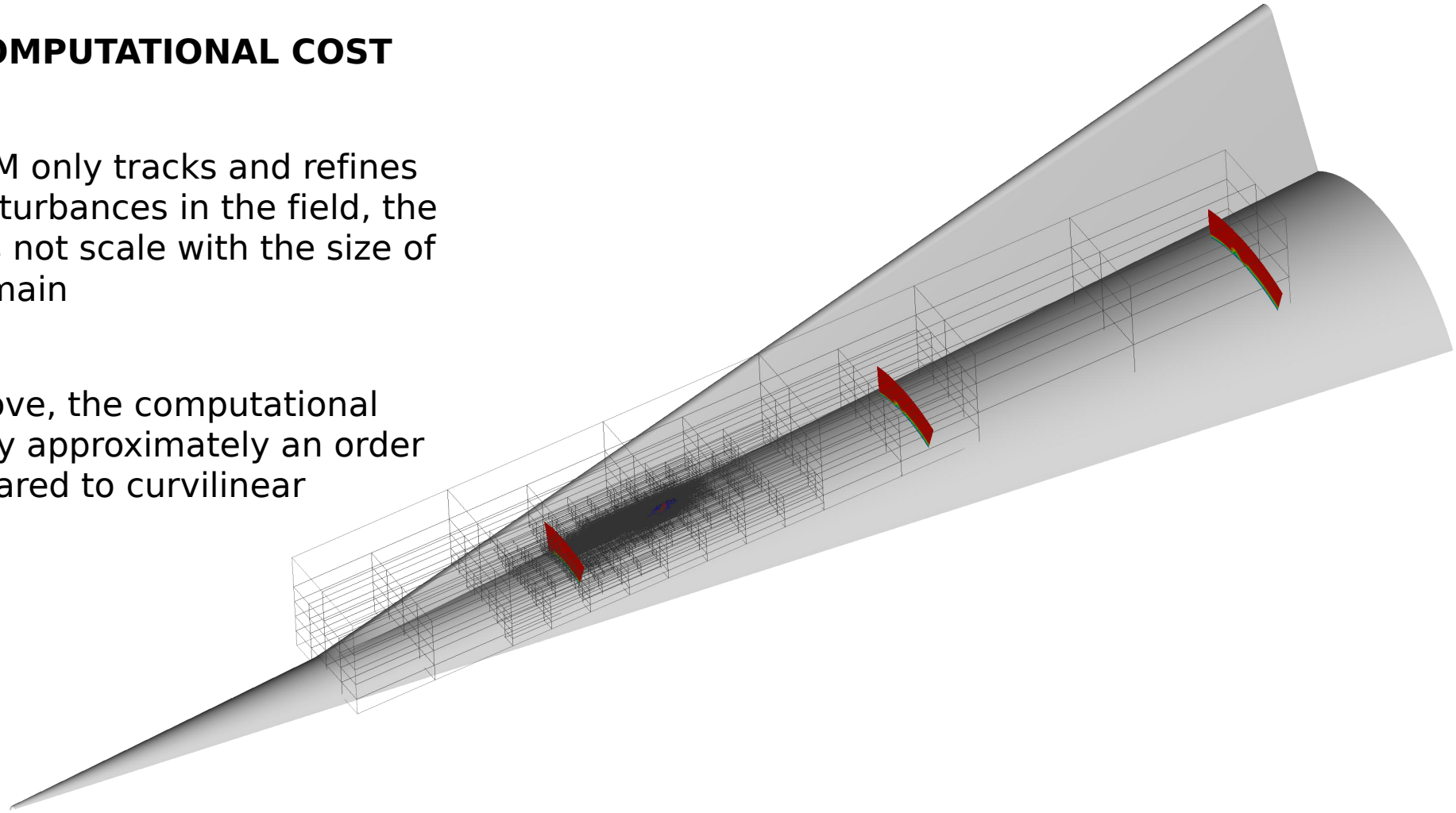


Assessment of linear methods for analysis of boundary layer instabilities on a finned cone at Mach 6, D. B. Araya, N. P. Bitter, B. M. Wheaton., O. Kamal, T. Colonius, A. Knutson, H. Johnson, J. Nichols, G. V. Candler, V. Russo, C. Brehm, AIAA Journal, submitted and currently under review.

A NOTE ABOUT THE COMPUTATIONAL COST

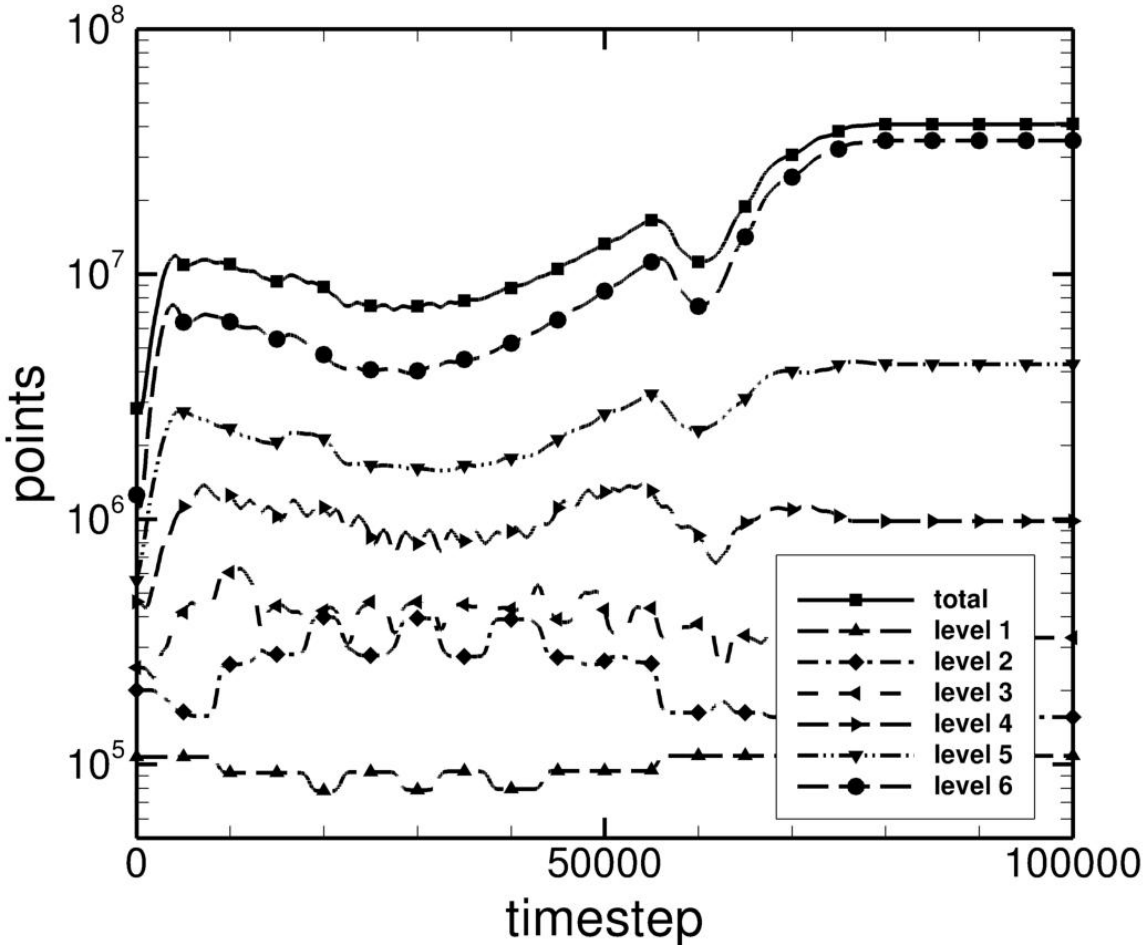
- Since the AMR-WPT-IBM only tracks and refines the most amplified disturbances in the field, the number of points does not scale with the size of the computational domain

- Given the premise above, the computational cost can be reduced by approximately an order of magnitude, if compared to curvilinear traditional approaches



A NOTE ABOUT THE COMPUTATIONAL COST

- Since the AMR-WPT-IBM only tracks and refines the most amplified disturbances in the field, the number of points does not scale with the size of the computational domain
- Given the premise above, the computational cost can be reduced by approximately an order of magnitude, if compared to curvilinear traditional approaches
- The specific validation case presented earlier remained relatively economical from a computational standpoint, with a count of only about 35 million points



OUTLINE

- Introduction and Research Motivation

On the relevance of Hypersonic Transition

- Computational Approach

Disturbance Flow Formulation, Adaptive Mesh Refinement and Immersed Boundary Method

- Results

Validation, Disturbance Flow Simulations for Complex Geometries and Particle Impingement

- Conclusions and Outlook

Summary of Presented Research and Future Work

OUTLINE

- Introduction and Research Motivation

On the relevance of Hypersonic Transition

- Computational Approach

Disturbance Flow Formulation, Adaptive Mesh Refinement and Immersed Boundary Method

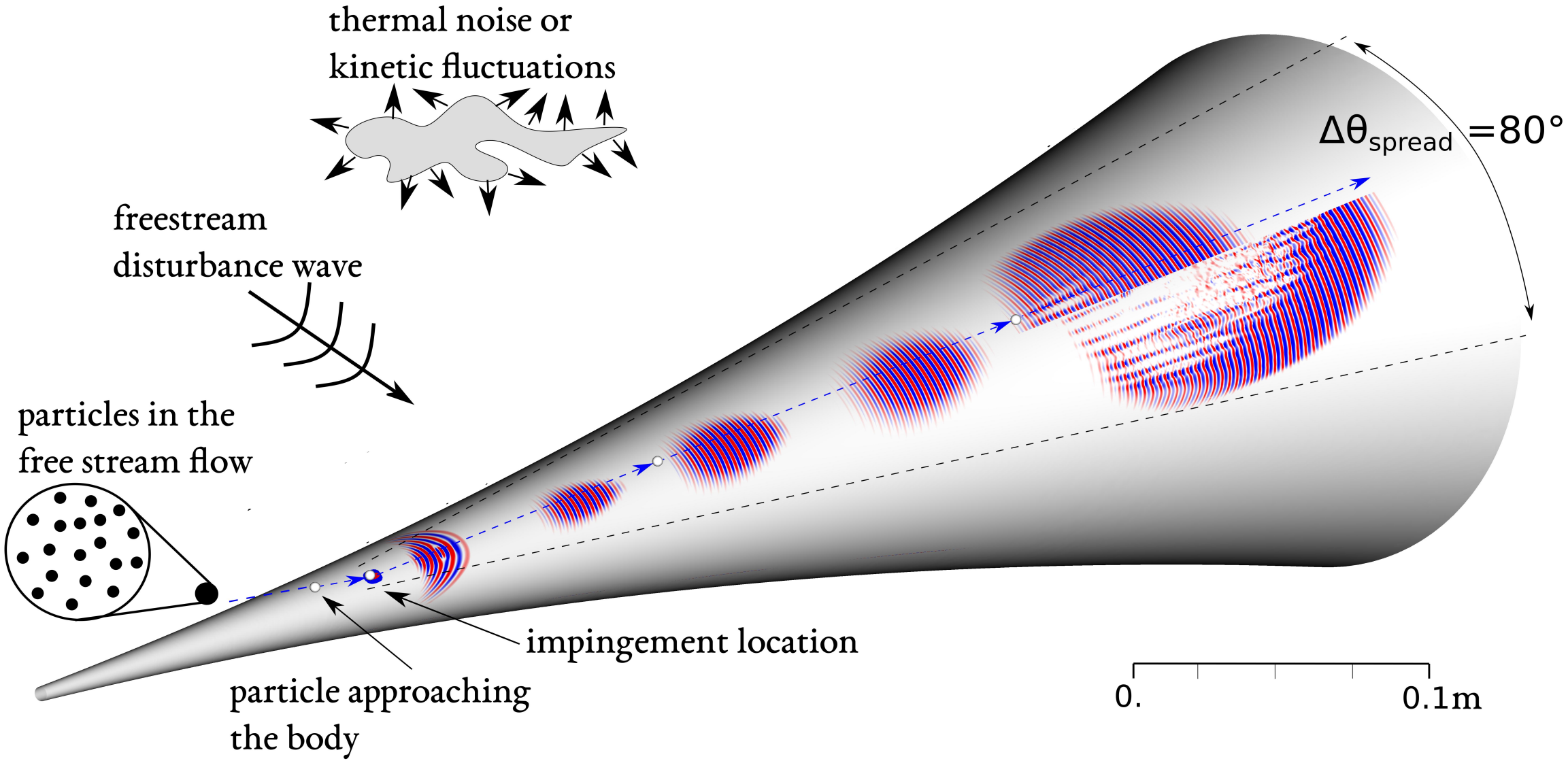
- Results

Validation, **Disturbance Flow Simulations for Complex Geometries and Particle Impingement**

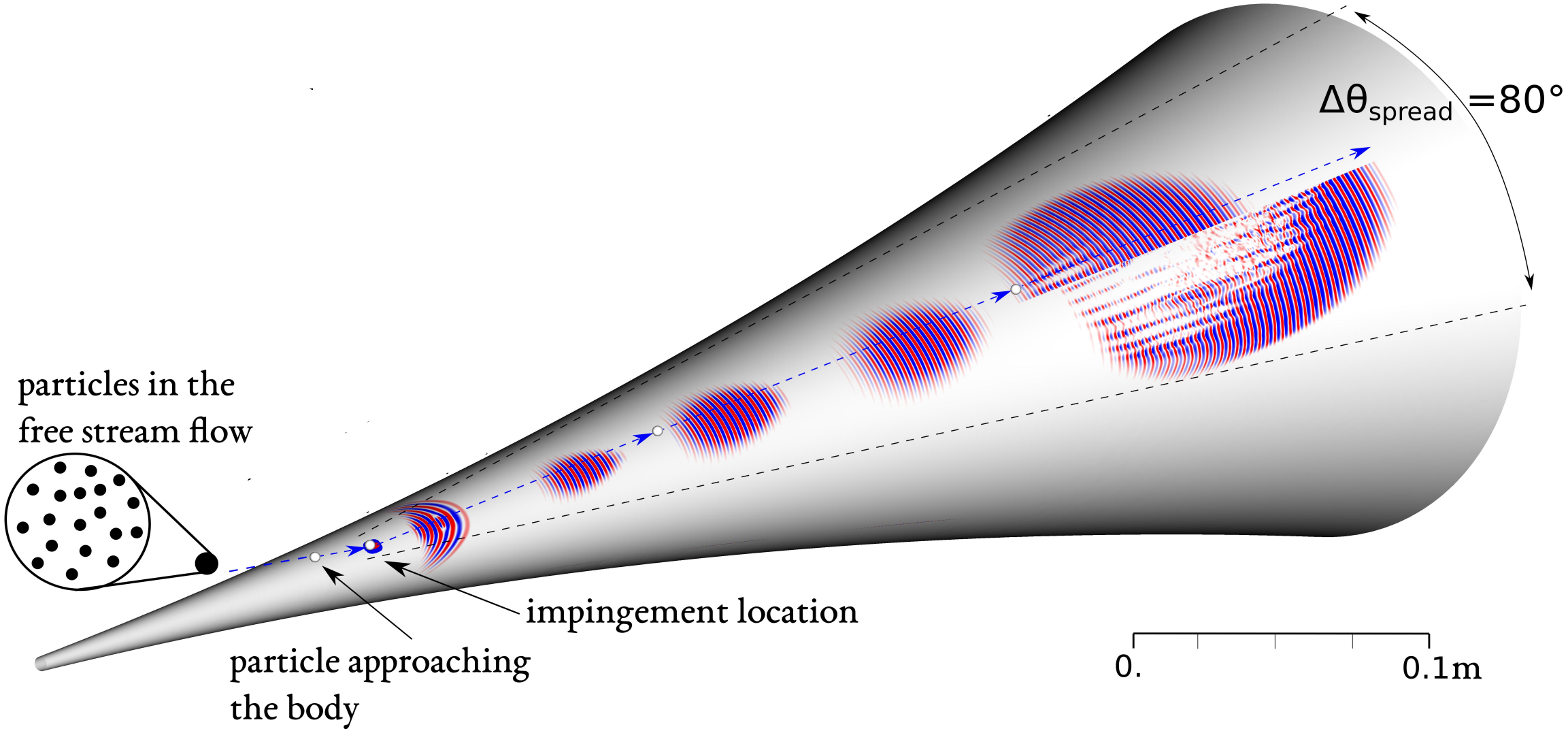
- Conclusions and Outlook

Summary of Presented Research and Future Work

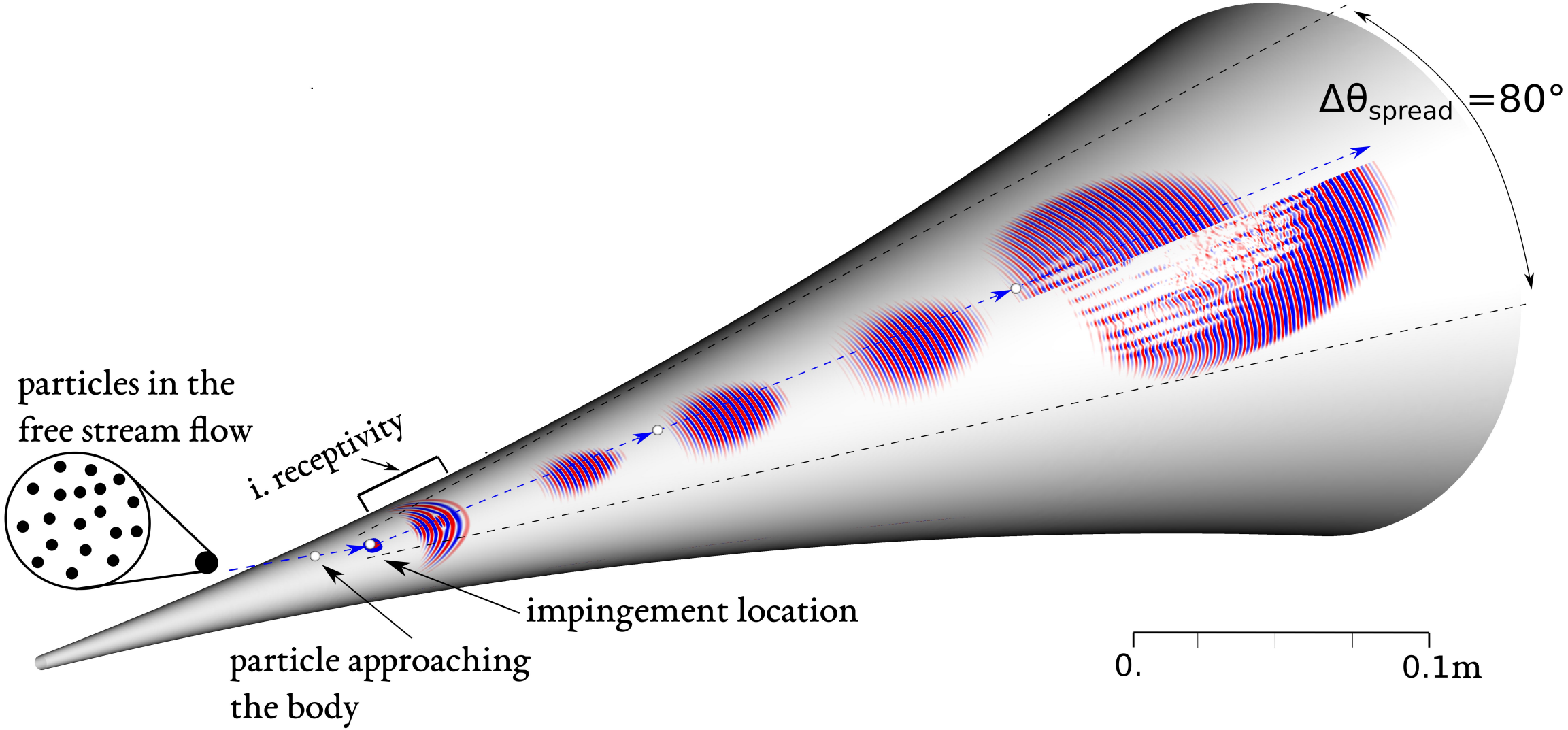
RESULTS: PARTICLE IMPINGEMENT SIMULATIONS



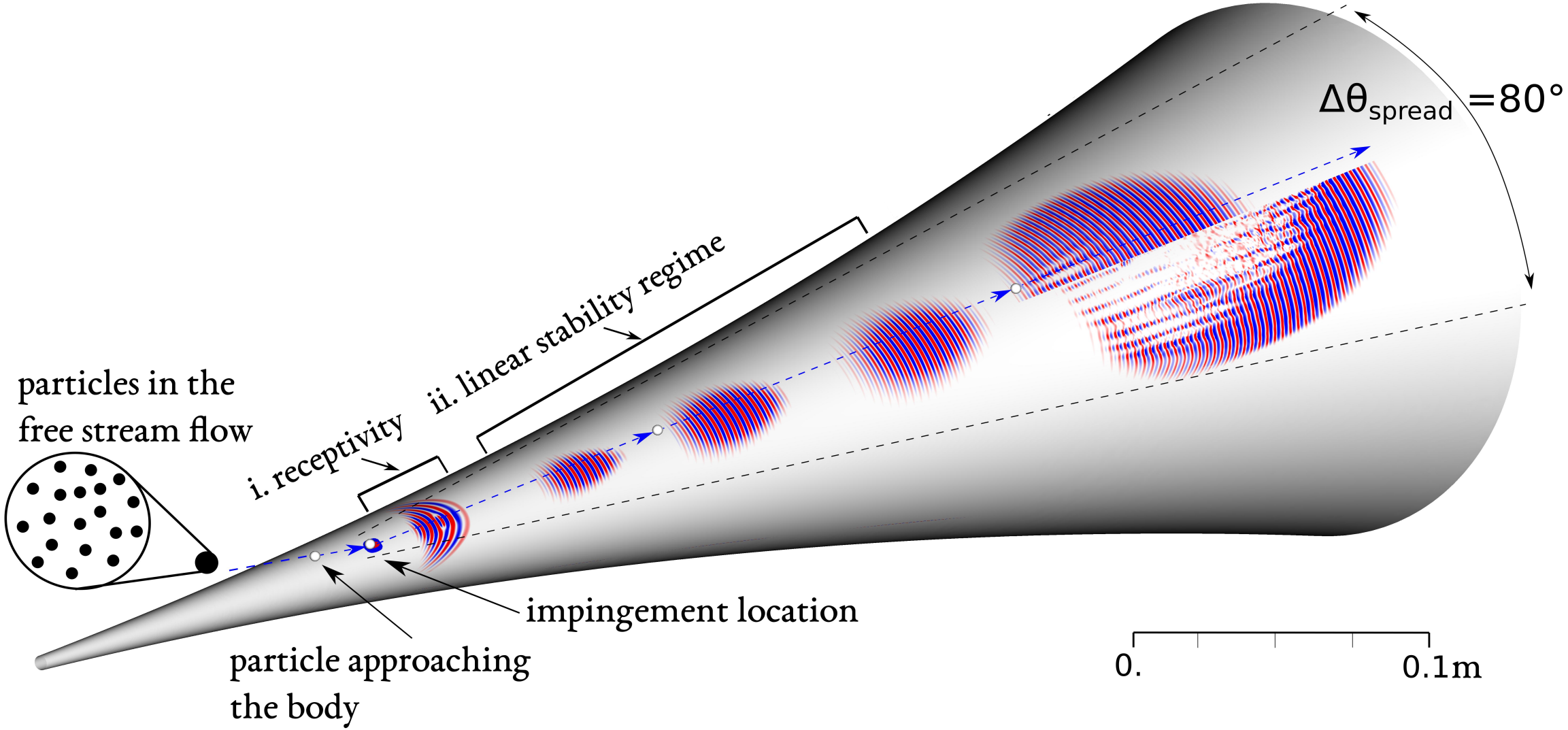
RESULTS: PARTICLE IMPINGEMENT SIMULATIONS



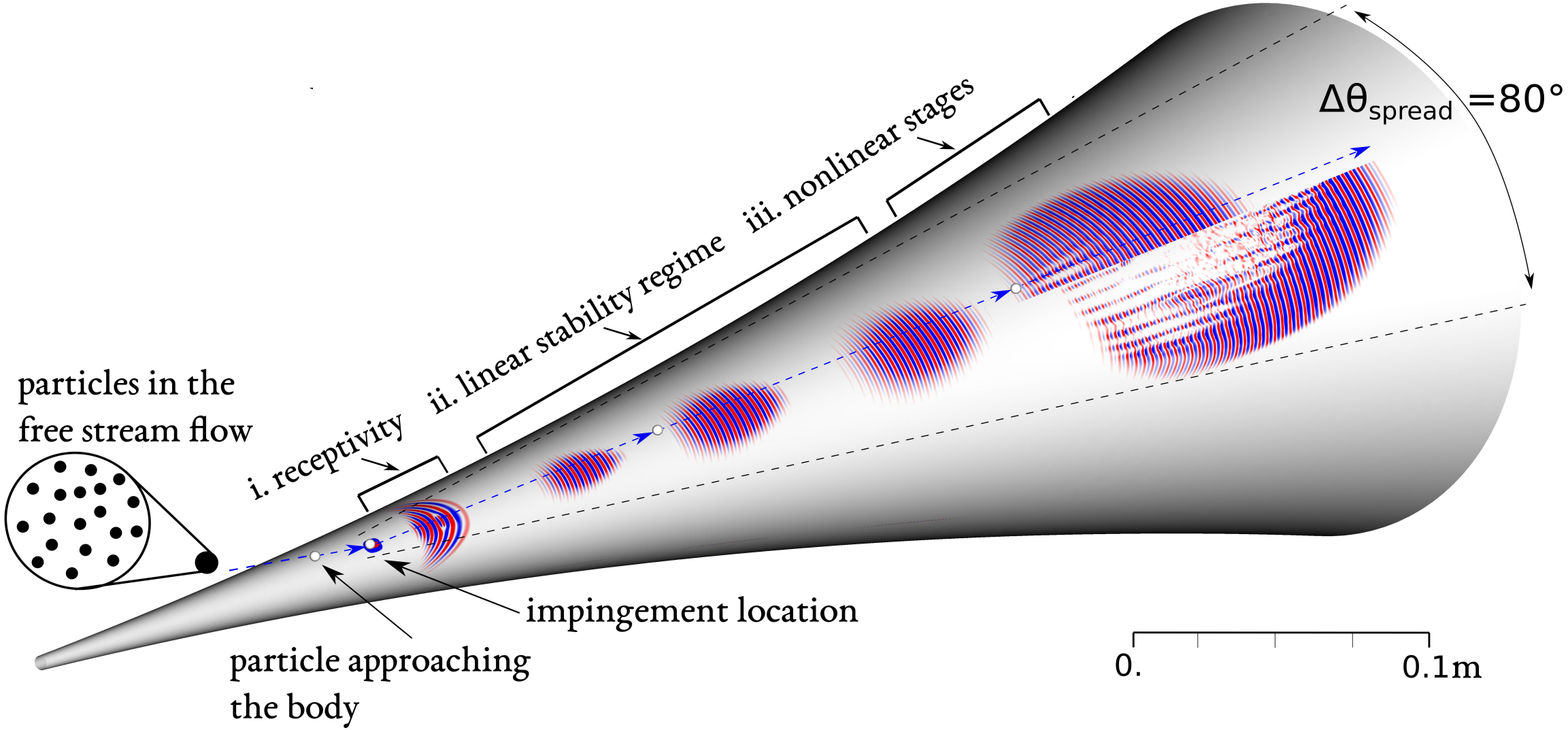
RESULTS: PARTICLE IMPINGEMENT SIMULATIONS



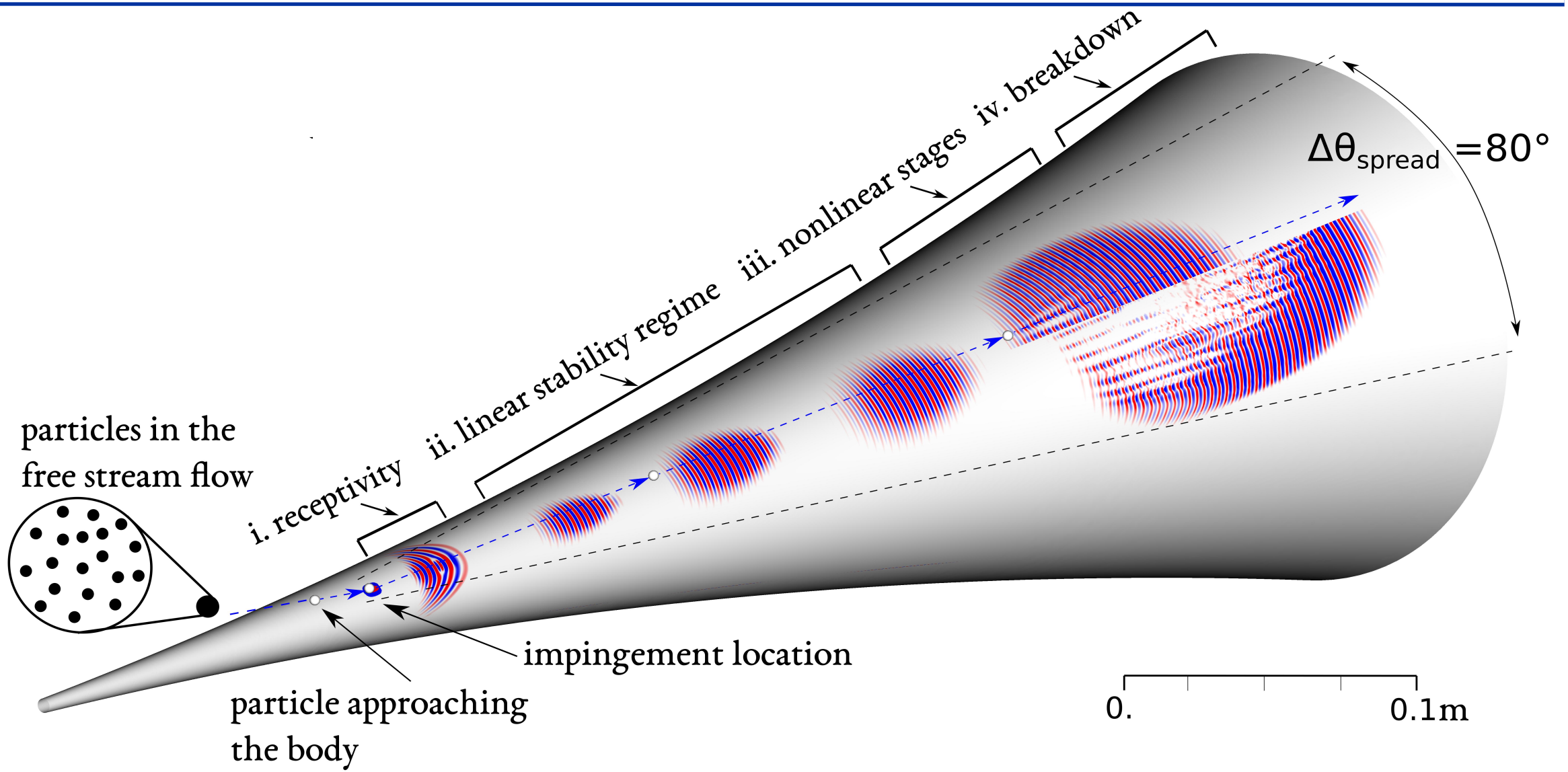
RESULTS: PARTICLE IMPINGEMENT SIMULATIONS



RESULTS: PARTICLE IMPINGEMENT SIMULATIONS



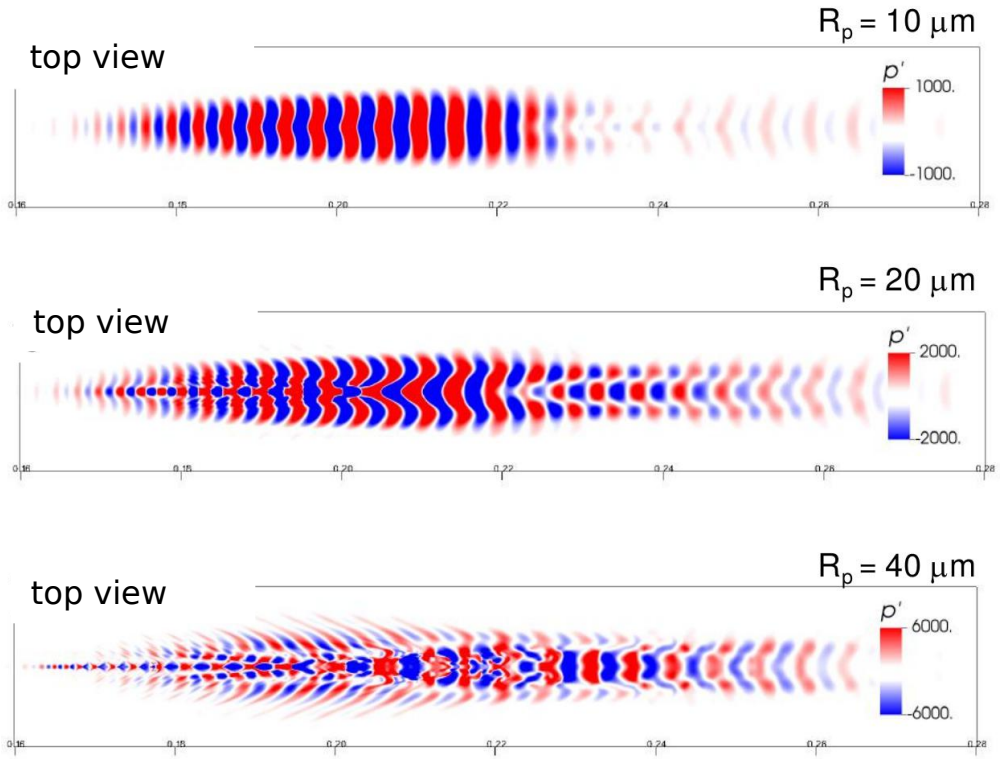
RESULTS: PARTICLE IMPINGEMENT SIMULATIONS



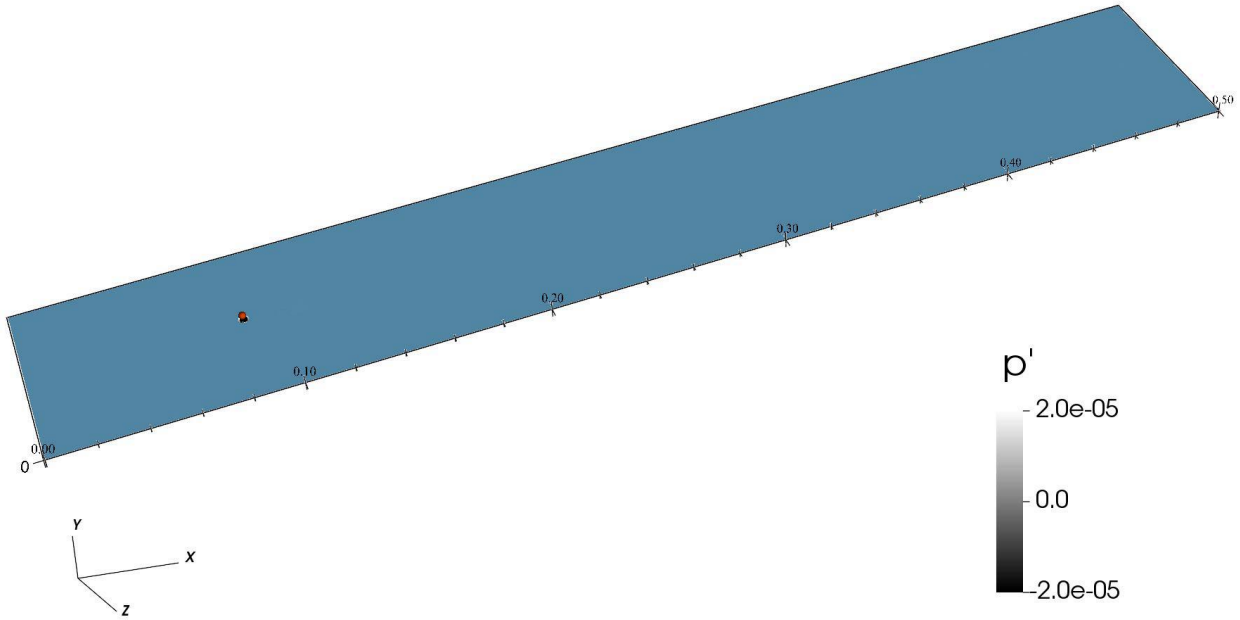
PARTICLE FLOW INTERACTION MECHANISMS: FLAT PLATES AND WEDGES

Initial tests demonstrated that **AMR-WPT (without Immersed Boundary)** could be successfully employed to simulate growth of instability waves (e.g. second Mack's mode) at dramatically reduced computational costs, for particle impingement on flat plates and wedges

collision different particle sizes on M=9.5 14º wedge



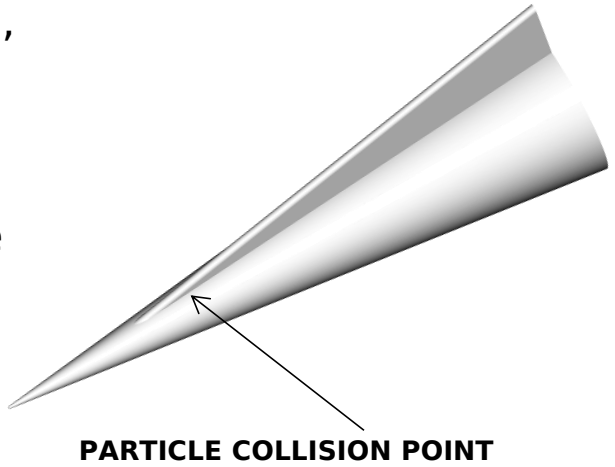
10μm particle impingement on M=9.5 14º wedge



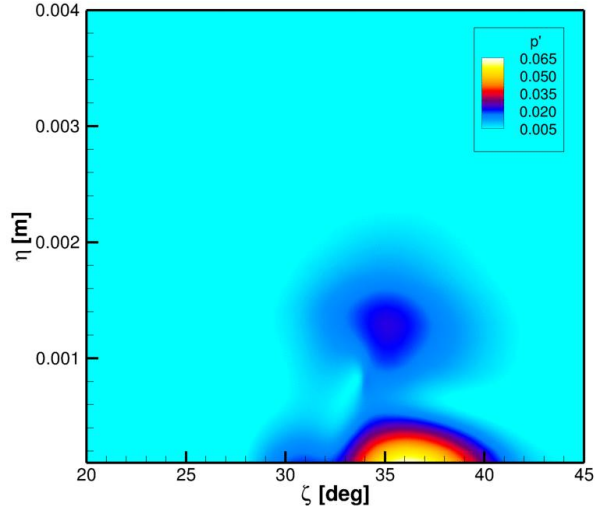
V. Russo *et al., "Towards understanding Particle Cloud Interactions with High Speed Boundary Layer Flows", AIAA Aviation 2021*

PARTICLE FLOW INTERACTION MECHANISMS: FINNED CONE

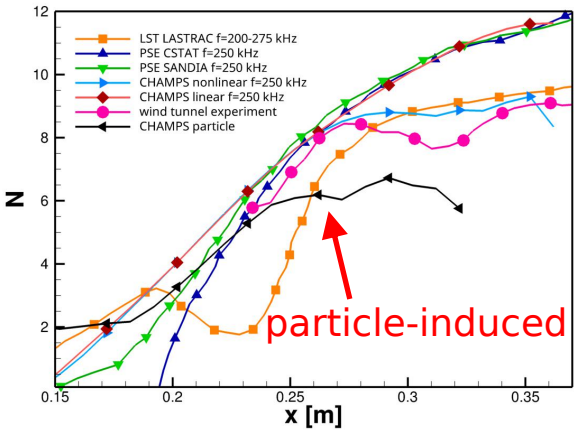
- subsequent tests on more complex geometries, like the fin-cone used for validation purposes, enabled the study of particle impingement on more realistic configurations
- particle impingement calculations revealed the capacity of particle collisions to induce complex instability mechanisms (such as vortical modes) and eventually trigger the transition of the boundary layer to a turbulent state



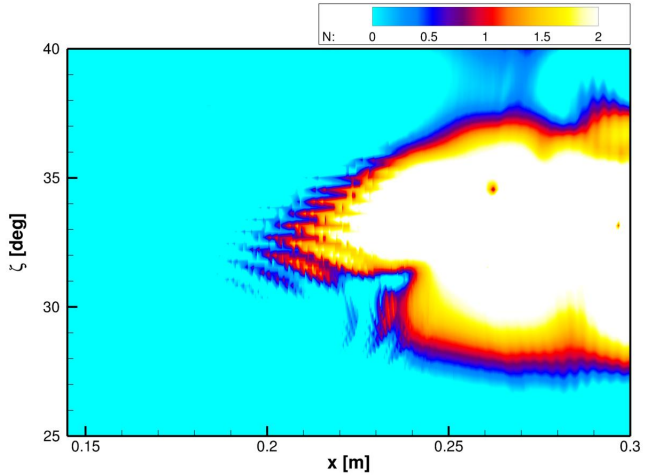
Disturbance Field



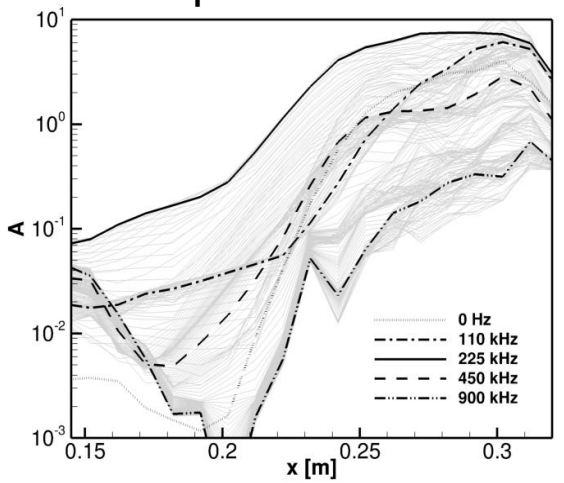
N-Factor Comparison



N-Factor on the Surface

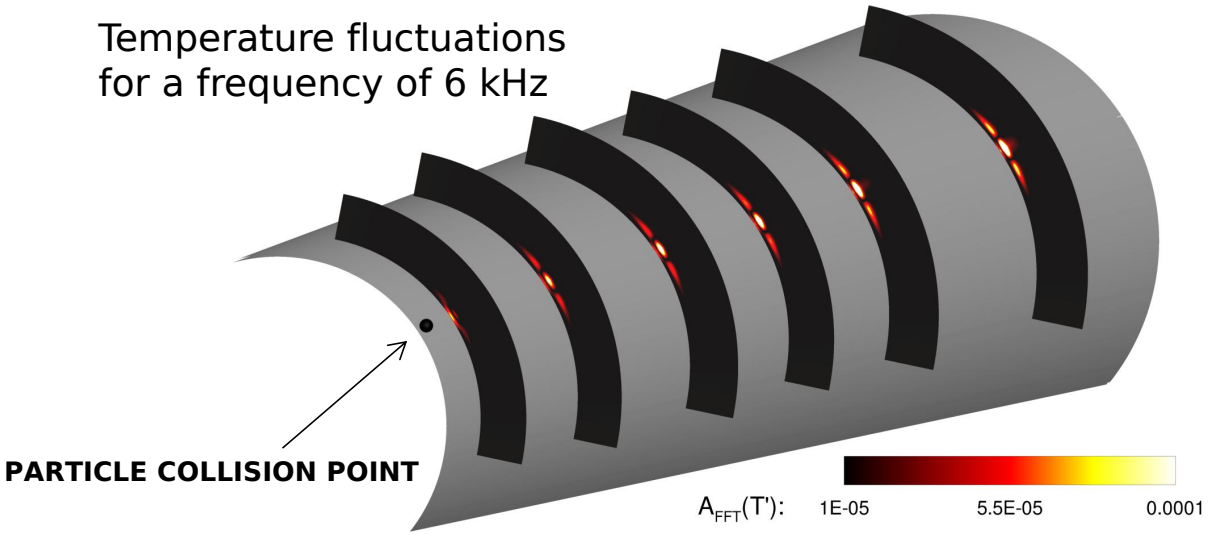


Amplitude Curves



PARTICLE FLOW INTERACTION MECHANISMS: TRANSIENT GROWTH

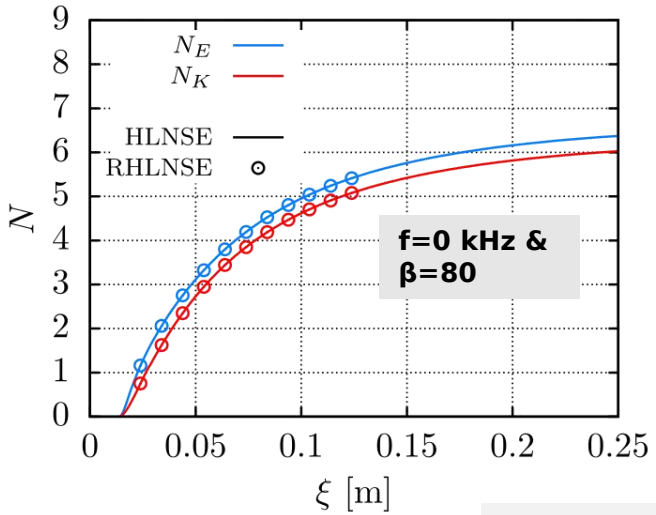
Temperature fluctuations
for a frequency of 6 kHz

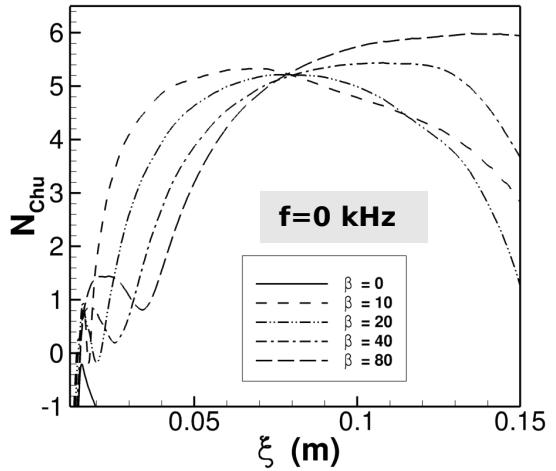


Particulate-Induced simuations Blunt Cone in Hypersonic Flow,
Russo et al., AIAA Scitech, 2021.

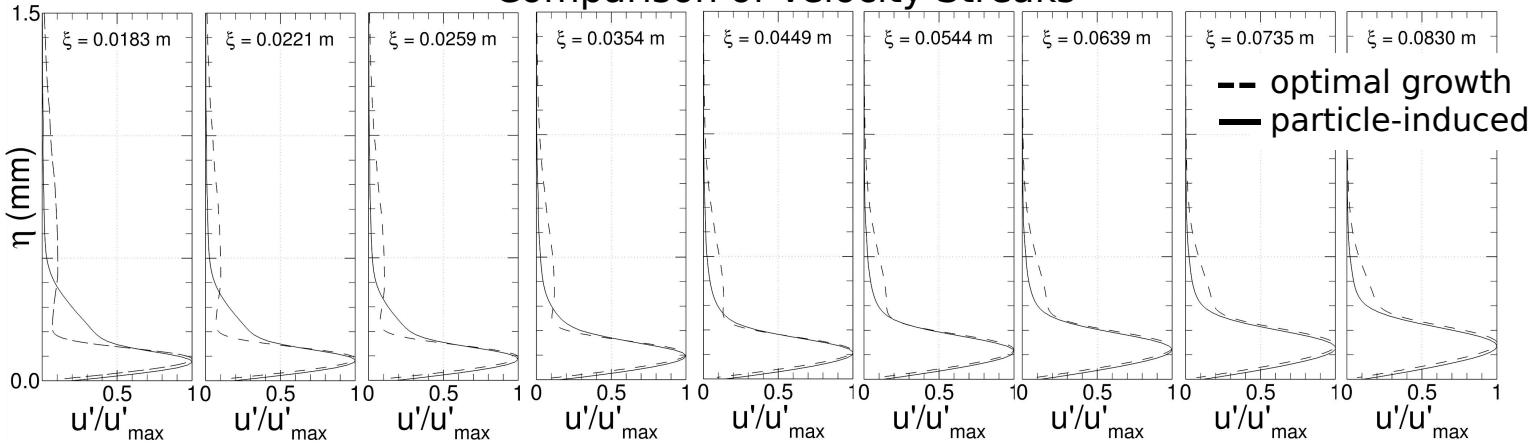
N-Factors

optimal growth (Paredes et al. 2019) *2D axisymmetric particle*



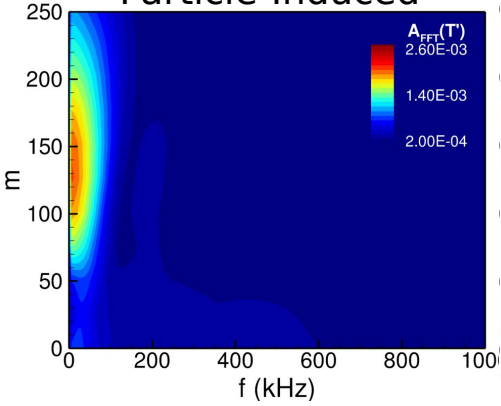


Comparison of Velocity Streaks

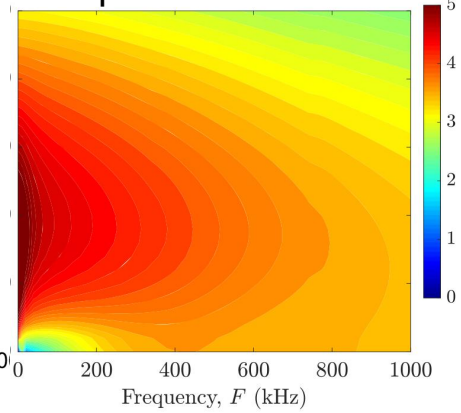


AMR-WPT-IBM *Paredes et al. (2019)*

Particle-Induced



Optimal Growth



CONCLUSIONS AND FUTURE WORK

CONCLUSIONS

- presented a **flexible** and **computationally efficient** framework to study boundary layer transition in hypersonic regimes on complex geometries with highly 3D baseflows, in cases where traditional methods (e.g. LST) would typically fail

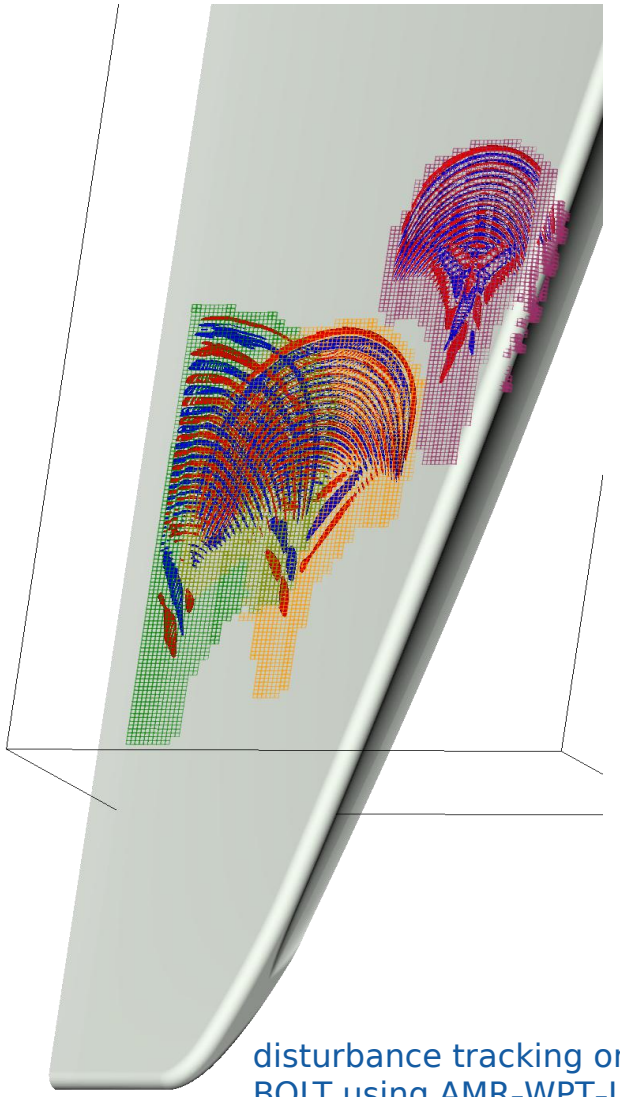
- provided a validation study for challenging cases with realistic geometries, and shown very good agreement with experimental data as well as other codes used by the transition community

- particle impingement simulations were also presented, and results indicated that particles could be responsible for the excitation of different types of disturbances in addition to traditional Mack first and second modes (namely vortical modes and transient growth)

FUTURE WORK

- study more realistic geometries and scenarios (BoLT, for instance) - to this purpose, the adaptive algorithm requires improvement in the strategies of refinement in order to attain the highest saving in computational cost without compromising on accuracy

- perform the computation of the entire path to transition, from receptivity to breakdown, until full turbulent flow - this scope will require additional work to guarantee the robustness of the adaptive refinement algorithm to handle the sudden transition of the boundary layer to turbulence



disturbance tracking on BOLT using AMR-WPT-IBM

AKNOWLEDGMENTS

- Professor Christoph Brehm, at the University of Maryland, College Park, for providing constant support

- Funding by the Office of Naval Research under contract N00014-19-1-2223, with Eric Marineau as Program Manager, is gratefully acknowledged

- Fruitful discussions with external collaborators: Dr. D. Araya (JHU Applied Physics Laboratory) and Dr. A. Knutson (University of Minnesota)

THANKS FOR THE ATTENTION

QUESTION?



BACKUP SLIDES

PUBLICATIONS

- *“Fully-Resolved Particulate-Induced Transition Simulations for High-Speed Boundary-Layers with an Immersed Boundary Method ,”* O. M. F. Browne, S. Hasnine, **V. Russo**, and C. Brehm, AIAA SciTech, Orlando, Florida, January 6, 2020.
- *“Disturbance Flow Field Analysis of Particulate Interaction with High Speed Boundary Layers ,”* S. M. A. Al Hasnine, **V. Russo**, O. M. F. Browne, A. Tumin, and C. Brehm, AIAA Aviation, virtual event, June 17, 2020.
- *“Particle Impingement Simulations for a Blunt Cone in Hypersonic Flow,”* **V. Russo**, S. Hasnine, O. Browne and C. Brehm, AIAA SciTech, Nashville, Tennessee, January, 2021.
- *“Three-Dimensional Spatio-Temporal Disturbance Flow Field Analysis of Particulate Induced High-Speed Boundary-Layer Transition ,”* S. Hasnine, **V. Russo**, O. M. F. Browne, A. Tumin, and C. Brehm, AIAA SciTech, Nashville, Tennessee, January, 2021.
- "*Towards understanding Particle Cloud Interactions with High Speed Boundary Layer Flows*",**V. Russo,** S. Hasnine and C. Brehm, AIAA Aviation Forum 2021.
- "*Particle Impingement Simulations for First and Second Mode Dominated High-Speed Boundary Layers*", S. Hasnine, **V. Russo** and C. Brehm, AIAA Aviation Forum 2021.
- "Low Frequency Streaks Upon Particle Collision on Blunt Cone in Hypersonc Flow", **V. Russo**, S. Hasnine and C. Brehm, in preparation, Journal of Fluid Mechanics.
- Assessment of linear methods for analysis of boundary layer instabilities on a finned cone at Mach 6, D. B. Araya, N. P. Bitter, B. M. Wheaton., O. Kamal, T. Colonius, A. Knutson, H. Johnson, J. Nichols, G. V. Candler, **V. Russo**, C. Brehm, AIAA Journal, submitted and currently under review.
- Assessment of linear methods for analysis of boundary layer instabilities on a finned cone at Mach 6, D. B. Araya, N. P. Bitter, B. M. Wheaton., O. Kamal, T. Colonius, A. Knutson, H. Johnson, J. Nichols, G. V. Candler, **V. Russo**, C. Brehm, AIAA Aviation Technical Forum, 2022, Chicago, Illinois.